HYDRAULIC AND SCOUR MODELING OF EXISTING AND ORIGINAL STRUCTURES AT INTERSTATE-35 AND CIMARRON RIVER

By

GABRIEL A. BRUEHL

Bachelor of Science

Oklahoma State University

Stillwater, Oklahoma

1998

Submitted to the Faculty of the
Graduate College of the
Oklahoma State University
in partial fulfillment of
the requirements for
the Degree of
MASTER OF SCIENCE
July, 2000

HYDRAULIC AND SCOUR MODELING OF EXISTING AND ORIGINAL STRUCTURES AT INTERSTATE-35 AND CIMARRON RIVER

Thesis Approved:

Avdhesh K. Tyagi
Thesis Advisor

Gerald D. Abraham

William F. McTernan

Dean of Graduate College

PREFACE

This study uses a common method of predicting scour to compare the existing bridge structure at the Interstate-35 and Cimarron River crossing to the original bridge that was damaged by a flood in 1986. The complexity of the site requires a two-dimensional analysis that was performed using the FESWMS-2DH computer model. Use of the program is simplified by using SMS, developed by Brigham Young University, to provide a graphical environment to input data and view the output. The results of this study validate the changes made to the Interstate-35 river crossing and can be used to further validate the use of FESWMS-2DH and SMS to model scour at other locations.

I wish to express my sincere gratitude to the individuals who assisted me in this project and during my course work at Oklahoma State University. In particular, I would like to thank my major advisor Dr. Avdhesh K. Tyagi for his guidance and invaluable assistance. I am also grateful to Dr. William F. McTernan and Dr. Garold D. Oberlender, both for serving on my committee and their enlightening courses. I would also like to thank Ms. Ramona Wheatley for her constant support and help.

TABLE OF CONTENTS

Chapter Page

LIST OF TABLES

LIST OF FIGURES

NOMENCLATURE

A_e = an element surface

D_{50} = median diameter of the bed material in feet

FESWMS-2DH = Finite Element Surface Water Modeling System: Two-Dimensional Flow in a Horizontal Plane.

f = a known function

g = acceleration due to gravity

H = water depth

L = a differential operator

N_i = the assumed interpolation function

NRCS = Natural Resources Conservation Service

n = Manning's n

n_x & n_y = the direction cosines between outward normal to the boundary and the positive x and y directions.

O.D.O.T. = Oklahoma Department of Transportation

Q_i = total source/sink flow attributed to node i

Q_{10} = flow from a 10 year storm

Q_{25} = flow from a 25 year storm

Q_{50} = flow from a 50 year storm

Q_{52} = flow from a 52 year storm

Q_{100} = flow from a 100 year storm

Q_{500} = flow from a 500 year storm

SMS = Surface Water Modeling System

s_e = an element boundary

subscript_0 = the known values at the start of a time step

Δt = the length of a time step

U = horizontal velocity in the x direction at a point along the vertical coordinate

u = the unknown nodal variable

USGS = United States Geological Survey

V = horizontal velocity in the y direction at a point along the vertical coordinate

V_c = the critical velocity above which bed material of a size D_{50} and smaller will be transported

W_1 = width of upstream main channel

W_2 = width of main channel in contracted section

y = flow depth

y_1 = average depth in upstream channel

y_2 = average depth in contracted section

z = the vertical direction

z_b =the bed elevation

z_s = the water surface elevation

$$\alpha_x = \arctan\left(\frac{\partial z_b}{\partial x}\right)$$

$$\alpha_y = \arctan\left(\frac{\partial z_b}{\partial y}\right)$$

$\alpha_z = \arccos\left(1 - \cos^2 \alpha_x - \cos^2 \alpha_y\right)$

$\beta_{uu}, \beta_{uv}, \beta_{vv}$ = momentum flux correction coefficients that account for the variation of velocity in the vertical direction

θ = a weighting coefficient ranging from 0.5 to 1

ρ = water mass density

τ_{bx}, τ_{by} = bed shear stress acting in the x and y directions

τ_{sx}, τ_{sy} = surface shear stress acting in the x and y directions

$\tau_{xx}, \tau_{xy}, \tau_{yy}$ = shear stress caused by turbulence, where τ_{xy} is the shear stress acting in the x direction on a plane that is perpendicular to the y direction

τ_2 = average bed shear stress in the contracted section

Ω = Coriolis parameter

CHAPTER 1

INTRODUCTION

Problem Statement

Description of the Watershed

The Cimarron River originates in New Mexico approximately one mile southeast of Dale Mountain peak. The river enters Oklahoma for the first time on the West side of Cimarron County. It then exits Oklahoma on the Northwest boundary of Cimarron County. The river enters Oklahoma for a second time on the North-central edge of Beaver County and exits the state for the second time at the North-central edge of Harper County. The river then enters the state for the third and final time and Forms part of the border between Harper and Woods County. The river then flows in a southeasterly direction to its termination into the Arkansas River at Keystone Reservoir near Mannford.

The Cimarron River crosses I-35 at the borders of Payne and Logan County approximately 7.5 miles North-Northeast of Guthrie. The drainage area contributing runoff upstream from the crossing is 17,505 square miles. Of the 17,505 square miles, 4,296 miles are controlled by NRCS water detention structures and are non-contributing. The river valley varies in width from 0.8 to 1.2 miles and is approximately one mile wide at the Interstate-35 crossing. The main channel may vary from 770 to 2000 feet in width and is contained by high banks and exhibits a high degree of meandering. Currently the river is located on the south edge of the floodplain. History indicates, however, that the

meander just upstream of the Interstate-35 crossing is moving downstream causing the main channel to gradually shift to the north side of the floodplain (Strongylis, 1988).

Crossing History

As mentioned, Interstate-35 crosses the Cimarron River at the border of Payne and Logan County. The original crossing, built in 1959, consisted of four lanes, with two lanes in both the north and south-bound directions, separated by a 40 foot median and shoulders. However, the structures were damaged in October of 1986 by a severe flood. Subsequently, the bridges were replaced by the existing structures in 1988.

The original crossing consisted of two bridges in the main channel and eight bridges in the floodplain. The two bridges in the main channel were installed parallel to each other on the south side of the flood plain, over the main river channel. Each bridge was 805 feet long and had a flowline of approximately 870.2 feet. The eight overflow bridges extended north across the floodplain and were placed in a series of four parallel installations. The overflow bridges were placed at increments of 900 feet, 450 feet, and 650 feet apart. The overflow bridges ranged in length from 160 to 280 feet, while the flowlines ranged from 885 to 887 feet.

The current design includes two structures spanning the main channel with two overflow structures extending north into the floodplain. The two main bridges are parallel to each other and span 800 feet in length with a flowline elevation of 870.5 feet. The two overflow structures are located in a parallel installation and both are 1,360 feet in length and have a flowline elevation of 887.0 feet.

Flood Events

There have been two major flood events recorded at the crossing. The first occurred in May of 1957. The high water elevation was recorded at 899.0 feet, but the corresponding discharge was not recorded. The second occurred in October of 1986 and had a peak water elevation of 898.0 feet. The flood, based on ODOT calculations, had a discharge of 156,000 cubic feet per second which is approximately a 52 year flood event (Q_{52}).

Scope of the Investigation

The scope of this investigation was to provide an advanced hydraulic and scour analysis of the original and existing structures at the Interstate 35 and Cimarron River Crossing. From this analysis the scour depths were calculated at each of the respective crossings and compared. The comparison will validate the design changes in 1988. The results may also be used to validate the use of scour equations as a design tool.

CHAPTER 2

FINITE ELEMENT METHOD

General

The finite element method is a numerical procedure for solving differential equations encountered in problems of physics and engineering. Originally devised to analyze structural systems, the finite element method has developed into an effective tool for evaluating a wide variety of problems in the field of continuum mechanics. Development of the finite element method has been encouraged primarily by the continued advancement of computers, which enables the user to rapidly perform the many complex calculations that are needed to obtain a solution. Only until recently has the finite element method been used to solve surface-water flow problems. However, in just a brief time a large amount of literature on the subject has already emerged. Lee and Froehlich (1986) provide a detailed review of literature on the finite element solution of the equations of two-dimensional surface-water flow in a horizontal plane.

Solution Technique

SMS is a graphical user interface that allows the simple transfer of the input data set into the FESWMS-2DH compiler and then allows the user to graphically view the output. FESWMS-2DH uses the Galerkin finite element method to solve the governing system of differential equations that describes surface water flow. The process to derive

a solution begins by assigning specific points in a plane of interest. These points, or nodes, may be connected to form triangular or quadrangular shapes called elements. A list of nodes connected to each element is easily recorded for identification and use. A series of elements divide the physical region of study into several subregions, which can be used for analysis. Values of a dependent variable are approximated within each element using values defined at the element's node points, and a set of interpolation functions. Mixed interpolation is used in FESWMS-2DH, which helps stabilize the solution. Quadratic interpolation functions are used to interpolate depth-averaged velocities and linear functions are used to interpolate flow depth.

The method of weighted residuals is applied to the governing differential equations next to form a set of equations for each element. Approximations of the dependent variables are substituted into the governing equations, which generally are not satisfied exactly, forming residuals. The residuals are required to vanish when they are multiplied by a weighting function and summed at every point in the solution domain. In Galerkin's method, the weighing functions are the same as the interpolation functions. By requiring the weighted residuals to equal zero, integration of the finite element equations is made possible. Coefficients of the equations are integrated numerically, and all the element equations are assembled to obtain the complete, global, system of equations. The global set of algebraic equations is then solved simultaneously.

Basic Concepts

One of the techniques used to approximate solutions to partial differential equations is the method of weighted residuals. There are two basic steps to apply the

method of weighted residuals. The first step is to assume a general functional behavior of a dependent variable so the governing differential equation and boundary condition equations can be satisfied approximately. When the assumed value of the dependent variable is substituted into the governing equations there is typically a margin of error. The error that is introduced by the assumed value is called a residual. The second step of the method is to solve the residual equation for the parameters of the functional representation of the dependent variable. Mathematically, the differential equation for the problem is written as:

$$Lu - f = 0 \tag{2-1}$$

where

L = a differential operator

u = the dependent variable

f = a known function

The dependent variable is then defined in terms of some unknown parameters and a set of functions, and is represented as:

$$u \approx \tilde{u} = \sum_{i=1}^{n} N_i C_i \tag{2-2}$$

where

N = the interpolation function

C = an unknown parameter

It is unlikely that the equation will be satisfied exactly when $\tilde{u}$ is substituted for u in equation (2-2). So the trial solution is defined as:

$$L\tilde{u} - f = \epsilon \tag{2-3}$$

where

ϵ = the residual

The method of weighted residuals attempts to determine the number of unknown parameters so the error is as small as possible within the solution region. By forming a weighted average of the error, the error is required to vanish when integrated over the entire solution region. This process minimizes the error and produces a more accurate result. The weighted average is computed as:

$$\int_R W_i \, \epsilon \, dR = 0 \qquad \text{for i} = 1, 2, \ldots, \text{m} \tag{2-4}$$

where

R = solution domain

W = linearly independent weighting function

m = number of linearly independent weighting functions

Next, the application of equation 2-2 provides a solution for the unknown parameters (C) which allows for an approximate representation of the dependent variable u. There is a certain amount of flexibility when choosing the weighting functions that are used to form the residual expressions. The weighting functions are then equated to interpolation functions used to approximate the dependent variable ($W_i = N_i$). The finite element implementation mentioned is known as Galerkin's method. Galerkin's method provides that:

$$\int_R N_i \, (L\tilde{u} - f) \, dR = 0 \quad \text{for i} = 1, 2, \ldots, \text{m} \tag{2-5}$$

Once the interpolation functions are specified, the equations can be evaluated explicitly, and the solution found.

The fundamental concept of the finite element method is to divide an irregular shaped region into a smaller set of finite regions called elements. The value of a continuous quantity can be approximated by a set of functions using the values of that quantity at a finite number of points. The functions are known as interpolation or shape functions, and are analogous to the functions described previously. The points that define the continuous quantity are known as node points. The values of the nodal points are comparative to the undetermined parameters (C) from equation 2-2. Once this is known the approximation of a continuous quantity within an element can be described as:

$$\tilde{u}^{(e)} \approx \sum_{i=1}^{n} N_i^{(e)} u_i^{(e)} \qquad (2\text{-}6)$$

where

$N_i^{(e)}$ = interpolation function for an element

$u_i^{(e)}$ = unknown nodal variables

n = the number of node points in an element

Equation 2-6 can either apply to a single point or a collection of points (an element) in the solution region. When Galerkin's method is applied, the left-hand side of equation 2-5 is computed as the sum of expressions of the form:

$$\int_R N_i^{(e)} (L\tilde{u}^{(e)} - f^{(e)})\, dR^{(e)} \qquad \text{for i} = 1, 2, \ldots, \text{n} \qquad (2\text{-}7)$$

where

$R^{(e)}$ = an element domain

$f^{(e)}$ = defined element function

A set of expressions is then developed for each equation based on equation 2-7. The element expressions are then assembled to form the complete set of global equations. In a finite element solution, the values of a quantity at the node points are the unknowns.

The behavior of the solution within the entire assemblage of element is described by the element interpolation functions and the node point values, when they have been determined.

To assemble the element equations the particular types of elements that define the region in question and their corresponding interpolation functions must be specified. The interpolation functions that define the system depend on the shape of the element and the order of approximation desired. Based on the premise that a system with a complex shape can be divided into small regions to find a solution, the shape of the elements to define the complex area are generally simple polynomials. Even though there are many shapes that can be used to define an element, the most commonly used shapes to define an element are triangles and quadrilaterals.

When polynomial interpolation functions are used, linear variation of a quantity within an element are determined by the values provided at the corners of a triangular or quadrangular element. For quadratic variation of a quantity, additional values need to be defined along the sides, and sometimes the interior, of an element. FESWMS-2DH uses three types of two-dimensional elements: 6-node triangles, 8-node quadrilaterals, and 9-node quadrilaterals. The 9-node quadrilateral differs from the 8-node quadrilateral because of an additional node at the centroid of the quadrilateral element, however both use the same interpolation function. The common types of elements used in FESWMS-2DH are shown in Figure 1, Examples of three types of two-dimensional elements in FESWMS-2DH.

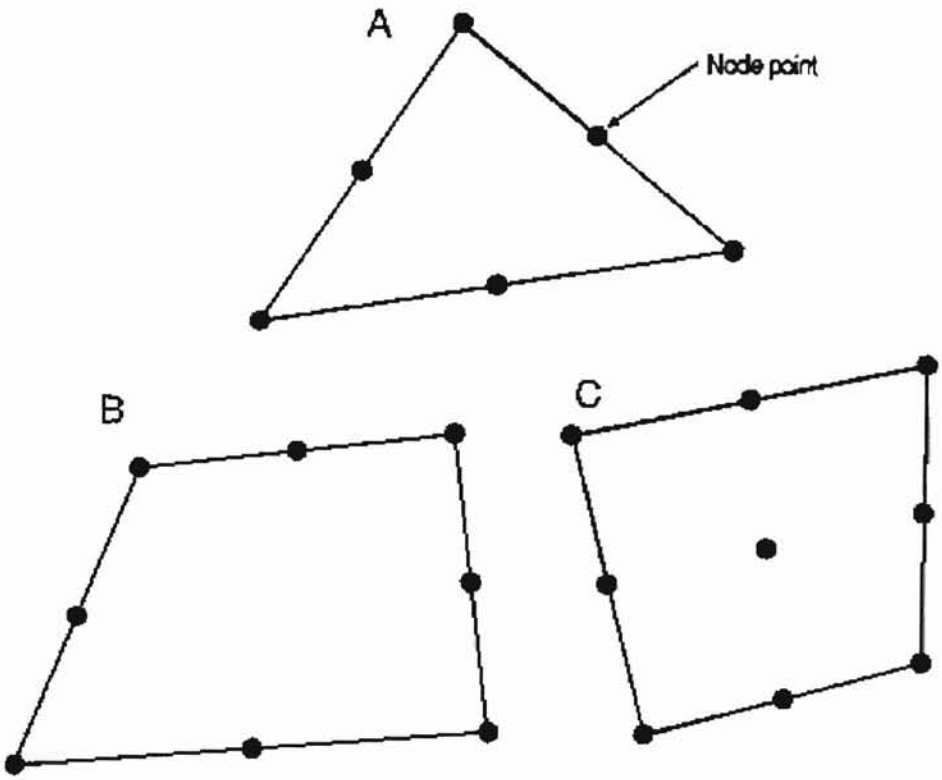

Figure 1. Examples of Three Types of Two-Dimensional Elements Used in FESWMS-2DH:

a) a six node triangle

b) an eight node quadrilateral

c) a nine node quadrilateral

(Source: Froelich, 1992, p. 3-6)

CHAPTER 3

GOVERNING EQUATIONS

General

In most practical engineering problems related to surface water, the width to depth ratio is very large. When the width to depth ratio of a water body is large, the knowledge of the full three dimensional nature is not required and the use of a two-dimensional flow application may be used. Examples of cases where two-dimensional analysis may be used include shallow coastal areas, harbors, estuaries, rivers and floodplains.

FESWMS-2DH calculates depth average horizontal velocities, flow depths, and the time derivatives of these quantities if a time dependent flow is modeled. To develop an accurate representation of surface water flow requires the in depth description of the physical conditions that are associated with depth averaged flow. The equations that govern depth averaged surface water flow take into consideration the effects of fluid stresses caused by turbulence, the effects of friction, stresses caused by surface wind, and the coriolis effect.

Steady State Solution

The equations that govern the hydrodynamic behavior of an incompressible fluid are based on the concepts of conservation of mass and momentum. The use of mean-flow quantities in two perpendicular horizontal directions is sufficient due to the large width to depth ratio. By integrating the three dimensional equations over the depth of water and assuming a constant fluid density, a set of three equations appropriate for modeling flow in shallow water bodies is found. Since the flow is assumed to be horizontal, the use of a Cartesian coordinate system with the x and y directions in the horizontal plane and z in the vertical direction is used. The coordinate system and is illustrated in Figure 2, Coordinate System. The depth averaged velocity components in the horizontal x and y coordinate directions are illustrated in Figure 3, Illustration of Depth Averaged Velocity, and are defined as:

$$U = \frac{1}{H} \int_{z_b}^{z_s} u\,dz \tag{3-1}$$

$$V = \frac{1}{H} \int_{z_b}^{z_s} v\,dz \tag{3-2}$$

where

H = the water depth

z_s = the vertical direction

z_b = the bed elevation

U = horizontal velocity in the x direction at a point along the vertical coordinate

V = horizontal velocity in the y direction at a point along the horizontal coordinate

$z_s = z_b + H$ = the water surface elevation

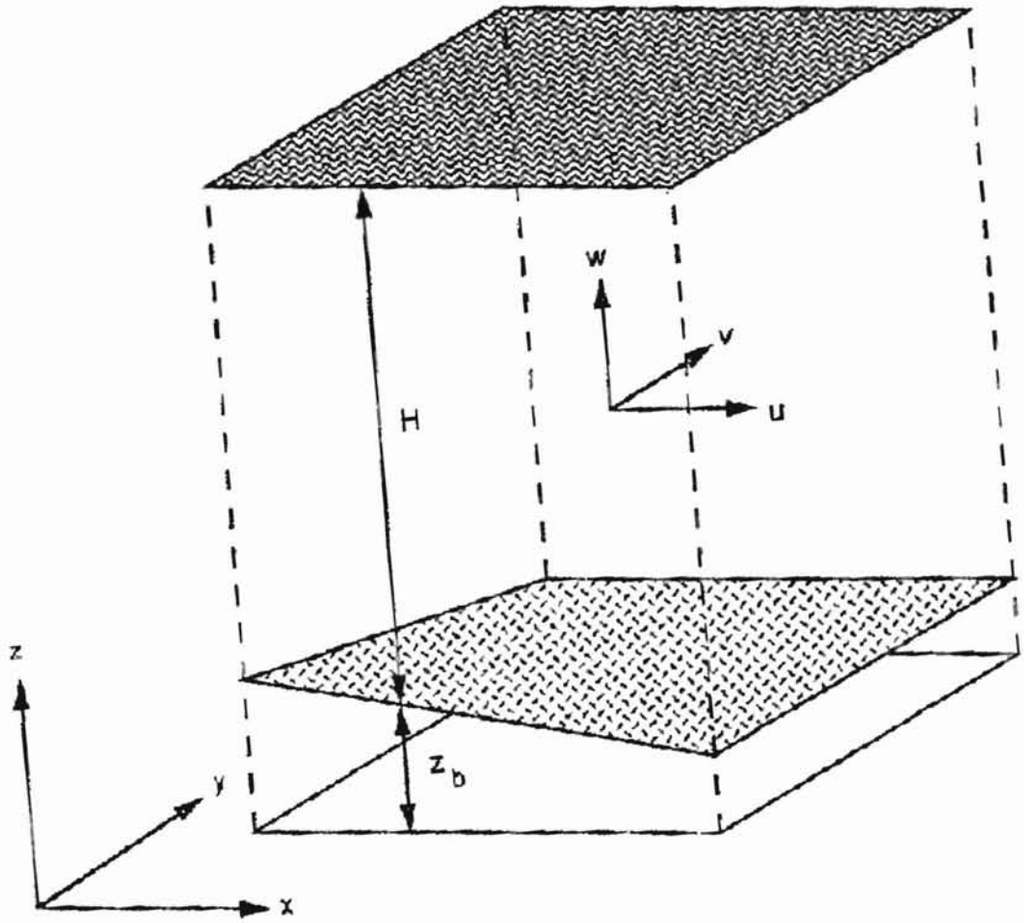

Figure 2. Coordinate System (Source: Froehlich, 1992, p. 4-2)

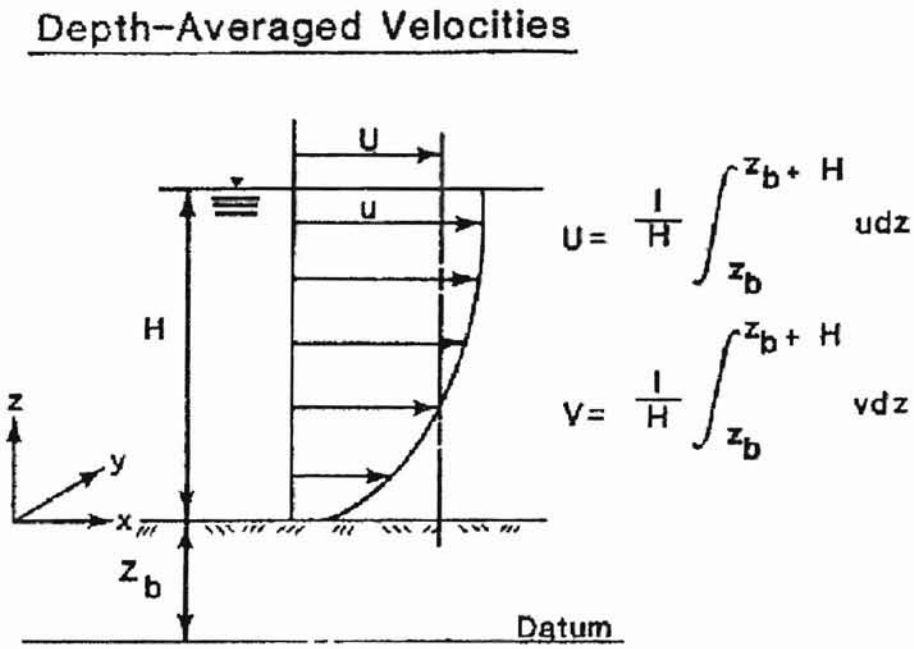

Figure 3. Illustration of Depth Averaged Velocities (Source: Froehlich, 1992, p. 4-3)

Jansen and others (1979) presents a thorough derivation of the depth averaged surface water flow equations by integrating the three dimensional mass and momentum transport equations with respect to the vertical coordinate from the bed to the water surface and assuming that vertical velocities and accelerations are negligible. The vertically-integrated momentum equations are:

$$\frac{\partial}{\partial t}(HU)+\frac{\partial}{\partial x}\left(\beta_{uu}HUU+\frac{1}{2}gH^2\right)+\frac{\partial}{\partial y}(\beta_{uv}HUV)+gH\frac{\partial z_b}{\partial x}-\Omega HV+\frac{1}{\rho}\left[\tau_x^b-\tau_x^s-\frac{\partial}{\partial x}(H\tau_{xx})-\frac{\partial}{\partial y}(H\tau_{xy})\right]=0 \quad (3\text{-}3)$$

For flow in the x direction, and

$$\frac{\partial}{\partial t}(HV)+\frac{\partial}{\partial y}\left(\beta_{vv}HVv+\frac{1}{2}gH^2\right)+\frac{\partial}{\partial x}(\beta_{vu}HVU)+gH\frac{\partial z_b}{\partial y}-\Omega HU+\frac{1}{\rho}\left[\tau_y^b-\tau_y^s-\frac{\partial}{\partial x}(H\tau_{yx})-\frac{\partial}{\partial y}(H\tau_{yy})\right]=0 \quad (3\text{-}4)$$

For flow in the y direction, where

β_{uu}, β_{uv}, β_{vu}, β_{vv} = momentum correction coefficients that account for the variation of velocity in the vertical direction

g = acceleration of gravity

Ω = Coriolis parameter

ρ = water mass density (constant)

τ_{bx} & τ_{by} = bed shear stress acting in the x and y directions

τ_{sx} & τ_{sy} = surface shear stress acting in the x and y directions

τ_{xx}, τ_{xy}, τ_{yy} = shear stresses caused by turbulence where τ_{xy} is the shear stress acting in the x direction on a plane that is perpendicular to the y

direction.

The vertically integrated mass balance (continuity equation) is:

$$\frac{\partial H}{\partial t}+\frac{\partial}{\partial x}(HU)+\frac{\partial}{\partial y}(HV)=q \tag{3-5}$$

Momentum Correction Coefficients

The momentum correction coefficients from the above equations result from the vertical integration of the momentum balance equations and account for vertical variations of U and V. The momentum correction coefficients are computed as follows:

$$\beta_{uu}=\frac{1}{HUU}\int_{z_b}^{z_s} uudz \tag{3-6}$$

$$\beta_{uv}=\beta_{vu}=\frac{1}{HUV}\int_{z_b}^{z_s} uvdz \tag{3-7}$$

$$\beta_{vv}=\frac{1}{HVV}\int_{z_b}^{z_s} vvdz \tag{3-8}$$

The momentum correction coefficients depend on the vertical velocity distribution, and upon further derivation are considered to be equal to each other, providing the equation:

$$\beta=\beta_o+c_\beta c_f$$

and

$$c_\beta=\frac{1}{k^2} \tag{3-9}$$

where

c_f = bed shear stress coefficient

k = Von Karman's constant

When the width to depth ratio of a water body is large the default values of β_o and c_β are 1.0 and 0.0 respectively. This provides that the vertical variations in velocity are negligible.

Coriolis Parameter

The Coriolis parameter is determined by the equation:

$$\Omega = 2\omega \sin\phi \tag{3-10}$$

where

ω = the angular velocity of the rotating earth

ϕ = mean angle of latitude of the area being modeled

However, for most shallow flows where the width to depth ratio is large the Coriolis effect will be small and can safely be ignored.

Bed Shear Stresses

The bottom friction coefficient, used to compute the bed shear stress, may be computed as:

$$c_f = g / C^2 \tag{3-11}$$

where

C = the Chezy discharge coefficient

or as

$$c_f = g\, n^2 / 2.208\, H^{1/3} \tag{3-12}$$

where

n = the Manning's roughness coefficient.

The values of Chezy discharge coefficients and Manning roughness coefficients can be obtained by using reference materials such as Chow (1959). It should be noted that the values found in reference materials such as these, are based on the assumption of one-dimensional flow and therefore, may be higher than necessary.

Surface Shear Stresses

The surface stress has been found to be a function of wind speed near the surface of the water body. The surface shear stress caused by wind in the x and y directions are as follows:

$$\tau_{sx} = c_s \rho_a W^2 \cos\varphi \tag{3-13}$$

$$\tau_{sy} = c_s \rho_a W^2 \sin\varphi \tag{3-14}$$

where

c_s = dimensionless surface stress coefficient

ρ_a = the density of air

W = a characteristic wind velocity near the surface

ψ = the angle between the wind direction and the positive x-axis

Turbulence

The effect of turbulence on a water body is computed by Boussinesq's eddy viscosity concept which assumes the turbulent stresses are proportional to the depth averaged velocity gradients. The turbulent stresses are computed as follows:

$$\tau_{xx} = \rho\tilde{\nu}_{xx}\left(\frac{\partial U}{\partial x} + \frac{\partial U}{\partial x}\right) \tag{3-15}$$

$$\tau_{xy} = \tau_{yx} = \rho\tilde{\nu}_{xx}\left(\frac{\partial U}{\partial y} + \frac{\partial V}{\partial x}\right) \tag{3-16}$$

$$\tau_{yy} = \rho\tilde{\nu}_{yy}\left(\frac{\partial V}{\partial y} + \frac{\partial V}{\partial y}\right) \tag{3-17}$$

where

$\tilde{\nu}_{xx}, \tilde{\nu}_{xy}, \tilde{\nu}_{yx}, \tilde{\nu}_{yy}$ = the directional values of the depth-averaged kinematic eddy viscosity

CHAPTER 4

FINITE ELEMENT EQUATIONS

General

The method of weighted residuals using Galerkin weighting is applied to the governing depth-averaged flow equations to form the finite element equations. Because the system of equations is nonlinear, Newton's iterative method (Zienkiwicz, 1977, p.452) is used to obtain a solution. To apply Newton's method, at each iteration the governing equations are used to define a residual. In addition, a matrix of derivatives with respect to each dependent variable for each residual expression is required. The matrix is referred to as the Jacobian matrix and each of its members is defined by a derivative expression. The finite element formulations of the residual and derivative expressions at the *i*th node point are presented in the following sections. Application of boundary conditions is also covered.

Residual Expressions

The finite element formulations for the residuals of the depth averaged flow equations, where the summation is with respect to all elements, written at node i are:

$$f_{1i} \equiv \sum_e \int_{A_e} \left\{ \begin{array}{l} N_i \left[H \frac{\partial U}{\partial t} + U \frac{\partial H}{\partial t} + gH \frac{\partial z_b}{\partial x} - \Omega HV + \frac{1}{\rho}\left(\tau_x^b - \tau_x^s\right) \right] \\ + \frac{\partial N_i}{\partial x}\left[-\beta HUU - \frac{1}{2} gH^2 + 2\tilde{\nu} H \frac{\partial U}{\partial x} \right] + \frac{\partial N_i}{\partial y}\left[-\beta HUV + \tilde{\nu} H \left(\frac{\partial U}{\partial y} + \frac{\partial V}{\partial x} \right) \right] \end{array} \right\} dA_e$$

$$+ \sum_e \int_{S_e} N_i \left[\left(\beta HUU + \frac{1}{2} gH^2 \right) l_x + \beta HUV l_y \right] dS_e - \sum_e \int_{S_e} N_i \left[2\tilde{\nu} H \frac{\partial U}{\partial x} l_x + \tilde{\nu} H \left(\frac{\partial U}{\partial y} + \frac{\partial V}{\partial x} \right) l_y \right] dS_e$$

for flow in the x direction, and (4-1)

$$f_{2i} \equiv \sum_e \int_{A_e} \left\{ \begin{array}{l} N_i \left[H \frac{\partial V}{\partial t} + V \frac{\partial H}{\partial t} + gH \frac{\partial z_b}{\partial y} - \Omega HU + \frac{1}{\rho}\left(\tau_y^b - \tau_y^s\right) \right] \\ + \frac{\partial N_i}{\partial y}\left[-\beta HVV - \frac{1}{2} gH^2 + 2\tilde{\nu} H \frac{\partial U}{\partial y} \right] + \frac{\partial N_i}{\partial x}\left[-\beta HUV + \tilde{\nu} H \left(\frac{\partial U}{\partial y} + \frac{\partial V}{\partial x} \right) \right] \end{array} \right\} dA_e$$

$$+ \sum_e \int_{S_e} N_i \left[\left(\beta HVV + \frac{1}{2} gH^2 \right) l_y + \beta HUV l_x \right] dS_e - \sum_e \int_{S_e} N_i \left[2\tilde{\nu} H \frac{\partial V}{\partial x} l_y + \tilde{\nu} H \left(\frac{\partial U}{\partial y} + \frac{\partial V}{\partial x} \right) l_x \right] dS_e$$

for flow in the y direction (4-2)

where

$\sum_e$ = the summation with respect to all elements

A_e = an element surface

S_e = an element boundary

l_x and l_y = the direction cosines between the outward normal to the boundary and the x and y directions, respectively

All second order derivatives in the moment expressions have been integrated by parts using the Green-Gauss theorem. Reduction of the order of the expressions in this way allows use of quadratic functions to interpolate velocities. Integration by parts of the advection terms simplifies the finite element terms facilitates application of normal-stress boundary conditions. The last boundary integral in the two momentum residual expressions represents the lateral stress resulting from the transport of momentum by turbulence.

The expression for the weighted residual of the continuity equation is:

$$f_{3i} \equiv \sum_{e} \int_{A_e} Mi \left[\frac{\partial H}{\partial t} + H \frac{\partial U}{\partial x} + U \frac{\partial H}{\partial x} + H \frac{\partial V}{\partial y} + V \frac{\partial H}{\partial y} \right] dA_e - Q_i \tag{4-3}$$

where

$$Q_i = \sum_{e} \int_{A_e} M_i q dA_e \tag{4-4}$$

is the total source/sink flow attributed to node i

Time Derivatives

Equations 3-18, 3-19, and 3-20 apply to a particular instant in time. For a steady-state solution the time derivatives are equal to zero and do not need to be evaluated. However, if the solution is time-dependent the residuals need to be integrated with respect to time. The derivative of U with respect to time at the end of a time step is:

$$\frac{\partial U^{j+1}}{\partial t} = \frac{1}{\theta} \left(\frac{U^{j+1} - U^{j}}{\Delta t} \right) - \left(\frac{1-\theta}{\theta} \right) \frac{\partial U^{j}}{\partial t} \tag{4-5}$$

where

Δt = the length of the time step

θ = a weighting function that varies from 0.5 – 1.0

For $\theta = 0$, the integration scheme is explicit (forward Euler), for $\theta = 1$, the integration is implicit (backward Euler), and for $\theta = 0.5$, a trapezoidal (Crank-Nicholson) integration scheme results. Setting $\theta = 0.67$ can provide an accurate and stable solution for even relatively large time steps. An expression of $\partial U/\partial t$ at the advanced time level can be rewritten as:

$$\frac{\partial U^{j+1}}{\partial t} = \alpha U^{j+1} + \beta_1 \tag{4-6}$$

where

$$\alpha = \frac{1}{\theta \Delta t} \tag{4-7}$$

and

$$\beta_1 = \alpha U^{j+1} + \left(\frac{1-\theta}{\theta}\right)\frac{\partial U^{j}}{\partial t} \tag{4-8}$$

The variable β_1 is the only quantity that is known at the start of the time step. In a similar Manner, time derivatives of V and M are defined as:

$$\frac{\partial V}{\partial t} = \alpha V + \beta_2 \tag{4-9}$$

and

$$\frac{\partial H}{\partial t} = \alpha H + \beta_3 \tag{4-10}$$

where

$$\beta_2 = \alpha V^j + \left(\frac{1-\theta}{\theta}\right)\frac{\partial V^j}{\partial t} \tag{4-11}$$

and

$$\beta_3 = \alpha H^i + \left(\frac{1-\theta}{\theta}\right)\frac{\partial H^j}{\partial t} \tag{4-12}$$

The finite element formulations of the derivatives of the depth-averaged flow equation residual are written for node i with respect to variables at node j. The derivative expressions for the residual of the conservation of momentum equation in the x direction are:

$$\frac{\partial f_i}{\partial U_j} \equiv \sum_e \int_{A_e} \left\{ \begin{array}{l} N_i N_j \left[\alpha H + \dfrac{\partial H}{\partial t} + \dfrac{1}{\rho}\tau_x^b \dfrac{\left(2U^2 + V^2\right)}{U\left(U^2 + V^2\right)} \right] + \dfrac{\partial N_i}{\partial x} N_j \left(-2\beta HU\right) \\ + \dfrac{\partial N_i}{\partial x}\dfrac{\partial N_j}{\partial x}\left(2\tilde{\nu}H\right) + \dfrac{\partial N_i}{\partial y} N_j \left(-\beta HV\right) + \dfrac{\partial N_i}{\partial y}\dfrac{\partial N_j}{\partial y}\left(\tilde{\nu}H\right) \end{array} \right\} dA_e$$
$$+ \sum_e \int_{S_e} \left\{ N_i N_j \left[2\beta HU\right]_x + \beta HV\big]_y - N_i \frac{\partial N_i}{\partial x}\left(2\tilde{\nu}H\right]_x - N_i \frac{\partial N_i}{\partial y}\left(\tilde{\nu}H\right]_y \right\} dS_e \tag{4-13}$$

$$\frac{\partial f_{1i}}{\partial V_j} \equiv \sum_e \int_{A_e} \left\{ N_i N_j \left[-\Omega H + \frac{1}{\rho}\tau_x^b \frac{V}{\left(U^2 + V^2\right)} \right] + \frac{\partial N_i}{\partial y} N_i \left(-\beta HU\right) + \frac{\partial N_i}{\partial y}\frac{\partial N_j}{\partial x}\left(\tilde{\nu}H\right) \right\} dA_e$$
$$+ \sum_e \int_{S_e} \left[N_i N_j \left(\beta HU\right]_y - N_i \frac{\partial N_j}{\partial x}\left(\tilde{\nu}H\right]_y \right] dS_e \tag{4-14}$$

$$\frac{\partial f_{1i}}{\partial H_j} \equiv \sum_e \int_{A_e} \left\{ \begin{array}{l} N_i M_j \left[\frac{\partial U}{\partial t} + \alpha U - \Omega V + g \frac{\partial z_b}{\partial x} + \frac{1}{\rho} \tau_x^b \frac{1}{c_f} \frac{\partial c_f}{\partial H} \right] \\ + \frac{\partial N_i}{\partial x} M_j \left[-\beta UU - gH + 2\tilde{\nu} \frac{\partial U}{\partial x} \right] + \frac{\partial N_i}{\partial y} M_j \left[-\beta UV + \tilde{\nu} \left(\frac{\partial U}{\partial y} + \frac{\partial V}{\partial x} \right) \right] \end{array} \right\} dA_e$$

$$+ \sum_e \int_{S_e} N_i M_j \left\{ \left[\beta UU + gH - 2\tilde{\nu} \frac{\partial U}{\partial x} \right] l_x + \left[\beta UV - \tilde{\nu} \left(\frac{\partial U}{\partial y} + \frac{\partial V}{\partial x} \right) \right] l_y \right\} dS_e$$

(4-15)

Derivative expressions for the residual of the conservation of momentum equation in the y direction are:

$$\frac{\partial f_{2i}}{\partial U_j} \equiv \sum_e \int_{A_e} \left\{ N_i N_j \left[\Omega H + \frac{1}{\rho} \tau_y^b \frac{U}{\left(U^2 + V^2 \right)} \right] + \frac{\partial N_i}{\partial x} N_i \left(-\beta HV \right) + \frac{\partial N_i}{\partial x} \frac{\partial N_j}{\partial y} \left(\tilde{\nu} H \right) \right\} dA_e$$

$$+ \sum_e \int_{S_e} \left\{ N_i N_j \left(\beta HV l_x \right) - N_i \frac{\partial N_j}{\partial y} \left(\tilde{\nu} H l_x \right) \right\} dS_e$$

(4-16)

$$\frac{\partial f_{2i}}{\partial V_j} \equiv \sum_e \int_{A_e} \left\{ \begin{array}{l} N_i N_j \left[\alpha H + \frac{\partial H}{\partial t} + \frac{1}{\rho} \tau_y^b \frac{\left(U^2 + 2V^2 \right)}{V \left(U^2 + V^2 \right)} \right] + \frac{\partial N_i}{\partial x} N_j \left(-\beta HU \right) \\ + \frac{\partial N_i}{\partial x} \frac{\partial N_j}{\partial x} \left(\tilde{\nu} H \right) + \frac{\partial N_1}{\partial y} N_j \left(-2\beta HV \right) + \frac{\partial N_i}{\partial y} \frac{\partial N_j}{\partial y} \left(2\tilde{\nu} H \right) \end{array} \right\} dA_e$$

$$+ \sum_e \int_{S_e} \left\{ N_i N_j \left[\beta HU l_x + 2\beta HV l_y \right] - N_i \frac{\partial N_i}{\partial x} \left(\tilde{\nu} H l_x \right) - N_i \frac{\partial N_i}{\partial y} \left(2\tilde{\nu} H l_y \right) \right\} dS_e$$

(4-17)

$$\frac{\partial f_{2i}}{\partial H_j} \equiv \sum_e \iint_{A_e} \left\{ \begin{array}{l} N_i M_j \left[\dfrac{\partial V}{\partial t} + \alpha V - \Omega U + g \dfrac{\partial z_b}{\partial x} + \dfrac{1}{\rho} \tau_x^b \dfrac{1}{c_f} \dfrac{\partial c_f}{\partial H} \right] \\ + \dfrac{\partial N_i}{\partial x} M_j \left[-\beta V V - gH + 2\tilde{\nu} \dfrac{\partial V}{\partial x} \right] + \dfrac{\partial N_i}{\partial y} M_j \left[-\beta U V + \tilde{\nu} \left(\dfrac{\partial U}{\partial y} + \dfrac{\partial V}{\partial x} \right) \right] \end{array} \right\} dA_e$$

$$+ \sum_e \int_{S_e} N_i M_j \left\{ \left[\beta V V + gH - 2\tilde{\nu} \frac{\partial U}{\partial x} \right] 1_y + \left[\beta U V - \tilde{\nu} \left(\frac{\partial U}{\partial y} + \frac{\partial V}{\partial x} \right) \right] 1_x \right\} dS_e \qquad (4\text{-}18)$$

where

$$\frac{\partial c_f}{\partial H} = \begin{cases} 0, \text{ if Chezy discarge coefficients are used} \\ \dfrac{\phi g n^2}{H^{4/3}}, \text{ if Manning roughness coefficients are used} \end{cases}$$

and

$$\phi = \begin{cases} 0.151 \text{ for U.S. Customary units} \\ 0.333 \text{ for S.I. units} \end{cases}$$

The derivative expressions for the equation continuity residuals are:

$$\frac{\partial f_{3i}}{\partial U_j} \equiv \sum_e \iint_{A_e} \left[M_i \frac{\partial N_j}{\partial x}(H) + M_i N_i \left(\frac{\partial H}{\partial x} \right) \right] dA_e - \frac{\partial Q_i}{\partial U_j} \qquad (4\text{-}19)$$

$$\frac{\partial f_{3i}}{\partial V_j} \equiv \sum_e \iint_{A_e} \left[M_i \frac{\partial N_j}{\partial y}(H) + M_i N_i \left(\frac{\partial H}{\partial y} \right) \right] dA_e - \frac{\partial Q_i}{\partial V_j} \qquad (4\text{-}20)$$

$$\frac{\partial f_{3i}}{\partial H_j} \equiv \sum_e \iint_{A_e} \left[M_i M_j \left(\alpha + \frac{\partial U}{\partial x} + \frac{\partial V}{\partial y} \right) + M_i \frac{\partial M_j}{\partial x}(U) + M_i \frac{\partial M_j}{\partial y}(V) \right] dA_e - \frac{\partial Q_i}{\partial H_j} \qquad (4\text{-}21)$$

Boundary Conditions

The Galerkin finite element formulation allows complicated boundary conditions to be automatically satisfied as natural conditions of the problem. The natural boundary conditions are implicitly imposed in the problem statement and require no further treatment. Those boundary conditions that are imposed explicitly are known as force, or essential, conditions. These boundary values are prescribed by modifying the finite element equation governing that variable. In addition, special boundary conditions imposed by one-dimensional flow at culverts and weirs can be easily applied.

Open Boundaries

Velocities and depth can be applied as essential boundary conditions at any node point on a boundary as long as the system of equations does not become overconstrained. Velocities and depth are prescribed at node i by replacing the residual expressions by:

$$F_{1i} = U_i \tag{4-22}$$

$$F_{2i} = V_i \tag{4-23}$$

$$F_{3i} = H_i \tag{4-24}$$

and replacing the derivative expressions by:

$$\frac{\partial f_{1i}}{\partial U_j} \equiv \begin{cases} 1, \text{if i} = \text{j} \\ 0, \text{if i} \neq \text{j} \end{cases}; \qquad \frac{\partial f_{1i}}{\partial V_j} = 0; \qquad \frac{\partial f_{1i}}{\partial H_j} = 0 \tag{4-25a,b,c}$$

$$\frac{\partial f_{2i}}{\partial U_j} = 0 \qquad \frac{\partial f_{2i}}{\partial V_j} \equiv \begin{cases} 1, \text{if i} = \text{j} \\ 0, \text{if i} \neq \text{j} \end{cases} \qquad \frac{\partial f_{2i}}{\partial H_j} = 0 \tag{4-26a,b,c}$$

Derivative expressions for the residual of the conservation of momentum equation in the y direction are:

$$\frac{\partial f_{3i}}{\partial U_j} = 0 \qquad \frac{\partial f_{3i}}{\partial V_j} = 0 \qquad \frac{\partial f_{3i}}{\partial H_j} \equiv \begin{cases} 1, \text{if i} = \text{j} \\ 0, \text{if i} \neq \text{j} \end{cases} \tag{4-27a,b,c}$$

where U_1, V_2, H_1 are the specified values. Unit flow rates are applied at node i in a similar manner by defining the momentum equation residuals as:

$$f_{1i} = U_i H_i - q^*_{xi} \tag{4-28}$$

and

$$f_{2i} = V_i H_i - q^*_{yi} \tag{4-29}$$

where

q^*_{xi} and q^*_{yi} = specified unit flow rates in the x and y directions, respectively, at node i

Depth can also be applied as a natural boundary condition by using the specified value of the depth at node i, H_i, to evaluate the boundary integral terms in the momentum equation residual expression 4-1 and 4-2. Contributions from the boundary-integral terms are taken as zero when derivatives of the momentum equation residuals with respect to H_i are computed.

When water depth is specified as a natural boundary condition, global mass conservation is insured and total inflow will equal total outflow in steady-state simulations. However, water depths computed at nodes where the water-surface elevation is applied as a natural boundary condition may differ slightly from the specified values. When water depth is specified as an essential boundary condition, the computed

depth will equal the specified depth, but the total outflow may differ slightly from the total inflow in steady-state simulations because the mass conservation equations at node points along the boundary have been replaced.

If the total flow through a cross section that forms part of the open boundary of a finite element network is specified, a constant friction slope along the section is assumed and the total flow is divided among the node points on the basis of conveyance. Each side of the element consists of three nodes where nodes one and two are the corner nodes and node three is the center node. Conveyance through each element side is defined as:

$$K = A\sqrt{\frac{gR}{c_f}} \tag{4-30}$$

where

R = the hydraulic radius

A = the area of the element side below the water surface

Total conveyance for the cross section is computed as the sum of the conveyance of each element side that is contained in the section. Conveyance through each element side is distributed among the three nodes that forms the sides as follows:

$$K_1 = \frac{1}{6}K(1-\zeta) \tag{4-31}$$

$$K_2 = \frac{2}{3}K_2 \tag{4-32}$$

$$K_3 = \frac{1}{6}K(1+\zeta) \tag{4-33}$$

where

$$\zeta = \frac{5\Delta H}{12\overline{H}} \tag{4-34}$$

and

$$\Delta H = H_3 - H_1 \tag{4-35}$$

and

$$\overline{H} = \frac{(H_1 + H_3)}{2} \tag{4-36}$$

where

H_1 & H_3 = the depth at nodes 1 and 3, respectively

Total flow normal to the open boundary at each cross section node point is computed on the basis of the ratio of conveyance assigned to each node to the total conveyance computed for the cross section. The velocities and depth computed at each node are required to satisfy the condition that the net flow across the open boundary resulting from flow at the node will equal the assigned portion of the total cross section flow.

Solid Boundaries

Solid boundaries define features such as shorelines, jetties, or seawalls. For viscous fluids, the velocity at a solid boundary is actually zero. This is generally referred to as a no-slip boundary condition. To accurately model the flow near a no-slip boundary a network composed of relatively small elements is necessary. Imposing a slip condition where the velocity is non zero at a solid boundary reduces the total number of elements needed in the network and thus decreases the number of equations that need to be solved. Slip conditions are applied at a solid boundary node by first transforming the x and y momentum equations that are associated with that node into equations that express

conservation of momentum in directions that are tangent and normal to the boundary. The conservation of momentum equation from flow in the normal direction is then replaced by a constraint equation that requires the net flow across the solid boundary that results from flow at the node point to equal zero.

Total Flow Across a Boundary

Total flow across a boundary, or normal flow, at a node point comes from several sources. Flow across an open boundary is defined as:

$$Q_i^o \equiv Q_{si}^o + Q_{xi} \tag{4-37}$$

where

Q_{si}^o = the flow normal to the boundary at node i that is specified directly

Q_{xi} = the amount of the total flow through a cross section at node i

Along a boundary, either open or solid, where flow normal to the boundary is to be specified, the conservation of momentum residual expressions for flows I the x and y directions first are transformed into conservation of momentum residual expressions for flows in directions that are tangent and normal to the boundary. At node point i, the transformation is accomplished as follows:

$$f_{1i}' = f_{1i}\cos\delta + f_{2i}\sin\delta \tag{4-38}$$

$$f_{2i}' = -f_{1i}\sin\delta + f_{2i}\cos\delta \tag{4-39}$$

where

f_{1i}' and f_{2i}' = the transformed residual expressions in the tangential and normal directions

δ = the angle between the positive x direction and tangent to the boundary at node i

If the flow normal to an open boundary at node i is specified, the residual expression for flow tangent to the boundary is redefined as:

$$f_{1i} \equiv a_i^o U_i + b_i^s V_i - Q_i^o \tag{4-40}$$

If flow normal to a solid boundary at node I is specified, the conservation of momentum equation for flow normal to the boundary is redefined as:

$$f_{2i} \equiv a_i^s U_i + b_i^s V_i - Q_i^s \tag{4-41}$$

The coefficients a_i^o, b_i^o, a_i^s, and b_i^s in equations 4-40 and 4-41 are determined by requiring the computed flow across an open or solid boundary at node i to equal the specified flow, that is:

$$U_i \sum_e \int_{S_e^o} N_i H \mathrm{l}_x dS_e^o + V_i \sum_e \int_{S_e^o} N_i H \mathrm{l}_y dS_e^o = Q_i^o \tag{4-42}$$

and

$$U_i \sum_e \int_{S_e^o} N_i H \mathrm{l}_x dS_e^s + V_i \sum_e \int_{S_e^o} N_i H \mathrm{l}_y dS_e^s = Q_i^s \tag{4-43}$$

where

N_i = the interpolation function for velocity at node i

S_e^o = part of the network boundary that is open

S_e^s = the part of the network boundary that is solid

Comparing equation 4-40 to 4-42 and 4-41 to 4-43 provides:

$$a_e^o \equiv \sum_e \int_{S_e^o} N_i H \mathrm{l}_x dS_e^o \tag{4-44}$$

$$b_e^o \equiv \sum_e \int_{S_e^o} N_i H \mathrm{l}_y dS_e^o \tag{4-45}$$

$$a_e^s \equiv \sum_e \int_{S_e^s} N_i H \mathrm{l}_x dS_e^s \tag{4-46}$$

$$b_e^s \equiv \sum_e \int_{S_e^s} N_i H \mathrm{l}_y dS_e^s \tag{4-47}$$

Derivatives of the residual expression for total flow across an open boundary are defined as follows:

$$\frac{\partial f_{1i}}{\partial U_j} \equiv \begin{cases} a_i^o, \text{if } i = j \\ 0, \text{if } i \neq j \end{cases} \tag{4-48}$$

$$\frac{\partial f_{1i}}{\partial V_j} \equiv \begin{cases} b_i^o, \text{if } i = j \\ 0, \text{if } i \neq j \end{cases} \tag{4-49}$$

$$\frac{\partial f_{1i}}{\partial H_j} \equiv \frac{\partial a_i^o}{\partial H_j} U_i + \frac{\partial b_i^o}{\partial H_j} V_i \tag{4-50}$$

where

$$\frac{\partial a_i^o}{\partial H_j} \equiv \sum_e \int_{S_e^o} N_i M_j \mathrm{l}_x dS_e^o \tag{4-51}$$

and

$$\frac{\partial b_i^o}{\partial H_j} \equiv \sum_e \int_{S_e^o} N_i M_j 1_y dS_e^o \tag{4-52}$$

Derivatives of the residual expression for total flow across a solid boundary are defined as follows:

$$\frac{\partial f_{2i}}{\partial U_j} \equiv \begin{cases} a_i^s, \text{if } i = j \\ 0, \text{if } i \neq j \end{cases} \tag{4-53}$$

$$\frac{\partial f_{2i}}{\partial V_j} \equiv \begin{cases} b_i^s, \text{if } i = j \\ 0, \text{if } i \neq j \end{cases} \tag{4-54}$$

$$\frac{\partial f_{2i}}{\partial H_j} \equiv \frac{\partial a_i^s}{\partial H_j} U_i + \frac{\partial b_i^s}{\partial H_j} V_i - \frac{\partial Q_{wi}}{\partial H_j} - \frac{\partial Q_{ci}}{\partial H_j} \tag{4-55}$$

where

$$\frac{\partial a_i^s}{\partial H_j} \equiv \sum_e \int_{S_e^s} N_i M_j \ell_x dS_e^s \tag{4-56}$$

$$\frac{\partial b_i^s}{\partial H_j} \equiv \sum_e \int_{S_e^s} N_i M_j 1_y dS_e^s \tag{4-57}$$

$$\frac{\partial Q_{wi}}{\partial H_j} \equiv \frac{3}{2}\left(\frac{Q_{wi}}{z_e^h - z_c}\right) \tag{4-58}$$

and

$$\frac{\partial Q_{ci}}{\partial H_j} \equiv \frac{1}{2}\left(\frac{Q_{ci}}{z_s^h - z_s^t}\right) \tag{4-59}$$

CHAPTER 5

SCOUR EQUATIONS

General

Scour is the erosion of soil from a streambed due to flowing water. The erosive action of the flow excavates and transports the material downstream. Different materials will scour at different rates. In general, loose soils are rapidly eroded by flowing water, while cohesive or cemented soils are more resistant to scour. According to Richardson, Harrison, Richardson, and Davis (1993) under constant flow conditions, scour will reach maximum depth in sand and gravel bed materials in hours, cohesive bed materials in days, sandstone and shale in months, limestone in years, and dense granites in centuries.

Scour that occurs at bridge piers and abutments, known as local scour, is of particular concern. When the material that a bridge rests on scours away, the bridge becomes unstable and is unsafe for travel. In 1987, the I-90 bridge over Schoharie Creek near Amsterdam, New York collapsed killing 10 people. In response to the tragedy the Federal Highway Administration (FWHA) and the United States Geological Survey (USGS) initiated the National Bridge Scour Program (Muehller, 1997). The program is dedicated to the understanding of scour processes and prediction methods. From this program the FWHA along with many researchers, such as Laursen and Richardson, have developed methods for predicting scour at bridges.

Total Scour

There are three individual components that account for the total scour at a bridge. These are:

1. Aggradation and Degradation
2. Contraction Scour
3. Local Scour

In addition, the lateral migration of the stream must be assessed when evaluating total scour at piers and abutments of highway crossings.

Aggradation and Degradation

Aggradation and degradation refer to long-term streambed elevation changes due to natural or man-induced causes. Aggradation is the raising of the streambed due to deposition of materials from upstream. Degradation is the lowering of the streambed due to erosion.

Long-term bed elevation changes may be the natural trend of the stream or may be the result due to a modification of the stream or of the watershed. The streambed may be aggrading, degrading, or achieved a state of equilibrium. Long-term trends may change during the life of a bridge. The changes generally result from the modification of the stream or watershed. Some examples of factors that affect long-term bed elevation changes are: dams and reservoirs, urbanization, deforestation, channelization, diversion of water, changes in flow levels, movement of a meander, tidal ebb, floods, and earthquake/tectonic activity.

The long term elevation change of the streambed can be determined by a simple mass balance equation. The inflow of material minus the outflow of material is equal to the rate of change for the particular reach in question. If the change is negative, erosion or degradation is occurring in the channel section. If the change is positive then sedimentation or aggradation is occurring.

The problem for the engineer is to estimate the long-term bed elevation changes that will occur during the life of the structure. The Corps of Engineers as well as other agencies have data for the long-term variations of various streams. If the required data is not available an assessment of long-term streambed elevations can be made using the principles of river mechanics. A quantitative measurement of the change in stream bed elevation may be calculated by using the methods outlined in the FHWA publication *HEC-20 Stream Stability at Highway Structures*.

Contraction Scour

Contraction scour occurs when the flow area of a stream is reduced. The reduction in cross-sectional area can be naturally occurring or by a man-made structure such as a bridge. At a bridge crossing, many factors can contribute to the occurrence of contraction scour. These factors may include: the main channel naturally contracting as it approaches the bridge opening; the road embankments at the approach to the bridge cause all or a portion of the overbank flow to be forced into the main channel; the bridge piers are blocking a significant portion of the flow area; and a drop in the downstream tail water elevation which causes increased velocities inside the bridge.

There are two forms of contraction scour that can occur depending on how much bed material is being transported by the flow upstream of the bridge contraction reach. The two types of contraction scour are referred to as live-bed contraction scour and clear-water contraction scour. Live-bed contraction scour occurs when bed material is already being transported into the contracted bridge section from upstream of the approach section (before the contraction reach). Clear-water contraction scour occurs when the bed material sediment transport in the uncontracted approach section is negligible or less than the carrying capacity of the flow.

Contraction scour equations are based on the principle of conservation of sediment transport. For scour analysis it is necessary to determine the maximum scour of a site. The maximum live-bed scour occurs when the shear stress reduces to the point that the sediment transport into the constricted section equals the sediment transported out of the constricted section, resulting in a net change in sediment of zero. During clear-water scour, the maximum scour occurs when the shear stress reduces to the critical shear stress of the material.

Contraction Scour Conditions

Four cases of contraction scour are commonly encountered as noted by Tyagi (1998):

Case 1

The overbank flow on a floodplain is being forced back to the main channel by the approaches to the bridge. Case 1 conditions include:

a. The river channel width becomes narrower either due to the bridge abutments projecting into the channel or the bridge being located at a narrowing reach of the river.
b. No contraction of the main channel, but the overbank flow area is completely obstructed by the road embankments.
c. Abutments are set back away from the main channel.

Case 2

Flow is confined to the main channel (i.e. there is no overbank flow). The normal river channel width becomes narrower due to the bridge itself or the bridge site is located at a narrowing reach of the river.

Case 3

A relief bridge in the overbank area with little or no bed material transport in the overbank area (i.e. clear-water scour).

Case 4

A relief bridge over a secondary stream in the overbank area with bed material transport (similar to case one).

Determination of Live-Bed or Clear-Water Scour

To determine if the flow upstream is transporting bed material, the critical velocity of the bed materials found upstream of the site should calculated. The critical

velocity determines the beginning of motion for a specific material base on grain size. If the critical velocity of the bed material is greater than the mean velocity at the approach section($V_c < V$), then clear water contraction scour is occurring. If the critical velocity of the bed material is less than the mean velocity at the approach section ($V_c > V$), then live-bed scour is occurring. To calculate the critical velocity the following equation developed by Laursen is used:

$$V_c = 10.95 y_1^{\frac{1}{6}} D_{50}^{\frac{1}{3}} \tag{5-1}$$

where

V_c = Critical velocity above which material of size D_{50} and smaller will be transported (ft/s)

y_1 = Average depth of flow in the main channel or overbank area at the approach section (ft)

D_{50} = median diameter of bed material (ft)

Live-Bed Contraction Scour

Richardson et al. (1993) recommends using the following version of Laursen's (1960) equation for computing live-bed contraction scour:

$$y_2 = y_1 \left(\frac{Q_2}{Q_1} \right)^{\frac{6}{7}} \left(\frac{W_1}{W_2} \right)^{K_1} \left(\frac{n_2}{n_1} \right)^{K_2} \tag{5-2}$$

and

$$y_s = y_2 - y_1$$

where

y_1 = average depth in the upstream main channel (ft)

y_2 = average depth in contracted section (ft)

y_s = average scour depth (ft)

W_1 = bottom width of upstream main channel (ft)

W_2 = bottom width of main channel in the contracted section (ft)

Q_1 = flow in the upstream channel transporting sediment (cfs)

Q_2 = flow in the contracted channel (cfs)

n_1 = Manning's n for the upstream main channel

n_2 = Manning's n for the contracted section

k_1 & k_2 = exponents determined from Table 1 that depend on the mode of bed material transport

Table 1 Values for Exponents k_1 & k_2

V_o/w	k_1	k_2	Mode of Bed Material Transport
< 0.50	0.59	0.066	Mostly contact bed material
0.50 to 2.0	0.64	0.21	Some suspended bed material
> 2.0	0.69	0.37	Mostly suspended bed material discharge

From Table 1:

$V_o = (gy_1S_1)^{1/2}$ shear velocity in the upstream section (ft/s)

W = median fall velocity of the bed material based on the D_{50} (see Figure 4)

g = acceleration of gravity

S_1 = slope of energy grade line of main channel (ft/ft)

D_{50} = median diameter of bed material (ft)

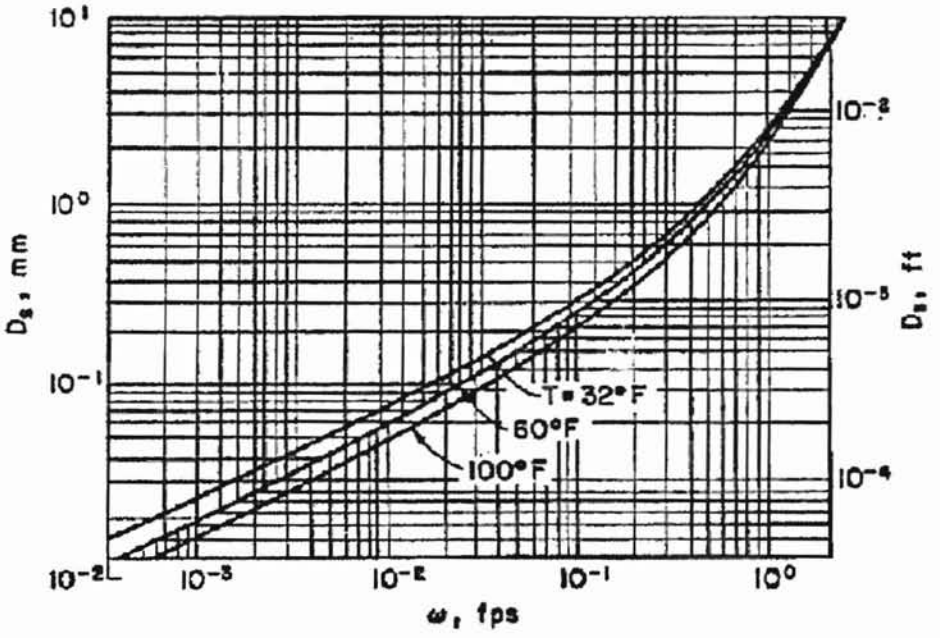

Figure 4. Fall Velocity of Sand Particles (Source: Richardson et al., 1993, p. 34)

Clear-Water Contraction Scour

Richardson et al. (1993) also recommends using an equation developed by Laursen (1960) to calculate clear-water contraction scour. The equation is based on the

assumption that the shear stress in the contracted section must equal the critical shear stress, or:

$$\tau_2 = \tau \tag{5-3}$$

where

τ_2 = average bed shear stress, contracted section

τ_c = critical bed shear stress at incipient motion

The bed shear can be expressed as:

$$\tau_2 = \gamma y_2 S_f = \frac{\gamma V^2 n^2}{(1.49)^2 y_2^{\frac{1}{3}}} \tag{5-4}$$

where

γ = the unit weight of water (62.4 lb/ft^3)

y_2 = average depth in the contracted section (ft)

S_f = slope of the energy grade line (ft/ft)

V_2 = average velocity in the contracted section (ft/s)

The use of Strickler's approximation for Manning's n, using the previous relationships, and in terms of discharge (using continuity), Laursen's (1960) equation for clear-water scour is determined as:

$$\frac{y_2}{y_1} = \left(\frac{W_1}{W_2}\right)^{\frac{6}{7}} \left(\frac{V_1^2}{120 y_1^{\frac{1}{3}} D_{50}^{\frac{2}{3}}}\right)^{\frac{3}{7}} \tag{5-5}$$

where

V_1 = average velocity in the upstream main channel (ft/s)

Froehlich (1996) presents equation 5-5 in terms of SI units and two-dimensional flow as:

$$d_{sc} = \left(\frac{\rho g n^2 q^2}{\tau_c}\right)^{\frac{3}{7}} - H \tag{5-6}$$

where

d_{sc} = clear-water contraction socur depth

ρ = density of water

H = water depth

and

$$q = H\sqrt{U^2 - V^2} \tag{5-7}$$

where

q = unit flow rate

U and V = the depth-averaged velocities in the x and y directions

Local Scour

Pier scour occurs due to the local acceleration of flow due to an obstruction. The acceleration of flow is due to the pileup of water on the upstream surface of the obstruction. The acceleration generates vortices, commonly referred to as a horseshoe vortex. The action of the horseshoe vortex removes bed material from around the base of the obstruction. As with contraction scour, local scour can occur in live-bed or clear-water situations.

Pier Scour

A bridge pier located in the flow-line of a stream will cause a system of vortices that are responsible for the occurrence of local scour. For a typical cylindrical pier design the vortex system will be comprised of the horseshoe vortex and wake vortex. The vortex systems are shown in Figure 5, Horseshoe and Wake Vortices around a Cylindrical Element.

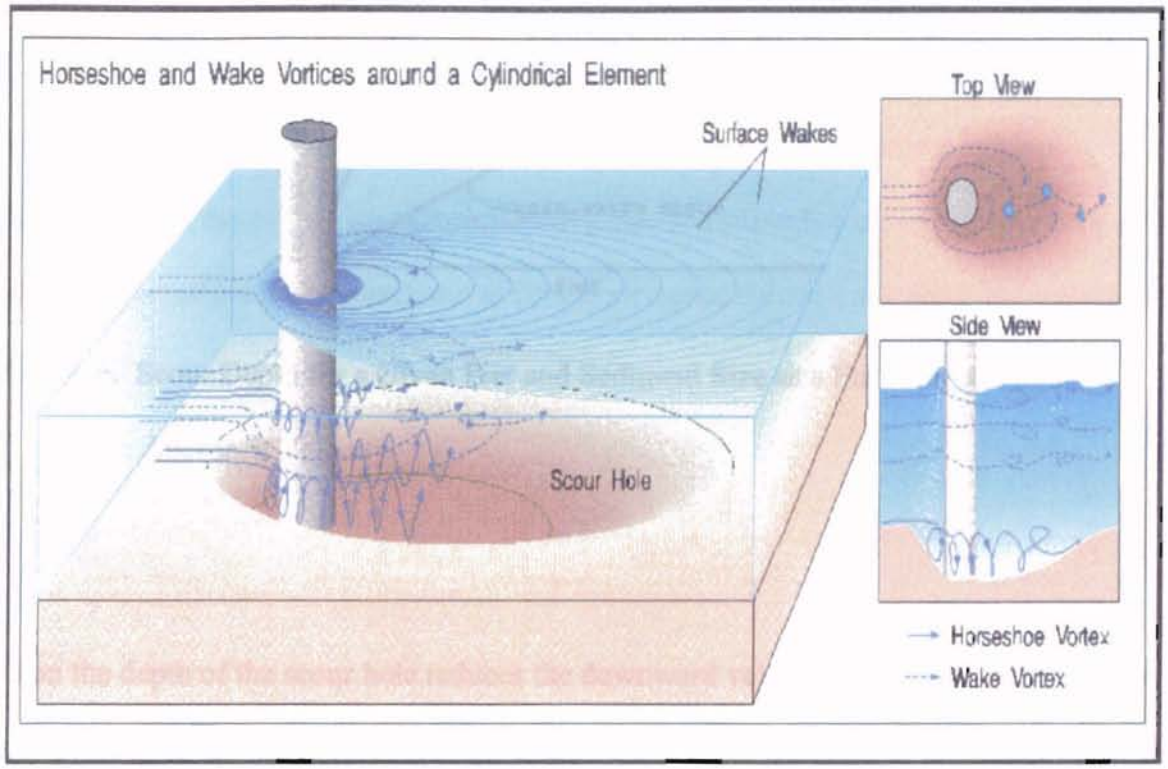

Figure 5. (Provided by The Missouri Department of Transportation, 1998)

When a pier is placed in the flow line the velocity distribution in the streamflow is interrupted. The varying velocities create a pressure field that creates a downward velocity along the lower leading face of the pier and produces a three-dimensional separation of the boundary layer leading to the formation of the horseshoe vortex. Once this process begins the downward flow reaches critical velocity, eroding the bed, and the horseshoe vortex that is produced then carries it away.

Figure 6, Scour Depth for a Given Pier and Sediment Size as a Function of Time and Approach Velocity, describes the effect of pier scour as a function of time and approach velocity for a given pier and sediment size. Maximum live bed scour is reached

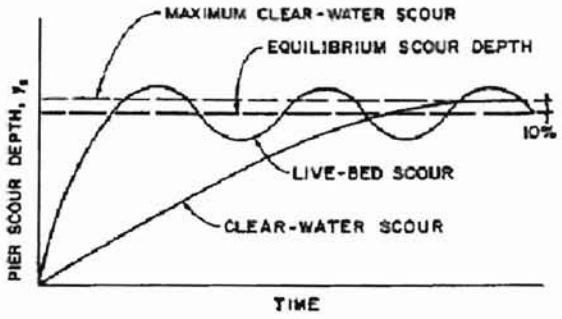

Figure 6. Scour Depth for a Given Pier and Sediment Size as a Function of Time and Approach Velocity.

when the depth of the scour hole reduces the downward velocity to the point that the flow is depositing as much as it is scouring. In the case of clear water scour maximum scour is reached when the depth of the scour increases to the point that downflow can no longer reach the critical velocity to increase the scour depth and equilibrium is reached.

There are several factors that affect the depth of local scour at a pier as noted by Tyagi (1998). These are:

1. Velocity of the flow just upstream of the pier
2. Depth of flow
3. Width of the pier
4. Length of the pier if skewed to the flow
5. Size and gradation of bed material
6. Angle of attack of approach flow
7. Shape of the pier
8. Bed configuration

9. Ice jams and debris

Several researchers have developed equations to incorporate each situation and form a universal equation to predict bridge scour. Most of the equations that researchers produced were developed based on laboratory data and provide varying results given a particular set of data. Richardson et al (1993) recommends the Colorado State University Equation:

$$\frac{y_s}{q} = 2.0K_1K_2K_3\left(\frac{y_1}{a}\right)^{0.35} Fr_1^{0.43} \qquad (5\text{-}8)$$

where

y_s = scour depth (ft)

K_1 = correction factor for pier nose shape

K_2 = correction factor for the angle of attack of the flow

K_3 = correction factor for bed condition

y_1 = flow depth directly upstream of the pier (ft)

a = pier width (ft)

Fr_1 = Froude number upstream of the pier

q = Unit flow rate

For round nose piers aligned with the flow, the maximum scour depth is limited as follows:

$y_s \leq 2.4$ times the pier width (a) for $Fr_1 \leq 0.8$

$y_s \leq 3.0$ times the pier width (a) for $Fr_1 > 0.8$

The correction factor for pier nose shape, K_1, is given in Table 2 below:

Table 2. Correction Factors, K_1, for Pier Nose Shape (Richardson et al, 1993)

Shape of Pier Nose	K_1
(a) Square nose	1.1
(b) Round nose	1.0
(c) Circular cylinder	1.0
(d) Group of cylinders	1.0
(e) Sharp nose (triangular)	0.9

The correction factor for angle of attack of the flow, K_2, is calculated by the following equation:

$$K_2 = \left(\cos\theta + \frac{L}{a} \sin\theta \right)^{0.65} \tag{5-9}$$

where

L = length of the pier along the flow line (ft)

θ = angle of attack of the flow, with respect to the pier

The correction factor for bed condition, K_3, is shown in Table 3, Increase in Equilibrium Pier Depth, K_3, for Bed Condition.

Table 3. Increase in Equilibrium Pier Depth, K_3, for Bed Condition (Richardson et al 1993)

Bed Condition	Dune Height H (ft)	K_3
Clear-Water Scour	N/A	1.1
Plane Bed and Antidune Flow	N/A	1.1
Small Dunes	$10 > H > 2$	1.1
Medium Dunes	$30 > H > 10$	1.1 to 1.2
Large Dunes	$H > 30$	1.3

CHAPTER 6

METHODOLOGY AND APPLICATION

Modeling Systems Operations

Froehlich (1996) recommends the following five steps to perform any hydraulic application.

1. Data Collection
2. Network Design
3. Model Calibration
4. Model Validation
5. Model Application

These five steps were performed while using the SMS modeling software to provide an analysis of the I-35 crossing of the Cimarron River.

After a surface water flow problem has been defined, the first step to develop an adequate hydraulic model is to gather the adequate topographic and hydraulic data. Topographic data describes the geometry of the physical system and allows an evaluation of surface roughness to be used in estimating bed friction coefficients. Hydraulic data include measurements of stage, flow, velocity, high-water marks left by floods, rating curves, and limits of flooding.

The next step when developing a hydraulic model is to design a finite element network. Design of a finite element network requires the definition of the number, size, shape, and configuration of elements. As long as the elements obey the basic requirements necessary for a convergent solution, the accuracy of the solution will improve with decreasing element size. However, increasing the number of elements by making them smaller adds to the computation expense of the model. The network design should provide a representation of the area being modeled that provides an adequate approximation of the true solution of the governing equations, while performing the analysis at a minimal cost.

The SMS computer solves complex surface water flow problems by providing a numerical approximation of the solution. The numerical approximation is described by the physics of surface water flow, from a series of equations, in which several empirical coefficients appear. When adequate data are available, the dimensions of the simplified geometric elements and empirical hydraulic coefficients need to be adjusted to provide a solution that corresponds to measured values. This process is referred to as model calibration.

Model testing is an important, but not always possible step in the analysis of a surface water flow problem. Model testing is accomplished by applying a calibrated model to other flow situations from which measured data are available.

Model application is the simulation of a variety of flow conditions. Model application is performed once the first four steps have been completed. A model still needs to be applied with caution, especially if it is used to evaluate condition far outside the range of calibration and validation. However, if a model has been calibrated and

validated properly, it can be used to provide valuable insights to various surface water flow situations over all flow regimes.

Site Overview

As mentioned previously, the site under investigation is the I-35 crossing of the Cimarron River (Appendix A). There are two separate flow conditions at the site that are of interest to this investigation, the original crossing and the existing crossing. The original crossing (in use until 1988) consisted of two main bridges and a series of eight overflow structures each of which were placed in a parallel installation. The existing crossing consists of two main bridges and two overflow bridges also in a parallel.

The original crossing utilized 803 foot main structures at the south side of the floodplain with overflow with parallel overflow structures each of which were 280 feet, 200 feet, 282 feet, and 162 feet in length, respectively. The overflow structures were placed at increments of 900 feet, 450 feet, 400 feet, and 650 feet apart, respectively. The plan view of this site is located in Figure 7, Plan View for Original Crossing. This configuration discouraged concentration of flow during large flood events on the north side of the crossing.

In 1988, the crossing was replaced due to a large flood in 1986 that damaged the original crossing. The current crossing consists of two 800 foot main structures located on the south side of the floodplain and two 1,360 foot overflow structures that extend north into the floodplain. The plan view of this site is located in Figure 8, Plan View for Existing Crossing. The redesign of the structure was made in an effort to lower the velocity of the water through the structures (Strongylis, 1988).

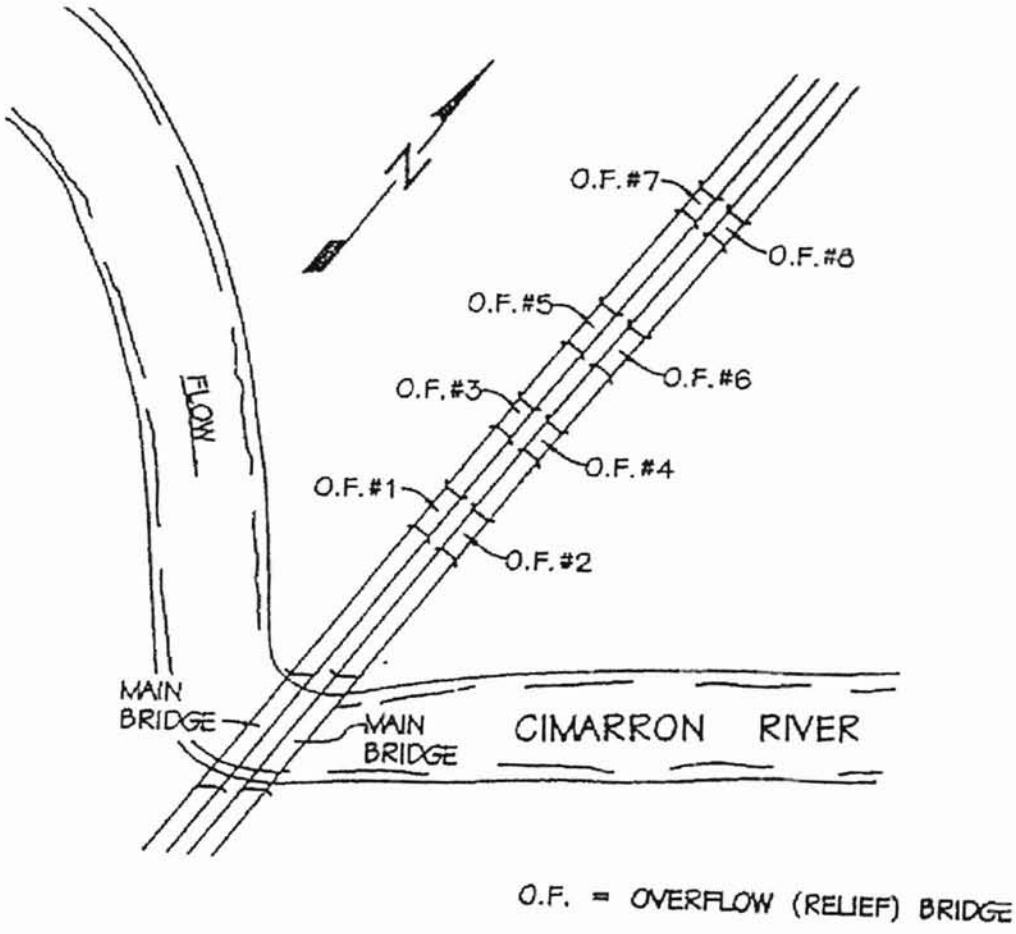

Figure 7. Plan View for Original Crossing

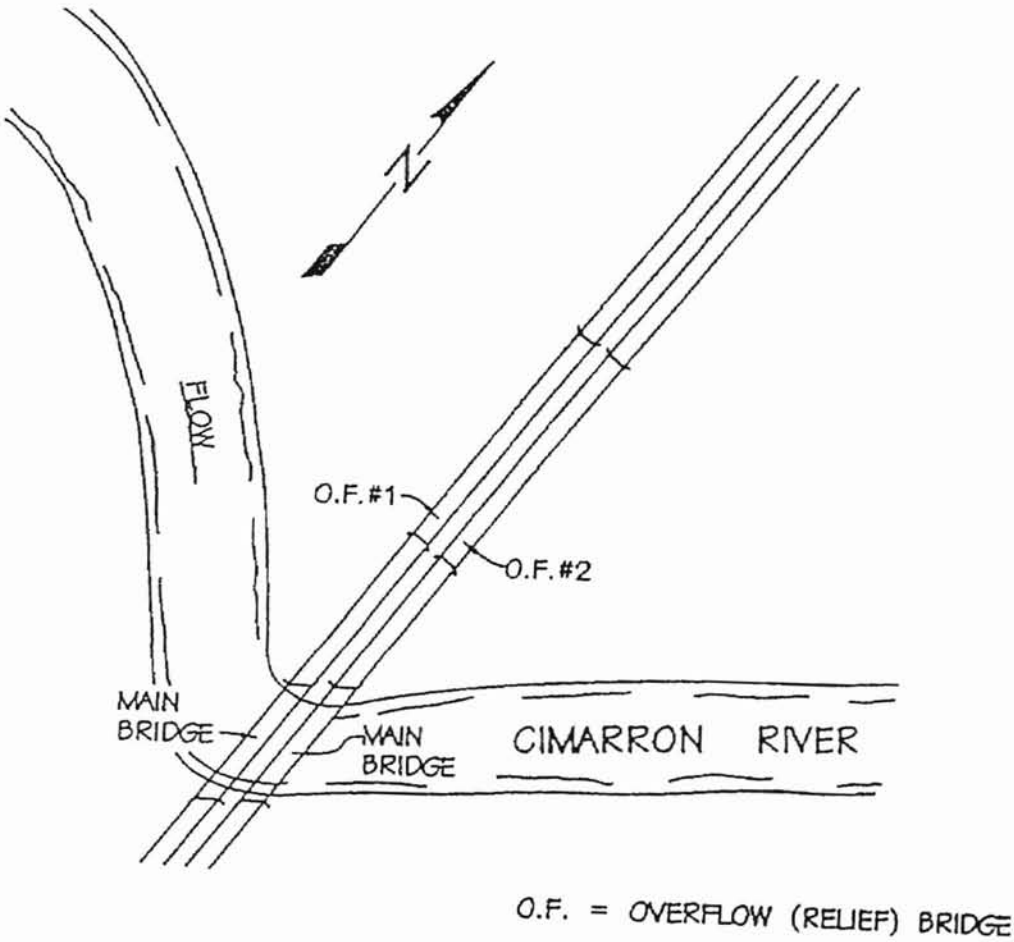

Figure 8. Plan View for Existing Crossing.

According to Strongylis (1988), comparison of aerial photos of the site taken in 1937, 1939, 1957, and 1990 reveals that the Cimarron River exhibited a fair degree of meandering. Meandering of a river is a phenomena that is prevalent in many stream systems yet not fully understood. According to Yalin (1992) a stream may be considered to be a meandering stream when the deformation of a stream exhibits a traceable periodicity along the general flow direction and this deformation is induced by the stream itself: it should not be "forced" upon the stream by its environment.

Currently, and prior to 1988, the main channel crossed under the main bridge on the south side of the floodplain. Immediately before crossing under the main bridge the channel formed a sharp bend from running perpendicular to the axis of the floodplain to crossing underneath the main bridge parallel to the axis of the flood plain. This occured because over the years the meander curves of the river moved downstream to the immediate vicinity of the bridge.

Hydraulic Data

The Hydraulics Branch of the O.D.O.T Bridge Division calculated the discharge information for the site while designing the current structures in 1987. The calculations used existing gage data and a statistical analysis using a Log Pearson Type III distribution. The results of this analysis are included in Appendix B and below.

$Q_5 = 63{,}805$ cfs

$Q_{10} = 88{,}650$ cfs

$Q_{25} = 125{,}040$ cfs

$Q_{50} = 154{,}600$ cfs

Q_{100} = 185,800 cfs

Q_{500} = 264,600 cfs

Soil Data

The soil data for the site were taken from the *Soil Survey of Payne County Oklahoma* (1989) completed by the Soil Conservation Service of the United States Department of Agriculture. The portions of the survey that applied to the site are listed in Appendix C. Additional information was taken from construction plans of the respective bridges.

Analysis of the soil data concluded that the soils present in the floodplain in the area of the previous and existing overflow structures, belong to the Yahola and Hawley groups. The Yahola group ranges in texture from a fine sandy loam near the surface to a stratified loam to loamy fine sand at a depth of approximately five feet. The Hawley group ranges in texture from a fine sand loam near the surface to a stratified loamy fine sand to silty clay loam at a depth of approximately five feet. The Cimarron River at the crossing consists of coarse sand in its bed (United States Geological Survey, 1989).

From the construction plans, it was determined that an underlying rock formation exists referred to as "Red-Bed". The "Red-Bed" denotes a layer of shale that exists at elevations ranging from 854.0 feet to 856.9 feet in the vicinity of the structures. The shale layer is the underlying material for the entire site under analysis.

Recorded Scour Data

The October 1986 flood caused a significant amount of damage to the structures, requiring replacement. The data collected by O.D.O.T. concluded that the flow rate of the flood was 156,000 cubic feet per second, which correlates to a 52-year flood event (Q_{52}). It was also concluded that the flood produced a water surface elevation of 898.0 feet approximately 5000 feet downstream from the main structures.

Tyagi (1988) presented a summary and analysis of the scour holes from the flood located at the eight overflow bridges. A summary of the maximum scour and location is presented in Table 4 Maximum Scour Depths Near Overflow Structures at the I-35 Bridge on the Cimarron River.

Table 4

Maximum Scour Depths Near Overflow Structures at the I-35 Bridge on the Cimarron River [Source: Tyagi, 1988, p. 4]

Overflow Structure	Maximum Scour Depth Location	Scour (feet)
1	Upstream	10.2
2	Downstream	27.0
3	Upstream	22.7
4	Downstream	12.2
5	Upstream	15.4
6	Downstream	11.4
7	Upstream	30.0
8	Downstream	10.7

The data contained in Tyagi's (1988) study were collected some time after the flood had receded using an Electronic Distance Meter and a small boat. The analysis revealed that the maximum scour depth recorded ranged from 10 to 30 feet. A trend can be seen from the data that suggests that most of the deep scour holes tend to be located on the upstream side of the structures where velocities would be expected to be the highest.

Modeling Strategy

Strongylis (1988) demonstrated that due to the complex nature of the flow, found at the I-35 crossing of the Cimarron River, that two-dimensional flow analysis is appropriate. Additionally, given the incorporation of scour calculation capabilities into two dimensional modeling software, the same software used for hydraulic analysis, may also be used for a scour analysis of the site. The hydraulic analysis for each of the sites was completed and the results from each of the studies were used to complete the scour analysis for the separate site conditions, respectively. The resources used to perform the hydraulic and scour analysis were:

a. The Surface Water Modeling System (SMS) Version 6.0, developed by Brigham Young University and provided by BOSS International was used for processing the data for this analysis.
b. The Finite Element Surface Water Modeling System: Two Dimensional Flow in a Horizontal Plane (FESWMS-2DH), developed by the United States Department of Transportation, was used to complete the hydraulic analysis

c. The procedure for conducting the scour analysis was obtained from the United States Department of Transportation Federal Highway administration's publication *HEC-18, Evaluating Scour at Bridges, Second Addition* (1993).

Hydraulic Modeling

The modeling of this site was performed using the following equipment and sources of information:

a. A 3 ½ foot x 3 ½ foot aerial photo (scale 1:200) of the site taken from an altitude of 2900 feet on 6-13-90.
b. Aerial photos (scale 1:200) of the site taken on 11-11-86 showing the scour damage to the overflow bridges.
c. A contour map of the site made by G.F.M. & Assosciates.
d. O.D.O.T site study files and photographs.
e. The S.C.S. Soil Survey *Soil Survey of Payne County Oklahoma.*
f. Tyagi's 1988 Report No. 88-1 *Scour Around Bridge Piers of Overflow Structures at I-35 Bridged on the Cimarron River.*
g. Strongylis' 1988 report "*Water Surface Profiles Using FESWMS-2DH Model.*"
h. Buechter's 1997 report "*Scour Analysis of the Interstate-35 and Cimarron River Crossing Using the FESWMS-2DH and SMS Computer Models.*"

The information from a, b, c, d, g, and h, provided the information for the design of the finite element networks used for the existing and previous site conditions. Items a, b, g, and g were used to determine the roughness coefficients for the element network. Information from items c and d were used for determining elevations to accurately create a contour map. The resulting element networks for the conditions prior to the 1988 redesign of the structures are included in Figure 9, Site Element Network for Original Conditions. The resulting element networks for the existing conditions are included in Figure 10, Site Element Network for Existing Conditions.

Buechter (1997) provides a summary of steps taken to generate the finite element network used for the previous structures at the site. Buechter's (1997) data was further developed by adding the pier locations in the main channel to allow for the computation of scour in the main channel for the previous site conditions. The data for the pier locations were obtained from the bridge construction plans completed by O.D.O.T. in 1959.

The generation of the finite element network for the current site conditions was based on work by Strongylis (1988). Due to loss of data over time, it was necessary to reconstruct the finite element mesh using previously collected data. The addition of pier locations in the main channel and overflow channel were added to allow for the computation of scour for the respective locations. The data for the pier locations were obtained from the bridge construction plans completed by O.D.O.T in 1987.

Due to the loss of data, several finite element networks were created for the existing structures. By progressively refining the data, various results were found and analyzed. Element shapes were varied slightly to analyze the results in hydraulically

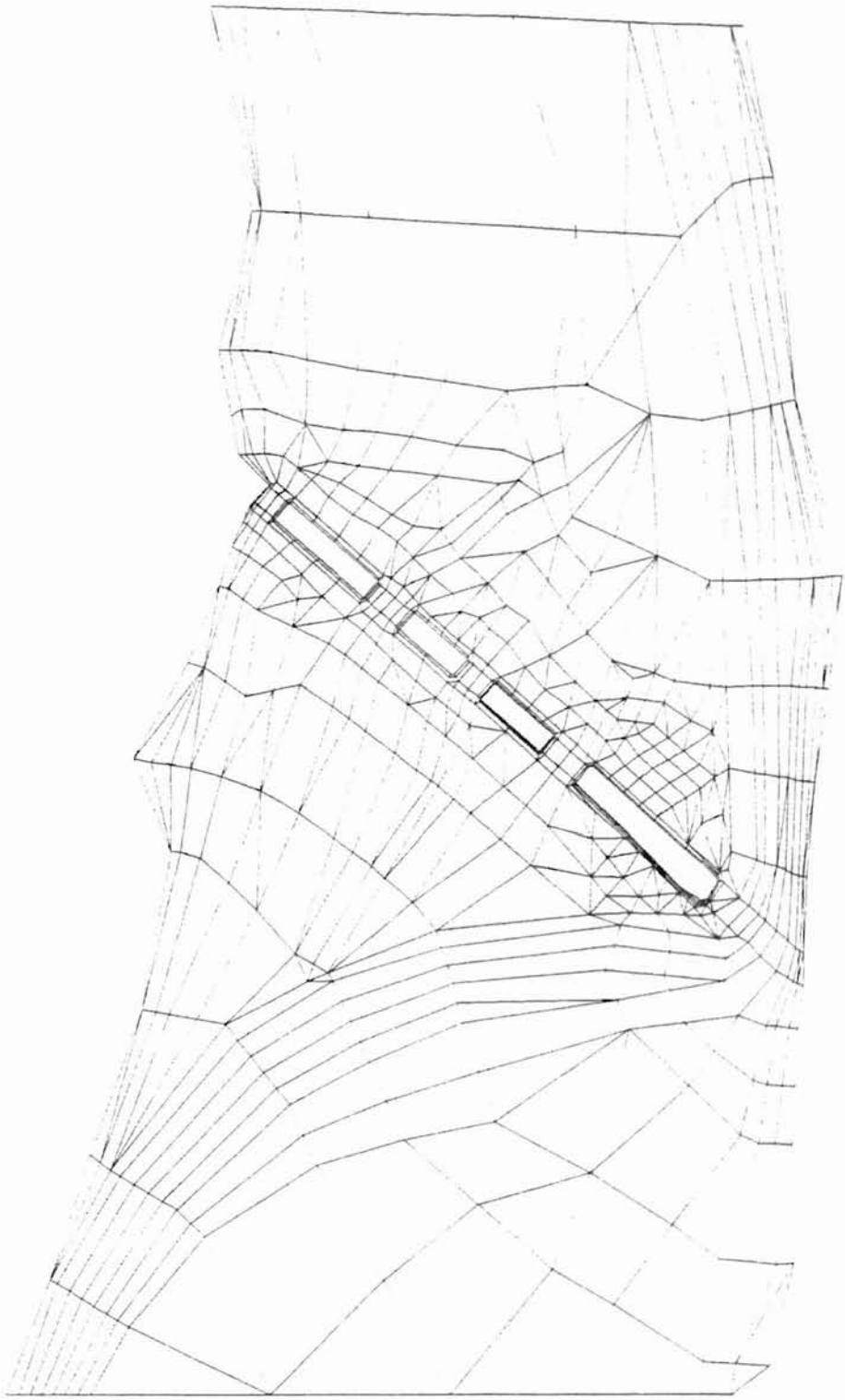

Figure 9. Site Element Network for Original Conditions

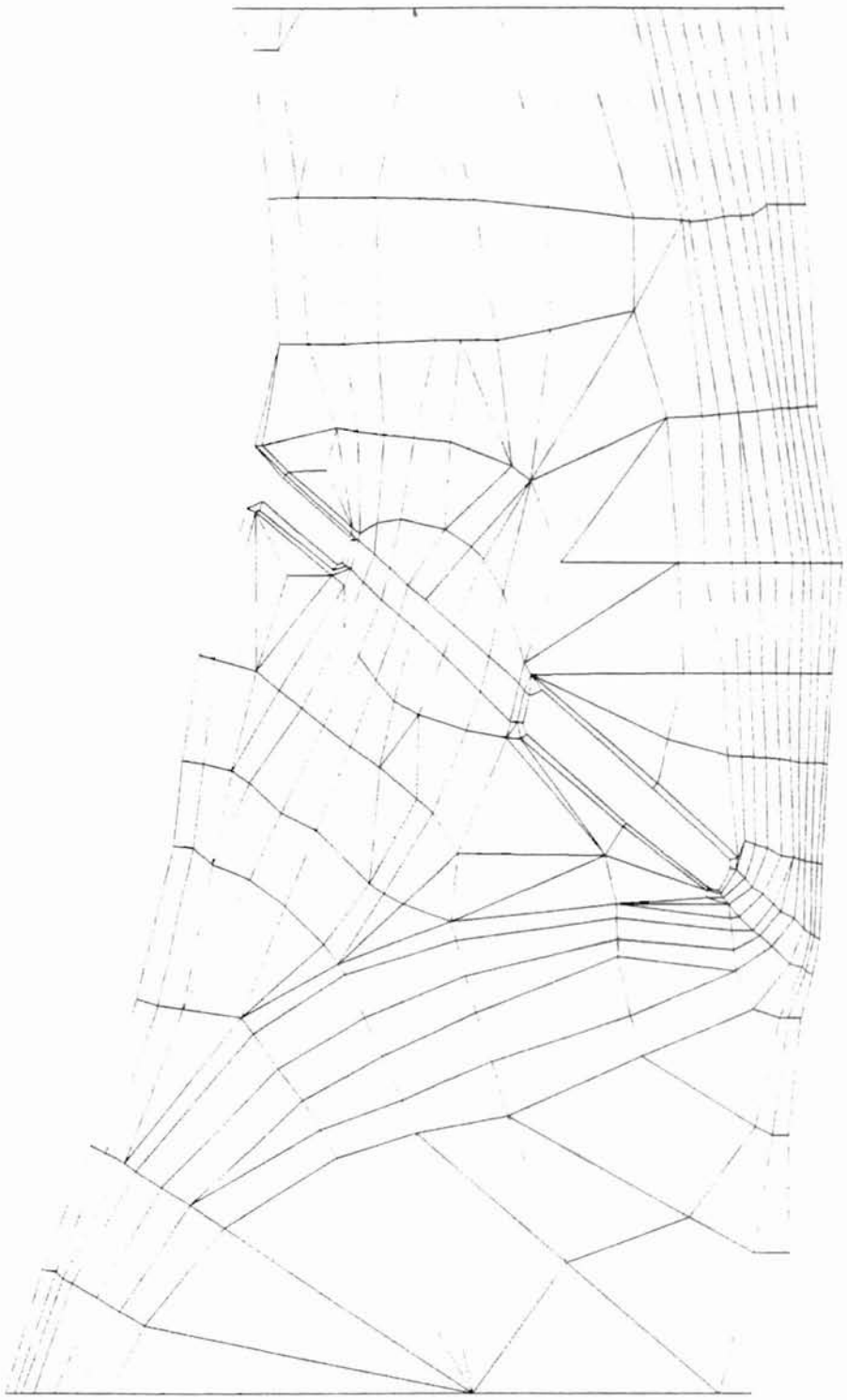

Figure 10. Site Element Network for Existing Conditions

sensitive areas near the bridge structures. Manning's n values were chosen according to standard engineering practice and text. The n values were varied and determined to have a small effect on the output, therefore the original values were used. After several complex variations of data, satisfactory results were obtained and the model was calibrated.

Once an accurate model has been developed and calibrated it can be used to model specific flood events. The model was used to calculate the water surface elevations and velocities for the Q_{10}, Q_{25}, Q_{50}, Q_{100}, and Q_{500} events. The water surface elevations for the existing and previous site conditions are shown in Figures 11-20. The water velocity distributions were also computed and are shown in Figures 21-30.

Scour Modeling

The FESWMS-2DH module in the SMS software package allows the computation of scour once the hydraulic analysis is complete. Clear-water contraction scour is computed by the methods listed in Chapter 5 . Pier scour is calculated by using the Colorado State University equation as noted in Chapter 5.

When modeling both the existing and previous structures the assumption of clear water scour conditions was made. Buechter (1997) provides evidence that this is a valid assumption because:

1. There is vegetation growing on the floodplain.
2. The velocities are large enough that the fine bed material would probably go into suspension at the bridge and not influence the contraction scour.

Computation of the contraction scour was made according to the recommendation in HEC-18. The contraction scour was calculated by choosing the proper n value and the correct shear value. The shear value was chosen based on the D_{50} value of the bed material.

The pier data was entered for scour modeling and to provide a more accurate hydraulic model. The previous crossing that was damaged in the 1986 flood utilized a different pier design than the existing structure. The previous design relied on piles anchored to the pier and driven into the "red bed." According to the methods outlined in HEC-18 the five piles in the pile bent were entered as one pier. After the 1986 flood, design modifications were made to the structural stability of the crossing to prevent the bridge from being damaged in the future. The new design specified that the piers would extend into the "red bed" no less than ten feet. This design eliminated the use of piles to anchor the structure to the underlying bed-rock. The piers were modeled using their corresponding diameters as recommended by HEC-18. The results of the scour model for the previous and existing crossing are located in Appendix D.

Figure 11. Water Surface Elevations for Q_{10} Original Crossing

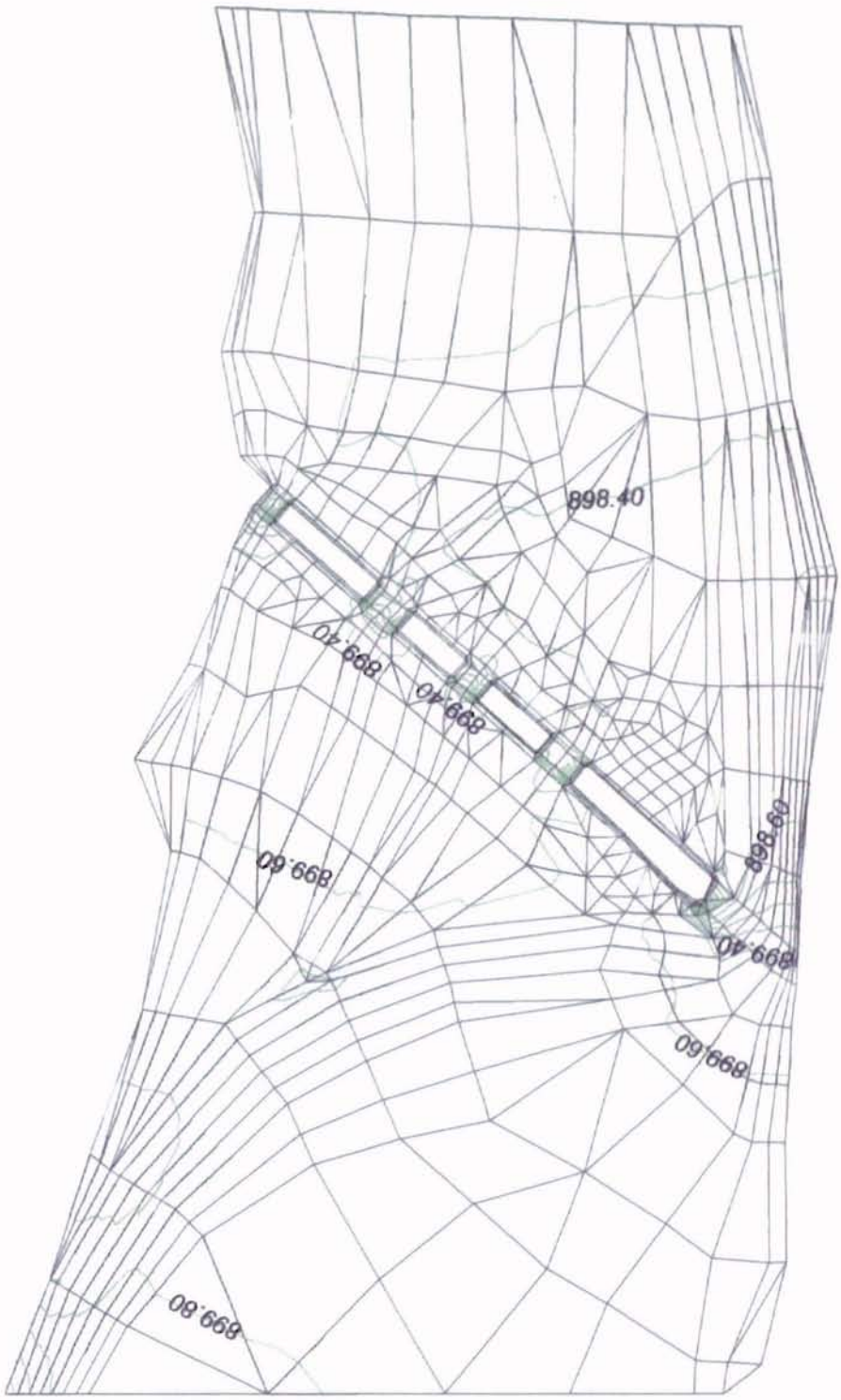

Figure 12. Water Surface Elevations for Q_{25} Original Crossing

Figure 13. Water Surface Elevations for Q_{50} Original Crossing

Figure 14. Water Surface Elevations for Q_{100} Original Crossing

Figure 15. Water Surface Elevations for Q_{500} Original Crossing

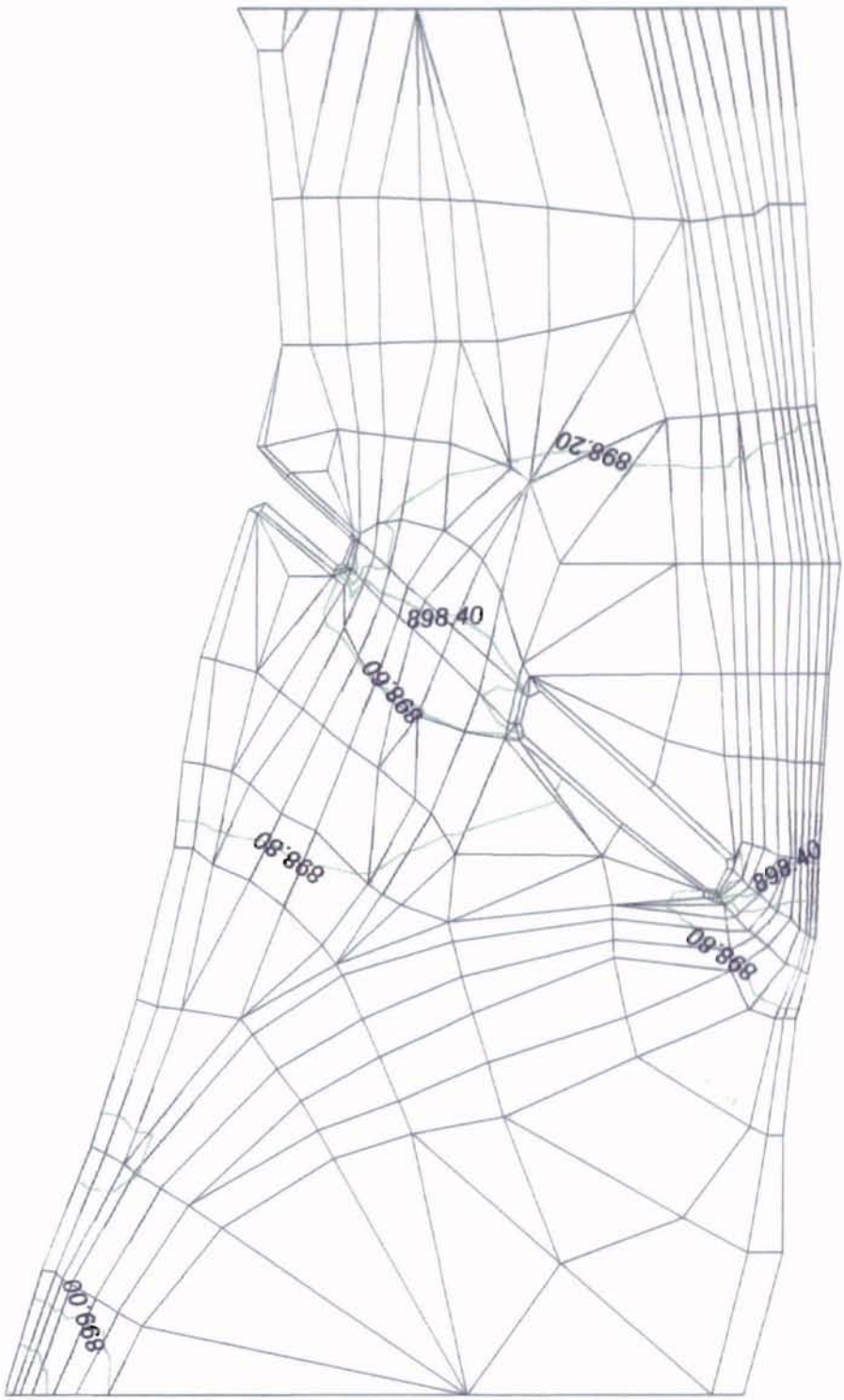

Figure 16. Water Surface Elevations for Q_{10} Existing Crossing

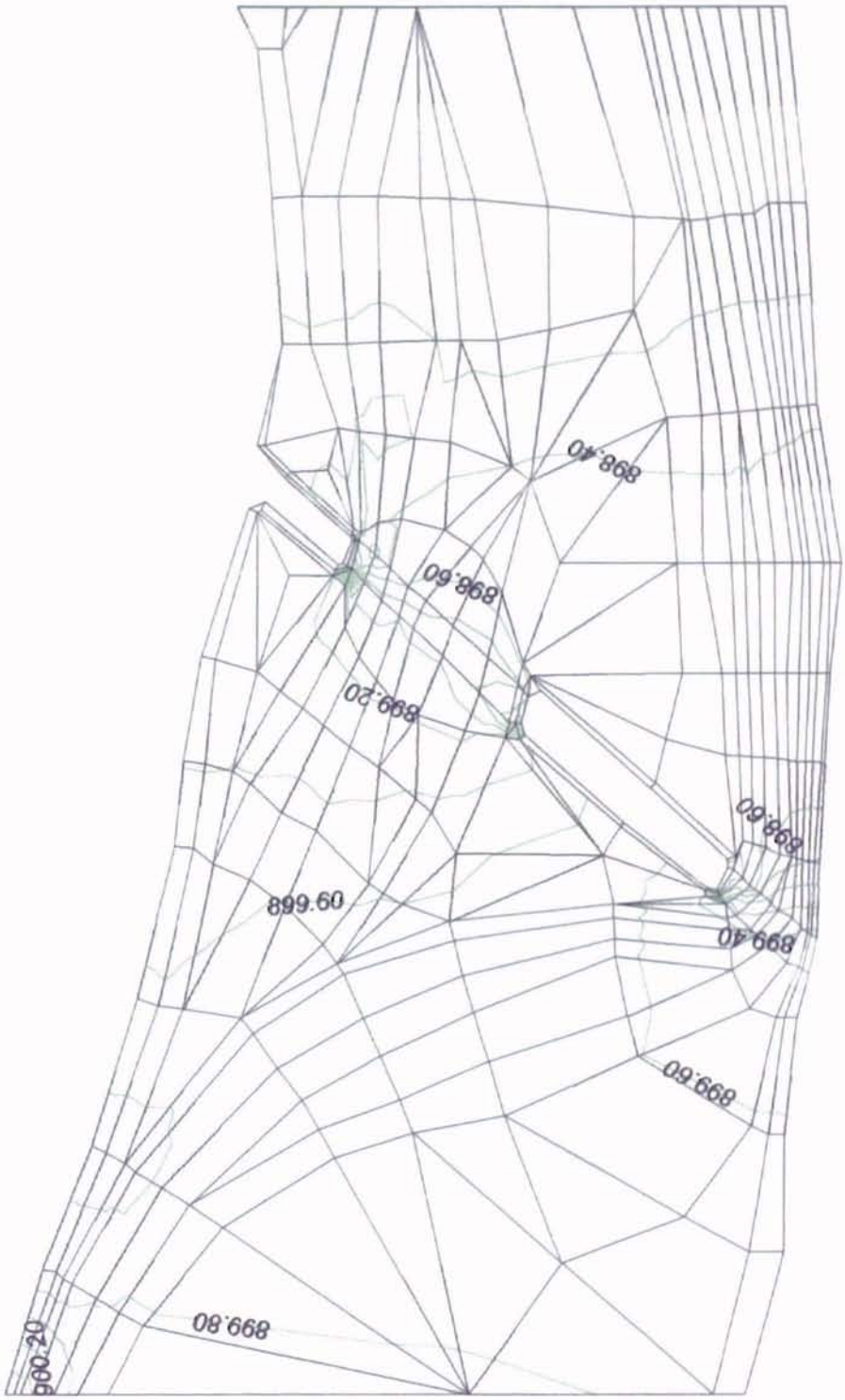

Figure 17. Water Surface Elevations for Q_{25} Existing Crossing

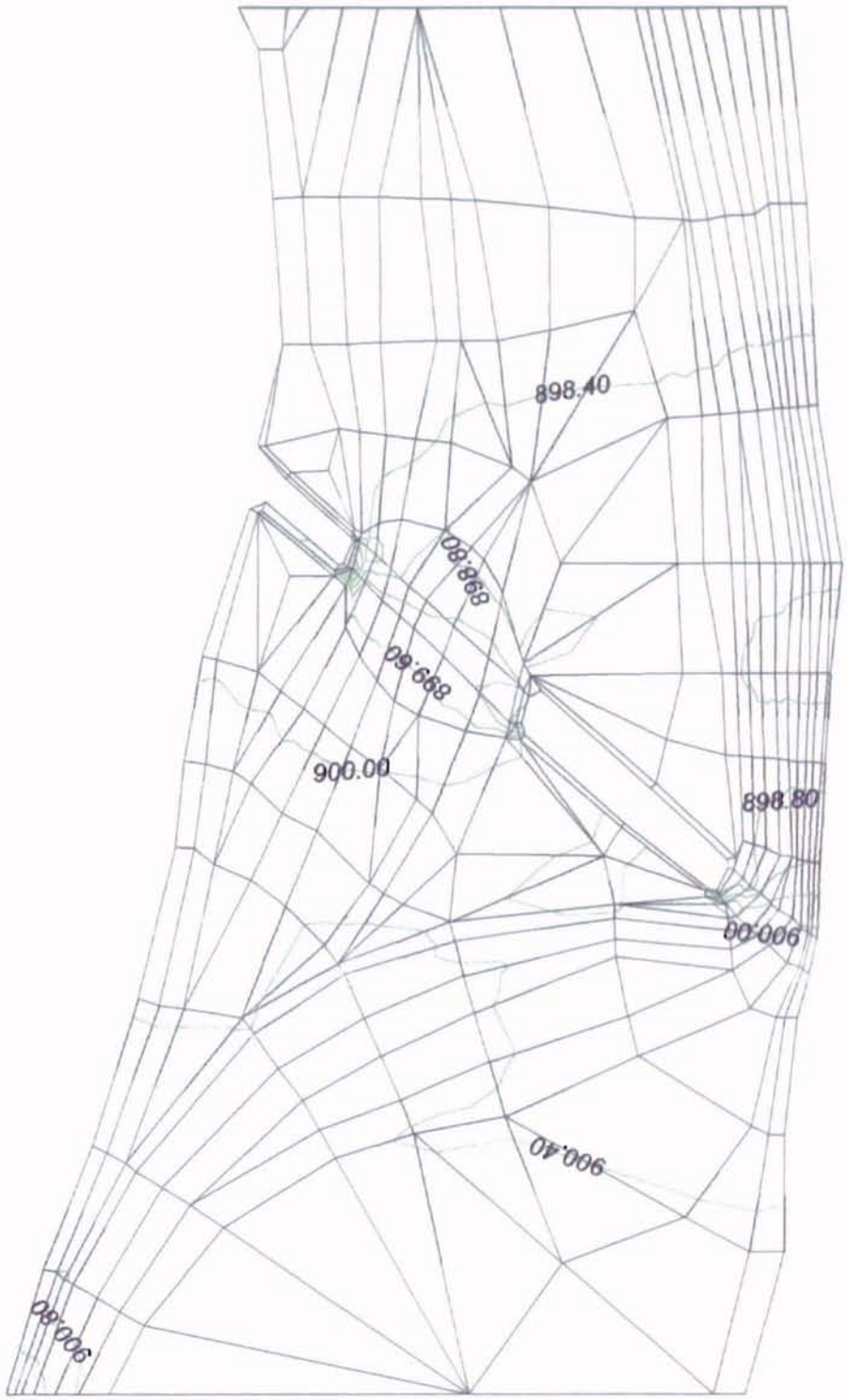

Figure 18. Water Surface Elevations for Q_{50} Existing Crossing

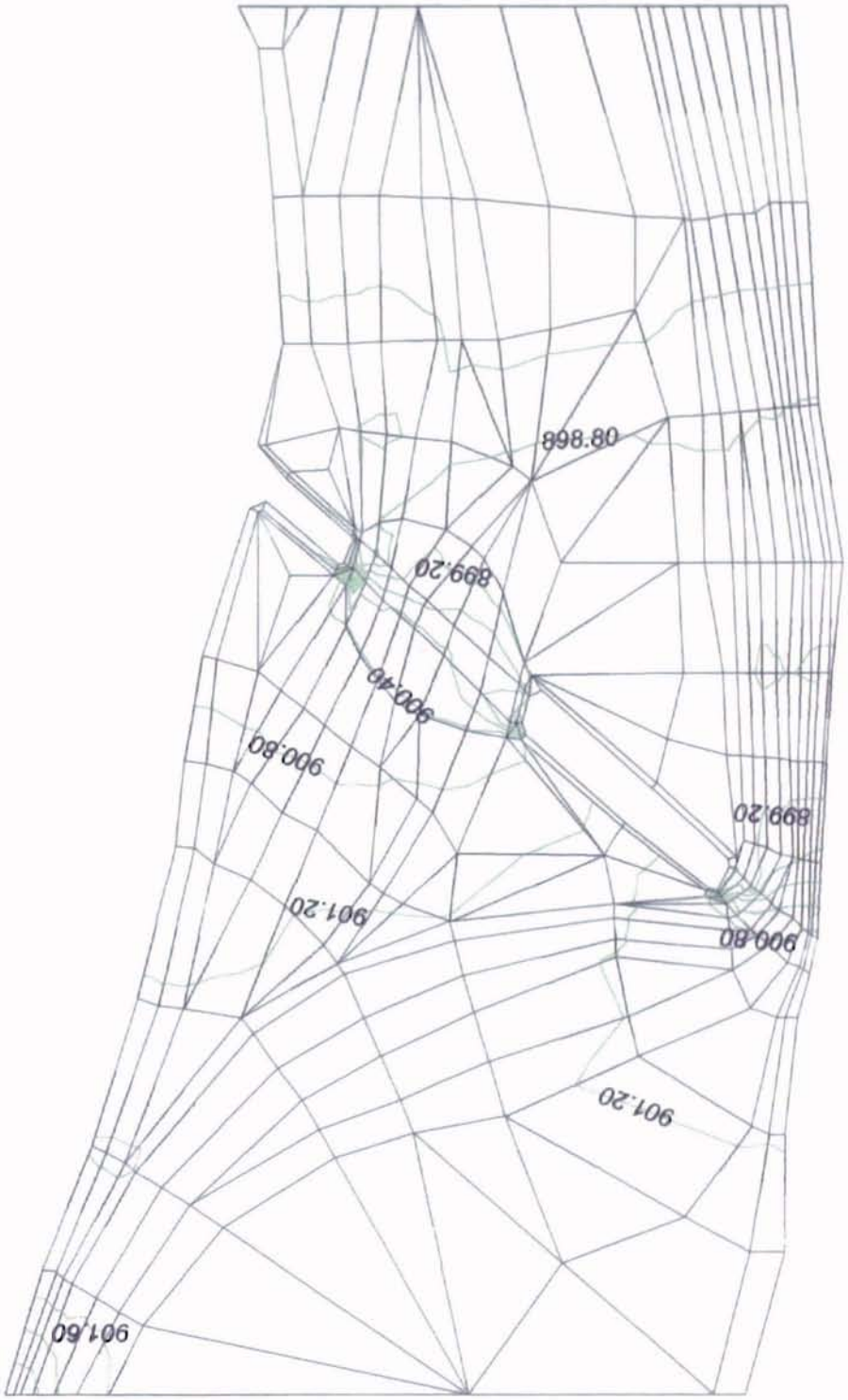

Figure 19. Water Surface Elevations for Q_{100} Existing Crossing

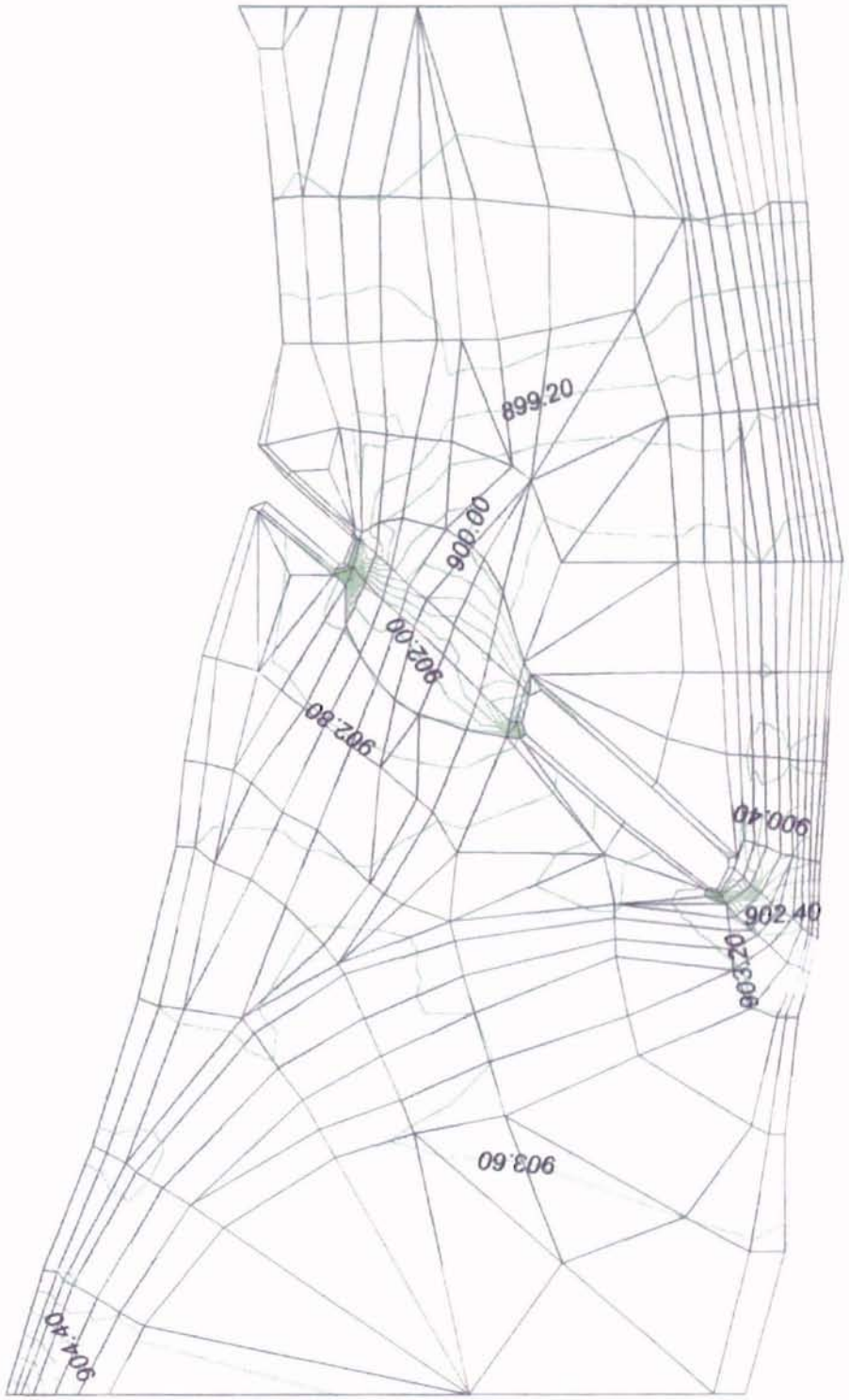

Figure 20. Water Surface Elevations for Q_{500} Existing Crossing

Figure 21. Velocity Vectors for Q_{10} Original Crossing

Figure 22. Velocity Vectors for Q_{25} Original Crossing

Figure 23. Velocity Vectors for Q_{50} Original Crossing

Figure 24. Velocity Vectors for Q_{100} Original Crossing

Figure 25. Velocity Vectors for Q_{500} Original Crossing

Figure 26. Velocity Vectors for Q_{10} Existing Crossing

Figure 27. Velocity Vectors for Q_{25} Existing Crossing

Figure 28. Velocity Vectors for Q_{50} Existing Crossing

Figure 29. Velocity Vectors for Q_{100} Existing Crossing

Figure 30. Velocity Vectors for Q_{500} Existing Crossing

CHAPTER 7

DISCUSSION OF RESULTS

Summary and Discussion of Hydraulic Results

The SMS computer software provides a graphical user interface to input data into the FESWMS-2DH compiler, which calculates scour and the hydraulic conditions at a site. A finite element mesh was constructed by entering topographic data, soil data, and roughness coefficients. The hydraulic and pier data were entered into the model and the following velocities of flow, water surface elevations, and scour at the bridge piers were calculated.

The maximum velocities for a given Q at the original and existing structures are presented in Table 5, Maximum Flow Velocities for Existing and Original Structures.

Table 5

Maximum Flow Velocities for Existing and Original Structures

Flow Event	Maximum Velocity (ft/s) At Previous Structure	Maximum Velocity (ft/s) At Existing Structure
Q_{10}	6.8	6.5
Q_{25}	9.8	9.2
Q_{50}	12.8	10.8
Q_{100}	16.3	12.6
Q_{500}	24.8	17.5

The goal of the I-35 crossing redesign was to reduce the flow velocities through the structures, thus reducing the scour and damage to the structures during floods. From the SMS model, the maximum velocity at the existing structures was reduced by 4.4% during a 10-year flood event, 6.1% during a 25-year flood event, 15.6% during a 50-year flood event, 22.7% during a 100-year flood event, and 29.4% during a 500-year flood event. A graphical representation of the velocity reduction is located in Figure 31, Percent Velocity Reduction.

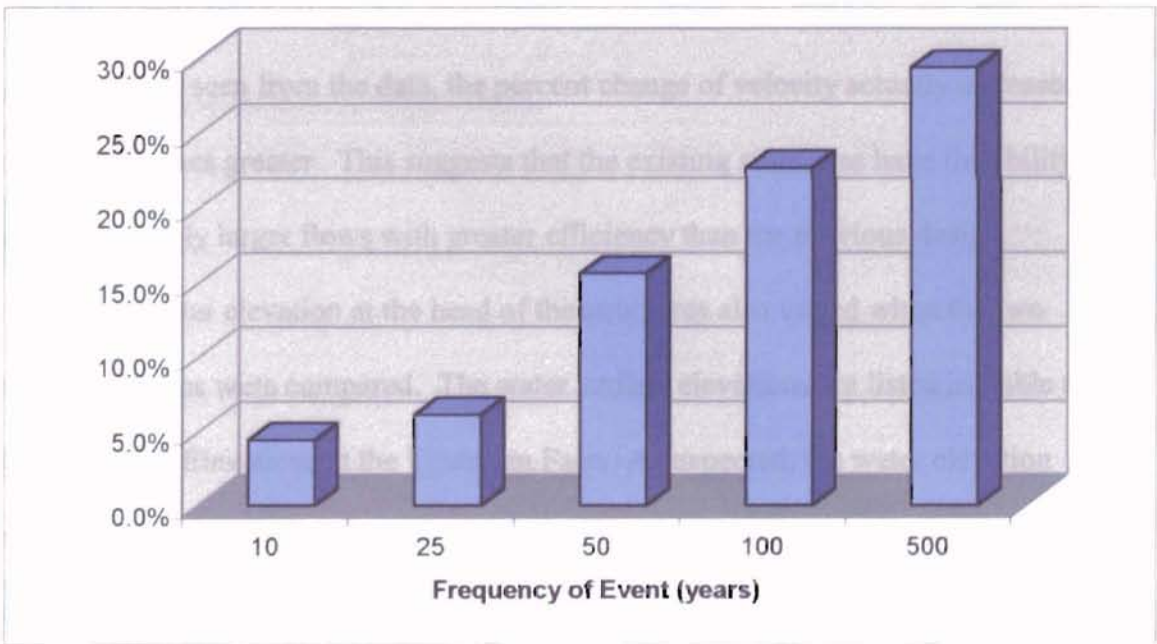

Figure 31. Percent Velocity Reduction

The results from the SMS model support the equation Q=VA, as expected. As the flow increased from a 10-year event to a 500-year event the velocities in both models also rose. However, the velocities rose at different rates because of the differences in the flow area between the original and existing models. From the data it was found that the maximum velocities associated with the existing crossing were less than the maximum velocities of the pre-1988 crossing. A decrease in maximum velocity was expected because of the increase in flow area of the overflow structures in the existing design. The expanded flow area in the floodplain had two effects. First, the expansion slowed the velocities of flow in the overflow structures, which was the area that received the most damage in the 1986 flood. Second, it increased the amount of flow through the overflow channels at high flood levels, which reduced the stress on the main channel structures. Also, as can be seen from the data, the percent change of velocity actually increases as the flow becomes greater. This suggests that the existing structures have the ability to pass increasingly larger flows with greater efficiency than the previous design.

The water elevation at the head of the structures also varied when the two structure designs were compared. The water surface elevations are listed in Table 6, Water Surface Elevations at the Upstream Face. As expected, the water elevation increased as the flow increased for both cases. The water surface elevations varied as little as 0.05 feet during the 10 year flow event to as much as 0.5 feet during the 500 year flood. The low chord of the existing structure has an elevation of 904.0 feet. From these data it was determined that the I-35 crossing was not under pressure flow at the existing crossing. The original crossing had a low chord elevation of 901.4 feet and would have been under pressure flow conditions during a 500-year flood.

Table 6

Water Surface Elevations at the Upstream Face

Flow Event	Water Surface Elevation (ft) At Previous Structure	Water Surface Elevation (ft) At Existing Structure
Q_{10}	898.5	898.4
Q_{25}	899.3	899.2
Q_{50}	900.1	899.9
Q_{100}	900.8	900.6
Q_{500}	903.2	902.7

Summary and Discussion of Scour Results

Once the hydraulic conditions of a site are known, the scour can be computed. The maximum scour for a given Q in the main channel is given in Table 7, Maximum Scour Depths for Existing and Original Structures in the Main Channel. The maximum scour for a given Q in the overflow channel is given in Table 8, Maximum Scour Depths for Existing and Original Structures in the Overflow Channel.

Table 7

Maximum Scour Depths for Existing and Original Structures in the Main Channel

Flow Event	Maximum Scour (ft) At Original Structure	Maximum Scour (ft) At Existing Structure
Q_{10}	20.7	16.2
Q_{25}	33.3	27.2
Q_{50}	42.8	35.9
Q_{100}	53.2	44.0
Q_{500}	76.8	60.4

Table 8

Maximum Scour Depths for Existing and Original Structures in the Overflow Channel

Flow Event	Maximum Scour (ft) At Original Structure	Maximum Scour (ft) At Existing Structure
Q_{10}	21.4	16.4
Q_{25}	35.1	26.6
Q_{50}	44.0	34.4
Q_{100}	54.2	42.1
Q_{500}	78.0	59.5

Upon initial inspection it was determined that the greater the flow rate, the greater the amount of scour for each structure system. From the scour data listed in the tables it

was found that the new design reduced the maximum scour in both the overflow and main structures. The reduction of scour was expected due to the aforementioned decrease in velocity.

It is also important to note that the maximum scour values are deeper than the limiting geologic strata known as the "red bed". The "red bed" varies in elevation from 854.0 to 856.9 feet above sea level. This elevation corresponds to a depth below the existing ground of approximately 16.5 feet in the main channel to 31.9 feet in the overflow channels. Therefore the maximum scour at the site is reached at Q_{25} in the original structures and Q_{50} in the existing structures. Currently FESWMS-2DH and SMS will not model multiple layers of soil and bedrock.

Comparing the maximum scour in the main channel of the existing structure and the structure that was replaced, for modeled flows the following was found: during the 10-year event the maximum scour was reduced by 21.7%, during the 25-year event the maximum scour was reduced by 18.3%, during the 50-year event the maximum scour was reduced by 16.1%, during the 100-year event the maximum scour was reduced by 17.3%, and during the modeled 500-year flood the maximum scour was reduced by 21.4%. From the data it can be proposed that the existing design reduces the maximum scour in the main channel by an average of 19.0%. A graphical representation of the results is located in Figure 32, Percent Scour Reduction - Main Structures.

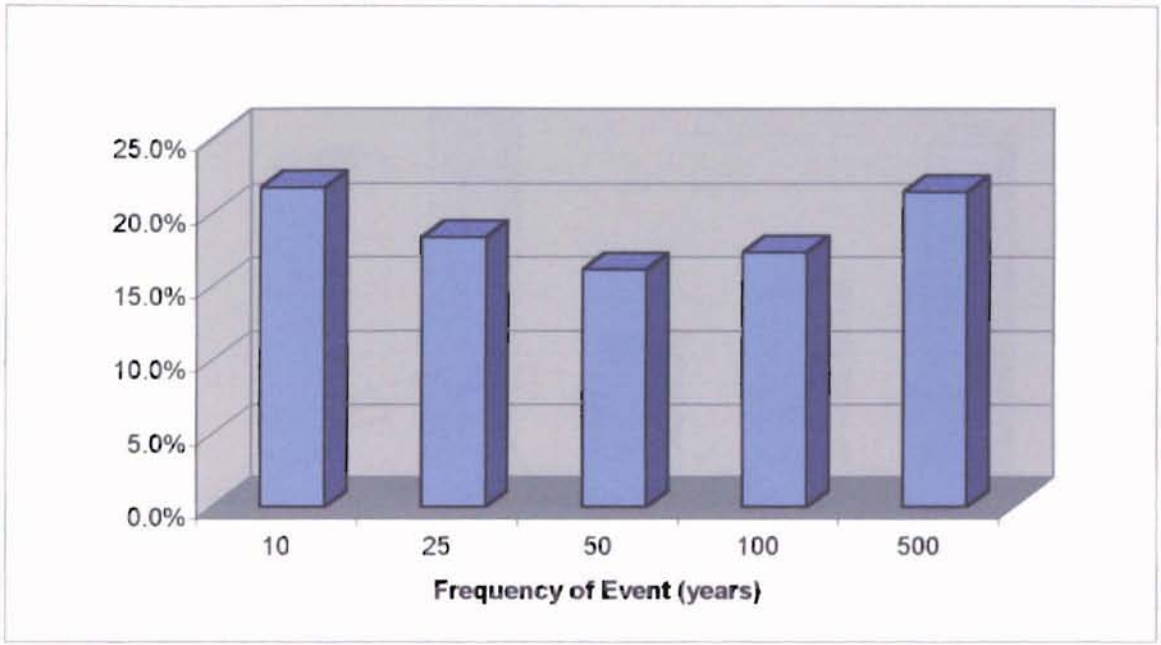

Figure 32. Percent Scour Reduction - Main Structures

Comparing the maximum scour in the overflow structure of the existing crossing and the crossing that was replaced, for modeled flows the following was found: during the 10-year event the maximum scour was reduced by 23.4%, during the 25-year event the maximum scour was reduced by 24.2%, during the 50-year event the maximum scour was reduced by 21.8%, during the 100-year event the maximum scour was reduced by 22.3%, and during the 500-year event the maximum scour was reduced by 23.7%. From the data it can be proposed that the existing design reduces the maximum scour to the overflow structures by an average of 23.1%. A graphical representation of the results is located below in Figure 33, Percent Scour Reduction - Overflow Structures.

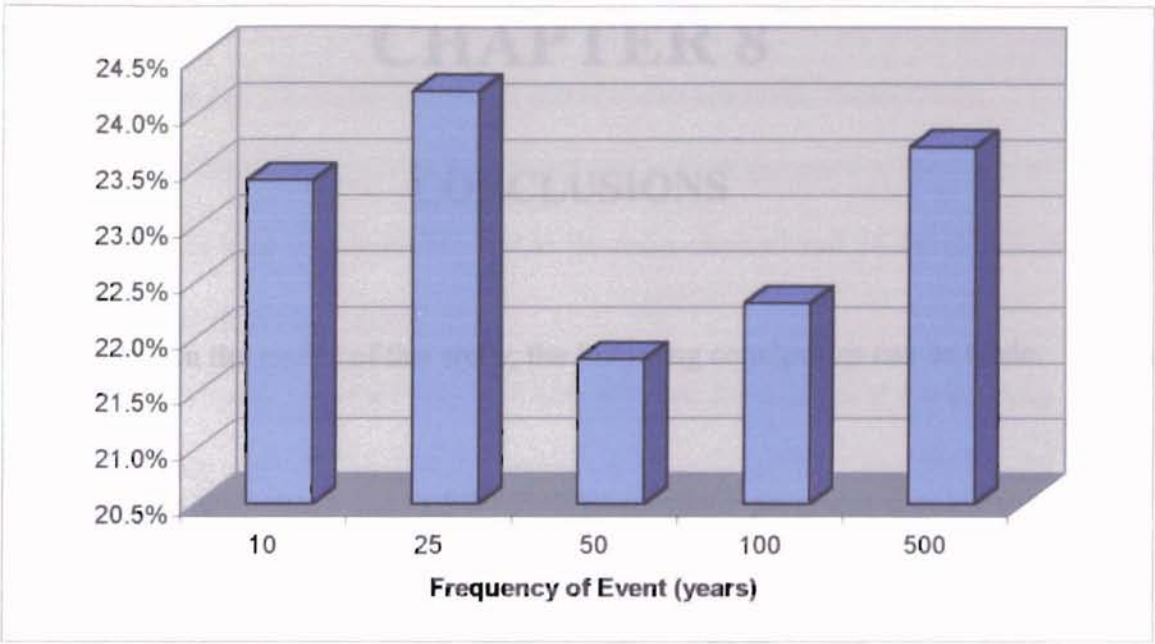

Figure 33. Percent Scour Reduction - Overflow Structures

The amount of scour reduction that occurred is not directly proportional to the decrease in velocity. This is evident from the fact that the percent reduction of scour did not increase as the velocity did when modeled with increasingly greater flows. The percent reduction in scour was lowest for the 50-year flood in both the main and overflow structures. While the highest percent reduction in the main channel was the 500-year flood and the highest percent reduction in the overflow channel occurred during the 25-year flood. The amount of scour is not directly proportional to the amount of scour, but it can be said that when the flow increases scour depth increases. This relation can be made because the amount of scour is based on several factors (Chapter 5) acting together that are related to the velocity of the flow.

CHAPTER 8

CONCLUSIONS

Based on the results of this study, the following conclusions can be made:

1. The use of the SMS and FESWMS-2DH computer programs should be used to perform the hydraulic analysis of complex flow problems such as the existing and previous I-35 crossings of the Cimarron River. SMS provides a graphical interface that facilitates the input and output of data from FESWMS-2DH. The depth averaged velocities, direction of flow, and water surface elevations can be calculated using this powerful two-dimensional analysis program. The information from the hydraulic analysis may be used to calculate scour. The results from the two-dimensional analysis using a program such as FESWMS-2DH may produce much more accurate results when applied properly than the traditional one-dimensional models.
2. The maximum velocity for 100-year and 500-year frequencies at the original structure were 16.3 and 24.8 feet per second, respectively.
3. The maximum velocity for 100-year and 500-year frequencies at the existing structure are 12.6 and 17.5 feet per second, respectively.
4. The water surface elevation for 100-year and 500-year frequencies at the original structures were 900.8 and 903.2 feet above mean sea level, respectively.

5. The water surface elevation for 100-year and 500-year frequencies at the existing structure are 900.6 and 902.7 feet above mean sea level, respectively.
6. The maximum scour for 100-year and 500-year frequencies at the original structures were 53.2 and 76.8 feet in the main channel and 54.2 and 78.0 in the overflow channel, respectively.
7. The maximum scour for 100-year and 500-year frequencies at the existing structures were 44.0 and 60.4 in the main channel and 42.1 and 59.5 in the overflow channel, respectively.
8. The limiting scour due to the "red-bed" shale formation ranges from approximately 31.9 ft to 34.8 ft.

REFERENCES

Blaisdell, F.W. (1981). Ultimate Dimensions of Local Scour. Journal of the Hydraulics Division. Proceedings of the American Society of Civil Engineers, Vol. 107, No. HY3, 327-337.

Buechter, M.T. (1997). Scour Analysis of the Interstate-35 and Cimarron River Crossing Using the FESWMS-2DH and SMS Computer Models. Stillwater, OK: Oklahoma State University. (Unpublished Master's Thesis).

Burkham, D.E. (1981). Uncertainties Resulting from Changes in River Form. Journal of the Hydraulics Division. Proceedings of the American Society of Civil Engineers, Vol. 107, No. HY5, 593-610.

Dargahi, B. (1990). Controlling Mechanism of Local Scouring. Journal of Hydraulic Egineering. American Society of Civil Engineers Hydraulics Division, Vol. 1116, No. 10, 1197-1214.

Chaudry, M.F. (1993). Open-channel Flow. Englewood Cliffs, NJ: Prentice-Hall.

Chow, V.T. (1988). Open Channel Hydraulics: Mc-graw Hill

Finnie, J.I., & Jeppson, R.W. (1991). Solving turbulent flows using finite elements. Hournal of Hydraulic Engineering. American Society of Civil Engineers, Hydraulic Division, Vol. 117, No. 11, 1515-1530.

Froehlich, D.C. (1996). Finite Element Surface Water Modeling System: Two-Dimensional Flow in a Horizontal Plane, Version 2, Draft User's Manual. McLean Virginia: Federal Highway Administration.

Froehlich, D.C. (1992). Finite Element Surface Water Modeling System: Two-Dimensional Flow in a Horizontal Plane, Version 2, User's Manual Preprint. McLean Virginia: Federal Highway Administration.

Hydrologic Engineering Center. (1993). HEC-6 Scour and Deposition in Rivers & Reservoirs User's Manual. Davis, CA: U.S. Army Corps of Engineers.

Jain, S.C. (1981). Maximum Clear-Water Scour Around Circular Piers. Journal of the Hydraulics Division. Proceedings of the American Society of Civil Engineers, Vol. 107, No. HY5, 611-626.

Lagasse, P.F., Schall, J.D., Johnson, F., Richardson, E.V., Richardson, J.R., & Chang, F. (1991). HEC-20 Stream Stability at Highway Structures. Washington, D.C.: Federal Highway Administration.

Laursen, E.M. (1960). Scour at Bridge Crossings. Journal of the Hydraulics Division. Proceedings of the American Society of Civil Engineers, Vol. 86, No. HY2, 39-54.

Laursen, E.M. (1963). An Analysis of Relief Bridge Scour. Journal of the Hydraulics Division. Proceedings of the American Society of Civil Engineers, Vol. 89, No. HY3, 93-118.

Muehller, David S. (1997). Field Based Research on Channel Scour at Bridges. Preceedings of the U.S. Geological Survey Sediment Workshop, February 4-7.

Richardson, E.V., Harrison, C.J., Richardson, J.R., & Davis, S.R. (1993). HEC –18 Evaluating Scour at Bridges, Second Edition. Washington, D.C.: Federal Highway Administration.

Strongylis, D.G. (1988). Water Surface Profiles Using FESWMS-2DH Model. Stillwater, OK: Oklahoma State University. (Unpublished Master's Thesis).

Tyagi, A.K. (1988). Scour Around Bridge Piers of the Overflow Structures at I-35 Bridge on the Cimarron River. Stillwater, OK: School of Civil Engineering, Oklahoma State University.

Tyagi, A.K. (1993). Scour Around Bridge Piers in Oklahoma Streams in 1986. Proceedings of Hydraulic Engineers, American Society of Civil Engineers, vol. 1, 934-938.

Tyagi, A.K. (1998). Hydraulic and Scour Analyses Black Bear Creek Bridge (0.8 M N. Jct. SH 64) Cimarron Turnpike. Stillwater, OK: School of Civil Engineering, Oklahoma State University.

Tyagi, A.K. (1998). Hydraulic and Scour Analyses Spunky Creek Bridge Will Rogers Turnpike. Stillwater, OK: School of Civil Engineering, Oklahoma State University.

Tyagi, A.K. and Buechter, M.T. (1999). Scour Modeling of I-35 Bridge on Cimarron River. Proceedings International Water Resources Engineering, American Society of Civil Engineers, p. 6.

United States Geological Survey (1989). Soil Survey of Payne County, Oklahoma. Washington D.C.: U.S. Department of the Interior.

Wanielista, M. (1990). Hydrology and Water Quantity Control. New York, New York: John Wiley & Sons.

Yalin, M.S. (1992). River Mechanics. Oxford, England: Pergamon Press.

Zienkiewicz, O.C. (1977). The Finite Element Method (3rd ed.). Maidenhead, England: Mc-Graw Hill.

APPENDIX A

SITE MAP

Site Map:

Langston 7 ½ Minute Quadrangle

APPENDIX B

HYDROLOGY DATA

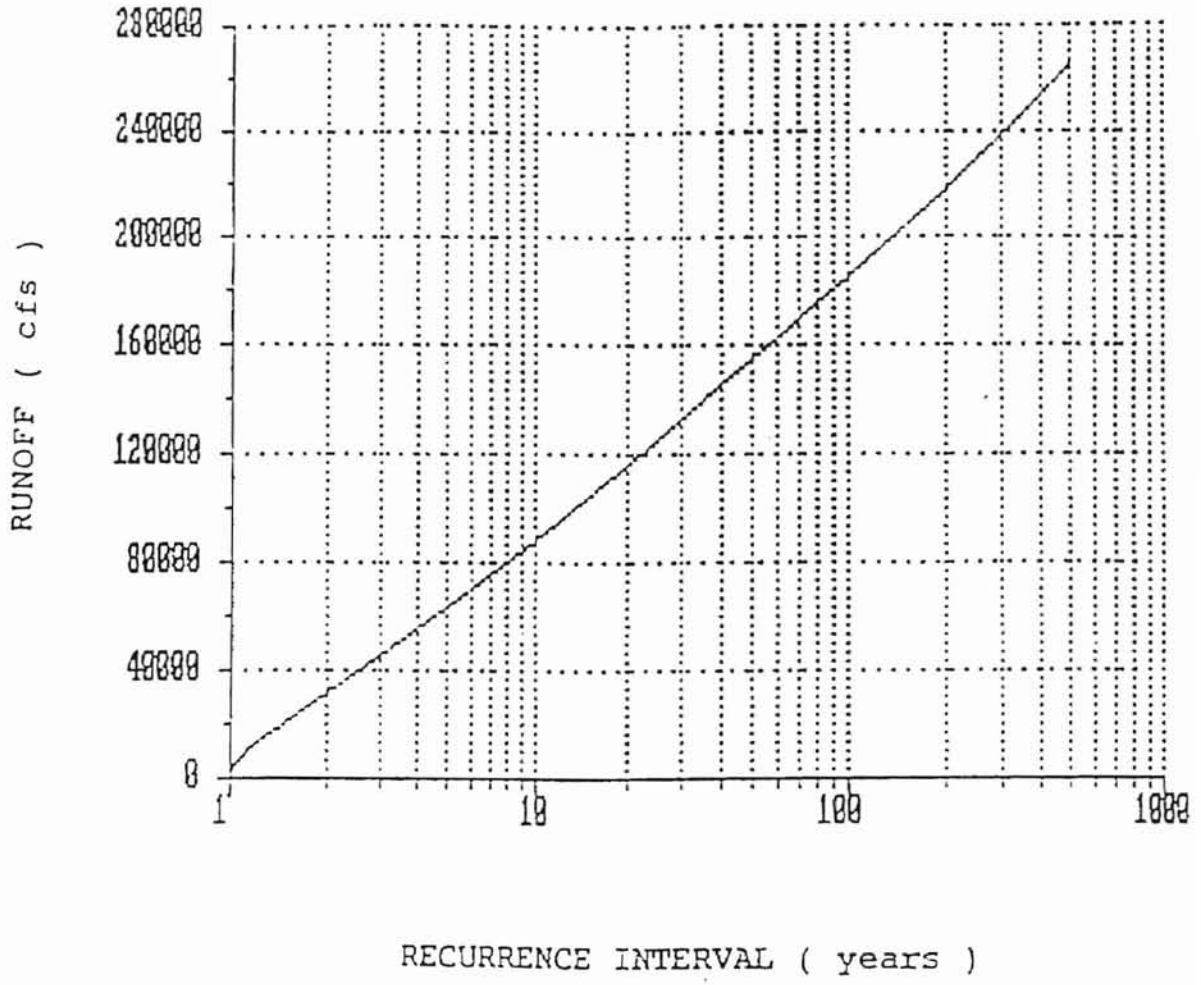

Runoff versus Recurrence Interval Curve

[Source: Strongylis (1992)]

APPENDIX C

SOIL DATA

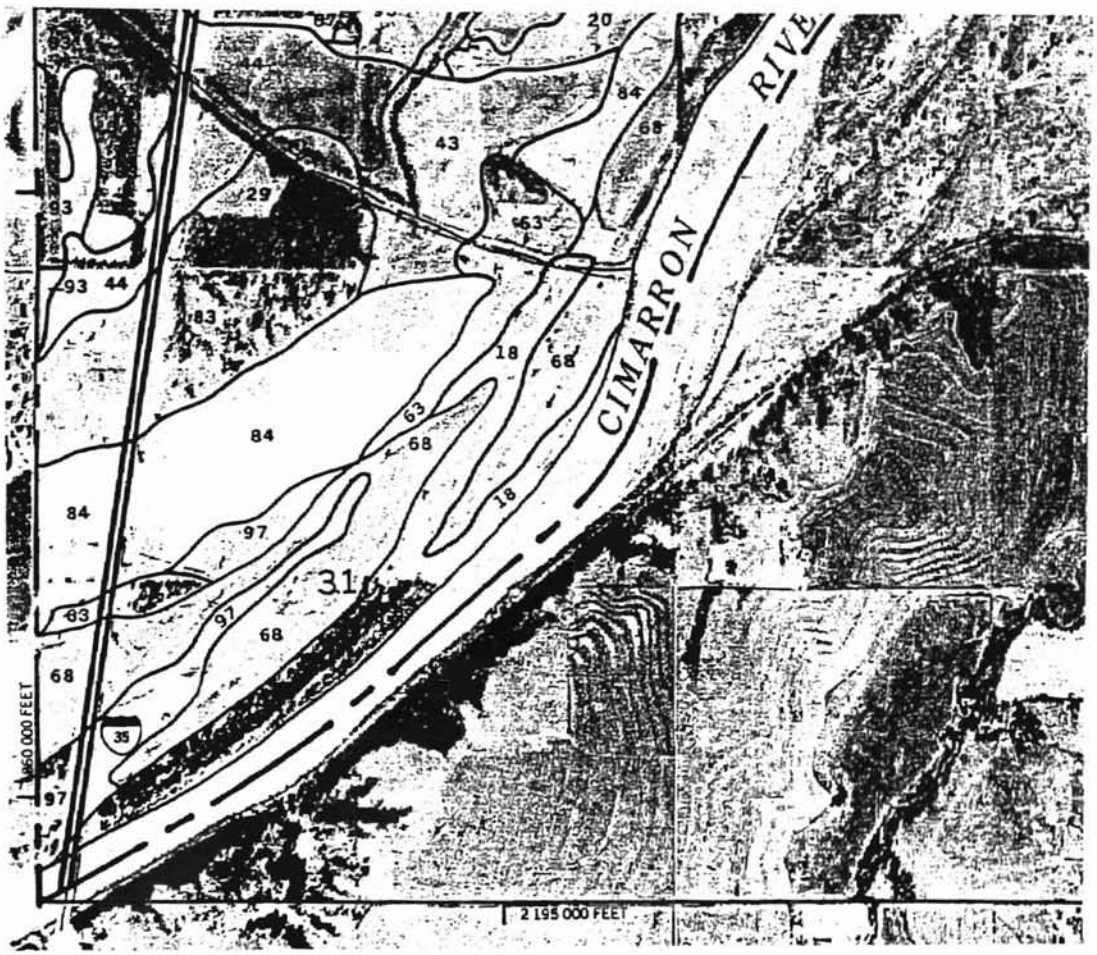
CIMARRON RIVE
84
68
43
29
63
93
44
83
18
68
63
84
68
18
84
97
31
63
97
68
68
35
97
660 000 FEET
2 195 000 FEET

8----------	0-8	Fine sandy loam	SM, ML, CL-ML, SM-SC	A-4	0	100	95-100	90-100	36-60	<26	NP-7
Yahola	8-46	Fine sandy loam, loam, very fine sandy loam.	SM, ML, CL SC	A-4	0	100	95-100	90-100	36-85	<30	NP-10
	46-64	Stratified loam to loamy fine sand.	SM, ML, CL SC	A-2, A-4	0	100	95-100	90-100	15-85	<30	NP-10
4----------	0-10	Fine sandy loam	ML, SM	A-4	0	100	98-100	94-100	36-60	<26	NP-4
Rawley	10-32	Fine sandy loam, loam.	SM, SC, SM-SC, CL-ML	A-4	0	100	98-100	90-100	45-75	<30	NP-10
	32-60	Stratified loamy fine sand to silty clay loam.	SM, ML, SM-SC, CL-ML	A-2, A-4	0	100	98-100	90-100	30-70	<30	NP-7

APPENDIX D

CALCULATED SCOUR DATA

Original Structure 10-year

*** PIER SCOUR REPORT ***

Pier No.	Pier Width (ft)	Pier Lngth (ft)	Pier Nose shape	Approach Flow Vel (ft/s)	Approach Flow Depth (ft)	Approach Flow Angle (deg)	Scour Depths Local (ft)	Scour Depths Genrl (ft)	Scour Depths Total (ft)	Riprap D50 (ft)
1	1.33	6.65	Square	4.88	9.05	75.8	8.07	0.00	8.07	0.45
2	4.00	4.00	Round	0.00	0.00	0.0	0.00	0.00	0.00	0.00
3	4.00	4.00	Round	0.00	0.00	0.0	0.00	0.00	0.00	0.00
4	4.00	4.00	Round	0.00	0.00	0.0	0.00	0.00	0.00	0.00
5	4.00	4.00	Round	0.00	0.00	0.0	0.00	0.00	0.00	0.00
6	4.00	4.00	Round	2.59	20.71	16.5	5.30	0.00	5.30	0.10
7	4.00	4.00	Round	2.66	21.02	17.1	5.36	0.00	5.36	0.10
8	4.00	4.00	Round	2.83	21.81	18.4	5.54	0.00	5.54	0.12
9	4.00	4.00	Round	2.93	22.22	19.0	5.63	0.00	5.63	0.13
10	4.00	4.00	Round	3.09	23.29	29.9	5.80	0.00	5.80	0.14
11	4.00	4.00	Round	3.24	23.42	29.7	5.93	0.36	6.28	0.15
12	4.00	4.00	Round	3.67	23.60	27.9	6.26	3.02	9.27	0.20
13	4.00	4.00	Round	3.90	23.62	26.8	6.42	4.44	10.87	0.22
14	4.00	4.00	Round	3.58	25.42	36.7	6.25	2.34	8.59	0.19
15	4.00	4.00	Round	3.73	25.70	35.8	6.38	3.35	9.73	0.20
16	4.00	4.00	Round	4.07	26.38	33.7	6.64	5.61	12.25	0.24
17	4.00	4.00	Round	4.17	26.72	33.3	6.72	6.33	13.05	0.26
18	4.00	4.00	Round	4.57	28.28	41.9	7.05	9.23	16.28	0.31
19	4.00	4.00	Round	4.60	27.35	40.7	7.03	9.29	16.32	0.31
20	4.00	4.00	Round	4.73	25.78	37.2	7.06	9.92	16.98	0.33
21	4.00	4.00	Round	4.78	25.32	35.3	7.08	10.13	17.21	0.33
22	4.00	4.00	Round	5.44	19.87	47.6	7.24	12.31	19.55	0.43
23	4.00	4.00	Round	5.69	19.41	46.2	7.36	13.38	20.74	0.47
24	4.00	4.00	Round	5.68	19.14	39.7	7.34	13.22	20.56	0.47
25	4.00	4.00	Round	5.52	19.14	36.4	7.25	12.42	19.67	0.45
26	4.00	4.00	Round	5.62	9.82	45.6	6.67	8.26	14.94	0.46
27	4.00	4.00	Round	5.32	9.17	40.8	6.46	7.12	13.58	0.42
28	4.00	4.00	Round	4.02	9.06	34.4	5.72	3.60	9.32	0.24
29	4.00	4.00	Round	3.51	9.01	30.8	5.39	2.20	7.59	0.18
30	1.33	6.65	Square	3.43	11.83	85.6	7.16	0.00	7.16	0.22
31	1.33	6.65	Square	2.42	11.69	88.5	6.13	0.00	6.13	0.11
32	1.33	6.65	Square	4.39	12.05	79.7	8.01	0.00	8.01	0.36
33	1.33	6.65	Square	3.53	11.96	87.1	7.25	0.00	7.25	0.24
34	1.33	6.65	Square	4.56	12.28	76.4	8.17	0.00	8.17	0.39
35	1.33	6.65	Square	4.25	12.25	81.5	7.92	0.00	7.92	0.34
36	1.33	6.65	Square	4.92	12.38	77.8	8.45	0.00	8.45	0.46
37	1.33	6.65	Square	5.02	12.36	79.1	8.52	0.00	8.52	0.47
38	1.33	6.65	Square	5.21	12.34	81.4	8.65	0.00	8.65	0.51
39	1.33	6.65	Square	4.89	12.36	78.7	8.43	0.00	8.43	0.45
40	1.33	6.65	Square	4.05	12.30	82.7	7.75	0.00	7.75	0.31
41	1.33	6.65	Square	3.39	12.36	75.6	7.20	0.00	7.20	0.22
42	1.33	6.65	Square	3.94	12.03	69.7	7.60	0.00	7.60	0.29
43	1.33	6.65	Square	3.39	12.19	88.0	7.13	0.00	7.13	0.22
44	1.33	6.65	Square	5.35	12.25	73.2	8.73	0.00	8.73	0.54
45	1.33	6.65	Square	5.17	12.22	80.3	8.62	0.00	8.62	0.50
46	1.33	6.65	Square	4.93	10.92	75.5	8.31	0.00	8.31	0.46
47	1.33	6.65	Square	5.20	11.04	76.3	8.52	0.00	8.52	0.51
48	1.33	6.65	Square	4.72	7.96	82.6	7.81	0.00	7.81	0.42
49	1.33	6.65	Square	3.33	10.14	89.7	6.88	0.00	6.88	0.21
50	1.33	6.65	Square	3.01	10.38	87.0	6.64	0.00	6.64	0.17
51	1.33	6.65	Square	4.60	10.66	81.0	8.04	0.00	8.04	0.40
52	1.33	6.65	Square	4.40	10.70	84.7	7.87	0.00	7.87	0.36
53	1.33	6.65	Square	4.75	11.07	80.7	8.20	0.00	8.20	0.42
54	1.33	6.65	Square	4.95	11.06	81.7	8.34	0.00	8.34	0.46
55	1.33	6.65	Square	4.73	11.24	82.5	8.20	0.00	8.20	0.42
56	1.33	6.65	Square	5.15	11.01	81.3	8.48	0.00	8.48	0.50
57	1.33	6.65	Square	4.91	10.80	84.7	8.27	0.00	8.27	0.45
58	1.33	6.65	Square	4.78	10.61	78.7	8.17	0.00	8.17	0.43
59	1.33	6.65	Square	4.24	10.28	78.8	7.73	0.00	7.73	0.34
60	1.33	6.65	Square	3.85	10.27	74.3	7.40	0.00	7.40	0.28

61	1.33	6.65	Square	3.28	10.13	86.3	6.87	0.00	6.87	0.20
62	1.33	6.65	Square	2.78	10.48	80.8	6.46	0.00	6.46	0.15
63	1.33	6.65	Square	4.89	11.11	76.8	8.31	0.00	8.31	0.45
64	1.33	6.65	Square	4.85	10.99	85.6	8.23	0.00	8.23	0.44
65	1.33	6.65	Square	5.02	10.50	80.4	8.34	0.00	8.34	0.48
66	1.33	6.65	Square	5.37	10.21	83.2	8.54	12.83	21.37	0.54

Note - Pier scour calculated using CSU equation.

Original Structure 25-year

*** PIER SCOUR REPORT ***

Pier No.	Pier Width (ft)	Pier Lngth (ft)	Pier Nose shape	Approach Flow Vel (ft/s)	Approach Flow Depth (ft)	Approach Flow Angle (deg)	Scour Depths Local (ft)	Scour Depths Genrl (ft)	Scour Depths Total (ft)	Riprap D50 (ft)
1	1.33	6.65	Square	7.05	9.19	76.1	9.47	17.40	26.87	0.94
2	4.00	4.00	Round	3.19	13.70	9.8	5.47	1.10	6.57	0.15
3	4.00	4.00	Round	3.08	11.37	7.9	5.26	0.88	6.14	0.14
4	4.00	4.00	Round	1.85	6.28	4.3	3.90	0.00	3.90	0.05
5	4.00	4.00	Round	0.84	3.92	0.4	2.61	0.00	2.61	0.01
6	4.00	4.00	Round	3.54	21.40	17.4	6.08	2.34	8.42	0.18
7	4.00	4.00	Round	3.66	21.71	16.7	6.18	3.04	9.22	0.20
8	4.00	4.00	Round	4.00	22.49	15.7	6.45	5.00	11.45	0.23
9	4.00	4.00	Round	4.20	22.90	15.2	6.61	6.24	12.85	0.26
10	4.00	4.00	Round	3.89	23.95	31.6	6.43	4.37	10.80	0.22
11	4.00	4.00	Round	4.09	24.07	30.7	6.58	5.66	12.23	0.25
12	4.00	4.00	Round	4.74	24.23	27.2	7.01	9.71	16.72	0.33
13	4.00	4.00	Round	5.12	24.24	25.6	7.25	12.03	19.27	0.38
14	4.00	4.00	Round	4.74	26.04	36.2	7.08	10.05	17.13	0.33
15	4.00	4.00	Round	4.95	26.30	35.1	7.22	11.47	18.69	0.36
16	4.00	4.00	Round	5.39	26.93	32.5	7.52	14.53	22.04	0.43
17	4.00	4.00	Round	5.47	27.25	32.0	7.57	15.13	22.70	0.44
18	4.00	4.00	Round	6.27	28.82	41.3	8.09	21.17	29.26	0.58
19	4.00	4.00	Round	6.23	27.86	40.1	8.03	20.43	28.46	0.57
20	4.00	4.00	Round	6.29	26.25	36.3	8.00	20.01	28.01	0.58
21	4.00	4.00	Round	6.19	25.76	34.0	7.93	19.18	27.11	0.56
22	4.00	4.00	Round	7.49	20.26	46.2	8.33	22.82	31.16	0.82
23	4.00	4.00	Round	7.94	19.77	45.4	8.51	24.54	33.05	0.92
24	4.00	4.00	Round	8.04	19.43	40.1	8.54	24.74	33.28	0.95
25	4.00	4.00	Round	7.73	19.39	36.7	8.39	23.22	31.62	0.88
26	4.00	4.00	Round	7.60	9.87	44.7	7.61	13.66	21.27	0.85
27	4.00	4.00	Round	7.24	9.16	39.5	7.38	12.02	19.40	0.77
28	4.00	4.00	Round	5.50	9.19	32.4	6.55	7.58	14.13	0.44
29	4.00	4.00	Round	4.85	9.20	28.9	6.21	5.88	12.09	0.34
30	1.33	6.65	Square	4.85	11.88	84.8	8.32	0.00	8.32	0.44
31	1.33	6.65	Square	3.27	12.05	86.9	7.03	0.00	7.03	0.20
32	1.33	6.65	Square	6.46	12.23	78.9	9.49	19.27	28.76	0.79
33	1.33	6.65	Square	5.18	12.32	86.7	8.58	0.00	8.58	0.50
34	1.33	6.65	Square	6.29	12.59	76.5	9.41	18.97	28.38	0.75
35	1.33	6.65	Square	5.81	12.61	81.4	9.09	16.90	26.00	0.64
36	1.33	6.65	Square	6.70	12.75	78.6	9.69	20.91	30.60	0.85
37	1.33	6.65	Square	6.98	12.71	79.6	9.86	22.06	31.91	0.92
38	1.33	6.65	Square	7.53	12.66	81.9	10.17	24.33	34.50	1.07
39	1.33	6.65	Square	7.02	12.71	79.1	9.88	22.22	32.10	0.93
40	1.33	6.65	Square	5.64	12.57	84.1	8.96	16.13	25.09	0.60
41	1.33	6.65	Square	4.46	12.70	74.2	8.12	0.00	8.12	0.38
42	1.33	6.65	Square	5.53	12.10	66.0	8.73	15.19	23.91	0.58
43	1.33	6.65	Square	4.72	12.35	86.5	8.26	0.00	8.26	0.42
44	1.33	6.65	Square	7.71	12.52	72.6	10.23	24.88	35.11	1.12
45	1.33	6.65	Square	7.66	12.42	79.6	10.23	24.52	34.75	1.11
46	1.33	6.65	Square	6.78	11.27	75.6	9.57	19.35	28.92	0.87
47	1.33	6.65	Square	7.26	11.23	76.4	9.86	21.14	31.00	0.99
48	1.33	6.65	Square	6.74	8.27	83.2	9.14	15.07	24.22	0.85
49	1.33	6.65	Square	4.66	10.19	89.8	7.95	0.00	7.95	0.41
50	1.33	6.65	Square	4.28	10.63	85.7	7.76	0.00	7.76	0.34
51	1.33	6.65	Square	6.60	10.92	80.8	9.43	18.19	27.61	0.82
52	1.33	6.65	Square	6.38	10.93	84.6	9.26	17.37	26.63	0.77
53	1.33	6.65	Square	6.63	11.39	80.8	9.49	18.89	28.38	0.83
54	1.33	6.65	Square	6.96	11.28	81.6	9.68	20.04	29.72	0.91
55	1.33	6.65	Square	6.59	11.58	82.3	9.48	18.97	28.46	0.82
56	1.33	6.65	Square	7.28	11.22	81.3	9.87	21.19	31.06	1.00
57	1.33	6.65	Square	6.93	11.10	84.8	9.61	19.66	29.28	0.90
58	1.33	6.65	Square	6.81	10.80	79.0	9.55	18.84	28.38	0.87
59	1.33	6.65	Square	6.12	10.43	78.9	9.07	15.79	24.86	0.71

60	1.33	6.65	Square	5.39	10.48	73.0	8.57	0.00	8.57	0.55
61	1.33	6.65	Square	4.84	9.97	84.8	8.12	0.00	8.12	0.44
62	1.33	6.65	Square	4.17	10.56	80.3	7.70	0.00	7.70	0.33
63	1.33	6.65	Square	7.04	11.23	76.7	9.73	20.29	30.02	0.93
64	1.33	6.65	Square	7.18	11.08	84.8	9.76	20.60	30.36	0.97
65	1.33	6.65	Square	7.10	10.76	81.1	9.71	19.85	29.55	0.95
66	1.33	6.65	Square	7.63	10.26	83.2	9.93	20.97	30.90	1.10

Note - Pier scour calculated using CSU equation.

Original Structure 50-year

*** PIER SCOUR REPORT ***

Pier No.	Pier Width (ft)	Pier Lngth (ft)	Pier Nose shape	Approach Flow Vel (ft/s)	Approach Flow Depth (ft)	Approach Flow Angle (deg)	Scour Depths Local (ft)	Scour Depths Genrl (ft)	Scour Depths Total (ft)	Riprap D50 (ft)
1	1.33	6.65	Square	8.73	9.33	76.9	10.41	22.99	33.39	1.43
2	4.00	4.00	Round	3.84	14.40	10.2	5.97	3.73	9.70	0.22
3	4.00	4.00	Round	3.74	12.07	8.3	5.76	3.15	8.92	0.20
4	4.00	4.00	Round	2.26	6.97	4.8	4.31	0.00	4.31	0.07
5	4.00	4.00	Round	1.01	4.61	0.9	2.88	0.00	2.88	0.01
6	4.00	4.00	Round	4.19	22.08	17.7	6.56	6.09	12.66	0.26
7	4.00	4.00	Round	4.34	22.38	16.9	6.68	7.00	13.68	0.28
8	4.00	4.00	Round	4.77	23.15	15.7	6.99	9.67	16.66	0.33
9	4.00	4.00	Round	5.04	23.56	15.1	7.17	11.35	18.52	0.37
10	4.00	4.00	Round	4.60	24.61	31.7	6.93	8.86	15.79	0.31
11	4.00	4.00	Round	4.84	24.72	30.8	7.09	10.41	17.51	0.34
12	4.00	4.00	Round	5.61	24.85	27.3	7.57	15.22	22.78	0.46
13	4.00	4.00	Round	6.06	24.85	25.8	7.82	17.95	25.77	0.54
14	4.00	4.00	Round	5.65	26.66	36.2	7.66	16.11	23.76	0.47
15	4.00	4.00	Round	5.89	26.91	35.1	7.81	17.81	25.61	0.51
16	4.00	4.00	Round	6.39	27.49	32.4	8.11	21.35	29.46	0.60
17	4.00	4.00	Round	6.41	27.78	31.7	8.13	21.62	29.76	0.60
18	4.00	4.00	Round	7.54	29.37	41.5	8.78	30.18	38.96	0.83
19	4.00	4.00	Round	7.42	28.39	40.5	8.68	28.66	37.35	0.81
20	4.00	4.00	Round	7.40	26.72	36.4	8.60	27.29	35.89	0.80
21	4.00	4.00	Round	7.14	26.22	33.9	8.45	25.32	33.77	0.75
22	4.00	4.00	Round	9.06	20.68	45.8	9.07	30.90	39.97	1.20
23	4.00	4.00	Round	9.66	20.15	45.3	9.29	33.15	42.44	1.37
24	4.00	4.00	Round	9.83	19.76	40.7	9.33	33.46	42.80	1.42
25	4.00	4.00	Round	9.40	19.69	37.1	9.15	31.35	40.50	1.30
26	4.00	4.00	Round	8.96	9.97	44.7	8.18	17.38	25.56	1.18
27	4.00	4.00	Round	8.56	9.19	39.4	7.93	15.34	23.27	1.07
28	4.00	4.00	Round	6.30	9.39	30.9	6.97	9.80	16.77	0.58
29	4.00	4.00	Round	5.49	9.48	27.6	6.58	7.73	14.31	0.44
30	1.33	6.65	Square	6.02	11.92	83.4	9.16	17.09	26.25	0.68
31	1.33	6.65	Square	4.00	12.41	86.2	7.69	0.00	7.69	0.30
32	1.33	6.65	Square	8.21	12.41	78.7	10.54	26.76	37.30	1.27
33	1.33	6.65	Square	6.63	12.69	86.3	9.59	20.52	30.11	0.83
34	1.33	6.65	Square	7.67	12.90	77.0	10.29	25.30	35.58	1.11
35	1.33	6.65	Square	7.03	12.98	81.6	9.91	22.63	32.54	0.93
36	1.33	6.65	Square	8.11	13.10	79.3	10.56	27.52	38.08	1.24
37	1.33	6.65	Square	8.53	13.07	80.0	10.79	29.25	40.04	1.37
38	1.33	6.65	Square	9.43	12.96	82.4	11.24	32.83	44.06	1.68
39	1.33	6.65	Square	8.73	13.05	79.3	10.89	30.05	40.95	1.44
40	1.33	6.65	Square	6.79	12.81	85.5	9.71	21.39	31.10	0.87
41	1.33	6.65	Square	5.07	13.02	73.2	8.60	0.00	8.60	0.48
42	1.33	6.65	Square	6.86	12.16	65.4	9.57	20.83	30.40	0.89
43	1.33	6.65	Square	5.88	12.54	85.7	9.10	17.14	26.24	0.65
44	1.33	6.65	Square	9.45	12.77	73.5	11.21	32.50	43.71	1.68
45	1.33	6.65	Square	9.50	12.63	79.9	11.25	32.44	43.69	1.70
46	1.33	6.65	Square	8.42	11.60	76.4	10.55	26.17	36.72	1.34
47	1.33	6.65	Square	9.06	11.42	77.0	10.87	28.27	39.13	1.55
48	1.33	6.65	Square	8.37	8.58	84.6	10.07	20.42	30.50	1.32
49	1.33	6.65	Square	5.73	10.26	88.9	8.71	14.18	22.89	0.62
50	1.33	6.65	Square	5.49	10.89	85.6	8.67	13.91	22.58	0.57
51	1.33	6.65	Square	8.25	11.19	81.1	10.41	24.80	35.21	1.28
52	1.33	6.65	Square	8.05	11.17	84.7	10.27	24.02	34.29	1.22
53	1.33	6.65	Square	8.12	11.72	81.0	10.40	25.24	35.64	1.24
54	1.33	6.65	Square	8.58	11.50	81.8	10.62	26.60	37.22	1.39
55	1.33	6.65	Square	8.11	11.94	82.5	10.42	25.56	35.98	1.24
56	1.33	6.65	Square	9.05	11.43	81.5	10.86	28.25	39.11	1.54
57	1.33	6.65	Square	8.53	11.41	85.0	10.55	26.26	36.82	1.37
58	1.33	6.65	Square	8.46	10.99	79.2	10.50	25.23	35.73	1.35
59	1.33	6.65	Square	7.79	10.57	79.5	10.08	22.06	32.14	1.14

60	1.33	6.65	Square	6.67	10.69	72.3	9.41	18.15	27.56	0.84
61	1.33	6.65	Square	6.18	9.81	82.2	9.02	15.28	24.30	0.72
62	1.33	6.65	Square	5.51	10.62	81.3	8.69	13.74	22.43	0.57
63	1.33	6.65	Square	8.74	11.36	77.3	10.70	26.95	37.65	1.44
64	1.33	6.65	Square	9.07	11.16	84.7	10.81	27.78	38.58	1.55
65	1.33	6.65	Square	8.88	11.00	81.2	10.72	26.78	37.50	1.49
66	1.33	6.65	Square	9.48	10.33	83.5	10.91	27.53	38.44	1.69

Note - Pier scour calculated using CSU equation.

Original Structure 100-year

*** PIER SCOUR REPORT ***

Pier No.	Pier Width (ft)	Pier Lngth (ft)	Pier Nose shape	Approach Flow Vel (ft/s)	Approach Flow Depth (ft)	Approach Flow Angle (deg)	Scour Depths Local (ft)	Scour Depths Genrl (ft)	Scour Depths Total (ft)	Riprap D50 (ft)
1	1.33	6.65	Square	10.55	9.52	77.3	11.32	29.18	40.51	2.10
2	4.00	4.00	Round	4.48	15.26	10.6	6.43	6.46	12.89	0.29
3	4.00	4.00	Round	4.38	12.93	8.8	6.23	5.58	11.81	0.28
4	4.00	4.00	Round	2.64	7.82	5.5	4.68	0.00	4.68	0.10
5	4.00	4.00	Round	1.14	5.46	1.4	3.10	0.00	3.10	0.02
6	4.00	4.00	Round	4.78	22.92	17.9	6.98	9.66	16.65	0.34
7	4.00	4.00	Round	4.96	23.22	17.1	7.11	10.79	17.90	0.36
8	4.00	4.00	Round	5.51	23.98	15.7	7.47	14.28	21.75	0.45
9	4.00	4.00	Round	5.86	24.38	15.0	7.69	16.51	24.20	0.50
10	4.00	4.00	Round	5.26	25.43	31.8	7.38	13.23	20.61	0.41
11	4.00	4.00	Round	5.54	25.53	30.8	7.55	14.98	22.53	0.45
12	4.00	4.00	Round	6.38	25.63	27.4	8.03	20.27	28.30	0.60
13	4.00	4.00	Round	6.85	25.61	25.9	8.28	23.17	31.45	0.69
14	4.00	4.00	Round	6.58	27.44	36.0	8.21	22.56	30.78	0.64
15	4.00	4.00	Round	6.87	27.66	35.0	8.37	24.57	32.94	0.69
16	4.00	4.00	Round	7.44	28.20	32.4	8.68	28.63	37.31	0.81
17	4.00	4.00	Round	7.32	28.47	31.6	8.64	28.05	36.68	0.79
18	4.00	4.00	Round	8.69	30.06	42.0	9.37	38.54	47.90	1.11
19	4.00	4.00	Round	8.51	29.06	41.2	9.24	36.40	45.64	1.06
20	4.00	4.00	Round	8.45	27.35	37.0	9.14	34.40	43.53	1.05
21	4.00	4.00	Round	8.00	26.82	34.2	8.90	31.14	40.04	0.94
22	4.00	4.00	Round	10.52	21.23	45.8	9.70	38.72	48.42	1.62
23	4.00	4.00	Round	11.25	20.67	45.8	9.95	41.39	51.34	1.85
24	4.00	4.00	Round	11.77	20.21	42.0	10.11	43.08	53.19	2.03
25	4.00	4.00	Round	11.06	20.09	37.6	9.84	39.63	49.47	1.79
26	4.00	4.00	Round	9.65	10.13	44.6	8.46	19.42	27.88	1.37
27	4.00	4.00	Round	9.31	9.27	36.9	8.23	17.29	25.52	1.27
28	4.00	4.00	Round	6.99	9.73	33.9	7.33	11.92	19.25	0.72
29	4.00	4.00	Round	6.04	9.93	32.8	6.90	9.51	16.41	0.54
30	1.33	6.65	Square	7.22	11.95	81.3	9.91	21.99	31.90	0.98
31	1.33	6.65	Square	4.64	12.82	85.9	8.24	0.00	8.24	0.41
32	1.33	6.65	Square	10.11	12.59	78.3	11.55	34.81	46.36	1.93
33	1.33	6.65	Square	8.22	13.11	85.7	10.57	28.00	38.57	1.27
34	1.33	6.65	Square	9.17	13.25	77.3	11.15	32.30	43.45	1.58
35	1.33	6.65	Square	8.29	13.42	81.7	10.68	28.79	39.47	1.29
36	1.33	6.65	Square	9.61	13.51	79.3	11.41	34.71	46.11	1.74
37	1.33	6.65	Square	10.08	13.51	80.0	11.64	36.72	48.36	1.91
38	1.33	6.65	Square	11.45	13.30	82.1	12.26	41.96	54.22	2.47
39	1.33	6.65	Square	10.54	13.48	79.2	11.86	38.59	50.45	2.09
40	1.33	6.65	Square	8.01	13.09	86.3	10.45	27.05	37.50	1.21
41	1.33	6.65	Square	5.81	13.43	73.5	9.15	17.71	26.87	0.64
42	1.33	6.65	Square	8.30	12.36	64.0	10.37	27.05	37.42	1.30
43	1.33	6.65	Square	7.12	12.80	84.0	9.93	22.81	32.73	0.96
44	1.33	6.65	Square	11.18	13.16	73.7	12.10	40.50	52.60	2.35
45	1.33	6.65	Square	11.48	12.93	79.5	12.24	41.13	53.37	2.48
46	1.33	6.65	Square	9.92	12.06	76.6	11.38	32.88	44.26	1.85
47	1.33	6.65	Square	10.82	11.69	77.0	11.77	35.44	47.21	2.21
48	1.33	6.65	Square	9.96	9.00	85.0	10.93	26.10	37.02	1.87
49	1.33	6.65	Square	6.73	10.30	87.8	9.36	17.84	27.21	0.85
50	1.33	6.65	Square	6.79	11.16	85.5	9.53	19.22	28.75	0.87
51	1.33	6.65	Square	10.01	11.52	81.3	11.35	32.01	43.36	1.89
52	1.33	6.65	Square	9.86	11.43	84.9	11.23	31.25	42.48	1.83
53	1.33	6.65	Square	9.66	12.13	80.8	11.26	32.02	43.28	1.76
54	1.33	6.65	Square	10.21	11.75	81.8	11.48	33.32	44.80	1.96
55	1.33	6.65	Square	9.74	12.38	82.1	11.32	32.84	44.16	1.79
56	1.33	6.65	Square	11.00	11.68	81.3	11.85	36.10	47.95	2.28
57	1.33	6.65	Square	10.27	11.79	84.8	11.48	33.60	45.08	1.99
58	1.33	6.65	Square	10.13	11.23	79.1	11.38	31.81	43.19	1.93
59	1.33	6.65	Square	9.45	10.76	79.2	10.98	28.31	39.29	1.68

60	1.33	6.65	Square	7.99	10.97	72.0	10.20	23.45	33.65	1.20
61	1.33	6.65	Square	7.65	9.60	79.9	9.87	19.99	29.86	1.10
62	1.33	6.65	Square	7.02	10.68	82.8	9.64	19.42	29.06	0.93
63	1.33	6.65	Square	10.27	11.47	78.6	11.48	32.89	44.37	1.99
64	1.33	6.65	Square	10.98	11.25	85.4	11.74	34.96	46.70	2.27
65	1.33	6.65	Square	10.86	11.31	81.8	11.73	34.66	46.39	2.22
66	1.33	6.65	Square	11.52	10.38	84.1	11.87	34.55	46.42	2.50

Note - Pier scour calculated using CSU equation.

Original Structure 500-year

*** PIER SCOUR REPORT ***

Pier No.	Pier Width (ft)	Pier Lngth (ft)	Pier Nose shape	Approach Flow Vel (ft/s)	Approach Flow Depth (ft)	Approach Flow Angle (deg)	Scour Depths Local (ft)	Scour Depths Genrl (ft)	Scour Depths Total (ft)	Riprap D50 (ft)
1	1.33	6.65	Square	14.45	10.22	78.0	13.09	43.62	56.71	3.93
2	4.00	4.00	Round	5.68	17.67	15.9	7.26	12.55	19.81	0.47
3	4.00	4.00	Round	6.02	15.32	15.1	7.30	12.79	20.09	0.53
4	4.00	4.00	Round	5.89	10.19	14.2	6.85	9.24	16.09	0.51
5	4.00	4.00	Round	5.41	7.81	13.9	6.37	6.60	12.97	0.43
6	4.00	4.00	Round	6.02	25.30	18.9	7.81	17.89	25.70	0.53
7	4.00	4.00	Round	6.20	25.58	18.1	7.92	19.13	27.05	0.56
8	4.00	4.00	Round	6.81	26.31	16.4	8.28	23.31	31.59	0.68
9	4.00	4.00	Round	7.20	26.69	15.6	8.50	26.05	34.55	0.76
10	4.00	4.00	Round	6.71	27.74	31.9	8.29	23.56	31.85	0.66
11	4.00	4.00	Round	7.05	27.81	30.9	8.47	25.82	34.30	0.73
12	4.00	4.00	Round	8.04	27.84	27.6	8.97	32.28	41.24	0.95
13	4.00	4.00	Round	8.57	27.79	26.2	9.21	35.55	44.76	1.08
14	4.00	4.00	Round	8.48	29.64	35.9	9.25	36.75	46.00	1.06
15	4.00	4.00	Round	8.86	29.83	34.8	9.43	39.42	48.85	1.15
16	4.00	4.00	Round	9.51	30.25	32.6	9.74	44.24	53.98	1.33
17	4.00	4.00	Round	8.97	30.48	31.9	9.51	40.87	50.39	1.18
18	4.00	4.00	Round	11.03	32.07	42.7	10.47	56.85	67.31	1.78
19	4.00	4.00	Round	10.68	31.02	42.9	10.28	53.07	63.35	1.67
20	4.00	4.00	Round	10.60	29.17	38.2	10.16	50.05	60.21	1.65
21	4.00	4.00	Round	9.63	28.57	34.2	9.72	43.16	52.89	1.36
22	4.00	4.00	Round	13.68	22.88	45.8	10.97	57.20	68.17	2.74
23	4.00	4.00	Round	14.78	22.22	46.5	11.30	61.23	72.53	3.20
24	4.00	4.00	Round	15.95	21.53	43.3	11.63	65.19	76.81	3.73
25	4.00	4.00	Round	14.68	21.26	38.5	11.20	58.65	69.85	3.16
26	4.00	4.00	Round	11.74	10.73	43.1	9.27	25.96	35.23	2.02
27	4.00	4.00	Round	11.94	9.62	34.7	9.21	24.30	33.51	2.09
28	4.00	4.00	Round	9.33	10.63	32.8	8.39	19.26	27.65	1.28
29	4.00	4.00	Round	8.60	11.08	32.7	8.15	17.83	25.99	1.09
30	1.33	6.65	Square	10.31	12.07	76.3	11.57	34.39	45.96	2.00
31	1.33	6.65	Square	6.58	13.97	85.8	9.69	21.89	31.58	0.82
32	1.33	6.65	Square	14.48	13.15	78.5	13.55	53.78	67.34	3.95
33	1.33	6.65	Square	11.98	14.32	85.6	12.58	46.87	59.45	2.70
34	1.33	6.65	Square	12.51	14.26	78.5	12.87	49.07	61.94	2.95
35	1.33	6.65	Square	11.06	14.67	82.1	12.24	43.67	55.91	2.30
36	1.33	6.65	Square	12.99	14.68	79.6	13.13	52.36	65.49	3.18
37	1.33	6.65	Square	13.73	14.73	80.5	13.45	55.77	69.22	3.55
38	1.33	6.65	Square	15.92	14.30	82.7	14.26	63.71	77.97	4.77
39	1.33	6.65	Square	14.69	14.62	79.7	13.83	59.58	73.42	4.07
40	1.33	6.65	Square	10.42	13.91	89.5	11.73	39.08	50.81	2.05
41	1.33	6.65	Square	6.79	14.48	73.3	9.89	23.53	33.42	0.87
42	1.33	6.65	Square	11.22	13.43	62.9	11.90	41.34	53.24	2.37
43	1.33	6.65	Square	9.90	13.90	81.4	11.59	36.77	48.36	1.85
44	1.33	6.65	Square	14.51	14.62	74.8	13.74	58.79	72.53	3.97
45	1.33	6.65	Square	15.48	14.05	78.9	14.07	60.95	75.02	4.51
46	1.33	6.65	Square	12.87	13.61	77.6	12.95	48.72	61.67	3.12
47	1.33	6.65	Square	14.62	12.64	76.7	13.53	52.60	66.13	4.03
48	1.33	6.65	Square	13.14	10.38	86.4	12.52	39.90	52.42	3.25
49	1.33	6.65	Square	8.87	10.55	85.1	10.62	25.86	36.48	1.48
50	1.33	6.65	Square	10.14	11.89	86.3	11.41	33.36	44.78	1.94
51	1.33	6.65	Square	13.88	12.55	82.2	13.21	49.48	62.69	3.63
52	1.33	6.65	Square	14.14	12.12	85.7	13.21	49.04	62.25	3.76
53	1.33	6.65	Square	13.06	13.40	80.8	12.99	48.85	61.85	3.21
54	1.33	6.65	Square	14.06	12.45	82.2	13.27	49.83	63.10	3.72
55	1.33	6.65	Square	13.33	13.71	82.3	13.14	50.91	64.05	3.35
56	1.33	6.65	Square	15.54	12.34	81.6	13.84	55.03	68.87	4.55
57	1.33	6.65	Square	13.93	12.97	84.8	13.26	51.04	64.30	3.66
58	1.33	6.65	Square	13.94	11.83	79.0	13.15	47.34	60.49	3.66
59	1.33	6.65	Square	14.09	11.36	80.5	13.13	46.35	59.48	3.74

60	1.33	6.65	Square	11.79	11.65	72.0	12.16	38.93	51.09	2.62
61	1.33	6.65	Square	15.81	8.67	79.2	13.30	41.81	55.12	4.71
62	1.33	6.65	Square	10.85	11.20	88.1	11.62	34.35	45.98	2.22
63	1.33	6.65	Square	10.03	10.27	89.2	11.08	29.26	40.35	1.90
64	1.33	6.65	Square	13.72	11.64	85.9	12.96	45.90	58.86	3.54
65	1.33	6.65	Square	18.45	11.57	85.9	14.71	62.22	76.94	6.41
66	1.33	6.65	Square	16.40	10.17	86.9	13.73	49.57	63.30	5.06

Note - Pier scour calculated using CSU equation.

Existing Structure 10-year

*** PIER SCOUR REPORT ***

Pier No.	Pier Width (ft)	Pier Lngth (ft)	Pier Nose shape	Approach Flow Vel (ft/s)	Approach Flow Depth (ft)	Approach Flow Angle (deg)	Scour Depths Local (ft)	Scour Depths Genrl (ft)	Scour Depths Total (ft)	Riprap D50 (ft)
1	4.50	4.50	Round	4.30	10.77	42.3	6.51	9.16	15.66	0.27
2	4.50	4.50	Round	4.12	10.80	35.2	6.39	8.44	14.83	0.25
3	4.50	4.50	Round	3.64	10.92	23.9	6.06	6.55	12.61	0.19
4	4.50	4.50	Round	3.34	11.01	22.1	5.86	5.36	11.21	0.16
5	4.50	4.50	Round	3.72	11.89	47.2	6.19	7.26	13.45	0.20
6	4.50	4.50	Round	3.83	11.91	44.2	6.27	7.76	14.03	0.22
7	4.50	4.50	Round	4.01	11.75	37.7	6.39	8.48	14.87	0.24
8	4.50	4.50	Round	4.04	11.57	35.1	6.39	8.50	14.89	0.24
9	4.50	4.50	Round	3.50	13.36	49.5	6.13	6.75	12.89	0.18
10	4.50	4.50	Round	3.50	13.84	49.4	6.16	6.85	13.01	0.18
11	4.50	4.50	Round	3.46	14.75	45.2	6.18	6.90	13.08	0.18
12	4.50	4.50	Round	3.45	15.11	41.5	6.19	6.95	13.14	0.17
13	4.50	4.50	Round	3.59	12.76	38.0	6.16	6.97	13.13	0.19
14	4.50	4.50	Round	3.68	13.19	39.2	6.25	7.55	13.80	0.20
15	4.50	4.50	Round	3.90	14.23	40.2	6.48	9.05	15.53	0.22
16	4.50	4.50	Round	4.01	14.76	40.0	6.59	9.81	16.40	0.24
17	4.50	4.50	Round	2.97	11.37	37.3	5.59	3.82	9.40	0.13
18	4.50	4.50	Round	2.97	11.40	36.9	5.59	3.84	9.43	0.13
19	4.50	4.50	Round	3.30	11.53	35.9	5.86	5.30	11.16	0.16
20	4.50	4.50	Round	3.57	11.66	35.4	6.07	6.50	12.57	0.19
21	4.50	4.50	Round	3.16	10.14	40.2	5.65	4.40	10.05	0.15
22	4.50	4.50	Round	3.20	10.31	40.8	5.70	4.59	10.28	0.15
23	4.50	4.50	Round	3.16	10.60	40.2	5.69	4.50	10.19	0.15
24	4.50	4.50	Round	3.10	10.71	38.9	5.65	4.29	9.94	0.14
25	4.50	4.50	Round	2.74	9.41	34.3	5.26	2.66	7.92	0.11
26	4.50	4.50	Round	2.82	9.54	35.2	5.34	2.99	8.33	0.12
27	4.50	4.50	Round	3.06	9.84	36.1	5.55	3.94	9.49	0.14
28	4.50	4.50	Round	3.18	9.99	36.1	5.66	4.43	10.08	0.15
29	4.50	4.50	Round	2.33	8.98	33.4	4.88	1.09	5.97	0.08
30	4.50	4.50	Round	2.33	9.06	33.5	4.89	1.12	6.01	0.08
31	4.50	4.50	Round	2.45	9.25	32.5	5.00	1.54	6.54	0.09
32	4.50	4.50	Round	2.55	9.35	31.7	5.10	1.92	7.02	0.10
33	4.50	4.50	Round	2.28	8.55	40.8	4.80	0.95	5.75	0.08
34	4.50	4.50	Round	2.24	8.58	40.5	4.76	0.78	5.54	0.07
35	4.50	4.50	Round	2.14	8.66	37.6	4.68	0.43	5.11	0.07
36	4.50	4.50	Round	2.12	8.71	35.3	4.67	0.36	5.02	0.07
37	4.50	4.50	Round	3.08	9.18	36.7	5.52	3.87	9.39	0.14
38	4.50	4.50	Round	3.02	9.13	37.5	5.46	3.64	9.10	0.13
39	4.50	4.50	Round	2.74	9.02	37.9	5.23	2.59	7.82	0.11
40	4.50	4.50	Round	2.54	8.97	37.2	5.06	1.88	6.94	0.09
41	4.50	4.50	Round	3.43	10.01	33.7	5.85	5.42	11.27	0.17
42	4.50	4.50	Round	3.40	9.97	34.6	5.82	5.29	11.11	0.17
43	4.50	4.50	Round	3.16	9.89	35.3	5.63	4.33	9.97	0.15
44	4.50	4.50	Round	2.97	9.86	35.0	5.48	3.57	9.05	0.13
45	4.50	4.50	Round	3.15	10.85	32.2	5.70	4.52	10.21	0.15
46	4.50	4.50	Round	3.12	10.82	33.3	5.67	4.39	10.06	0.14
47	4.50	4.50	Round	2.95	10.77	34.4	5.53	3.64	9.17	0.13
48	4.50	4.50	Round	2.81	10.74	34.3	5.41	3.05	8.46	0.12
49	4.50	4.50	Round	2.54	11.35	32.8	5.23	1.94	7.17	0.09
50	4.50	4.50	Round	2.46	11.37	33.9	5.16	1.57	6.72	0.09
51	4.50	4.50	Round	2.28	11.42	35.4	4.99	0.76	5.75	0.08
52	4.50	4.50	Round	2.20	11.44	35.6	4.91	0.36	5.28	0.07
53	4.50	4.50	Round	2.68	11.09	33.1	5.33	2.52	7.85	0.11
54	4.50	4.50	Round	2.55	11.16	34.3	5.22	1.94	7.16	0.10
55	4.50	4.50	Round	2.26	11.31	37.0	4.96	0.66	5.62	0.07
56	4.50	4.50	Round	2.12	11.38	38.3	4.84	0.03	4.87	0.07
57	4.50	4.50	Round	3.16	10.85	29.3	5.71	4.57	10.28	0.15
58	4.50	4.50	Round	3.00	10.96	30.9	5.59	3.90	9.49	0.13
59	4.50	4.50	Round	2.62	11.20	34.5	5.28	2.27	7.56	0.10

60	4.50	4.50	Round	2.43	11.31	36.2	5.12	1.42	6.54	0.09
61	4.50	4.50	Round	3.83	9.01	23.6	6.04	6.48	12.52	0.22
62	4.50	4.50	Round	3.70	9.16	27.0	5.97	6.08	12.05	0.20
63	4.50	4.50	Round	3.14	9.52	32.5	5.59	4.16	9.75	0.14
64	4.50	4.50	Round	2.76	9.70	34.3	5.30	2.76	8.06	0.11
65	4.00	4.00	Round	1.24	6.31	26.7	3.29	0.00	3.29	0.02
66	4.00	4.00	Round	1.28	6.38	25.3	3.33	0.00	3.33	0.02
67	4.00	4.00	Round	1.27	6.54	21.6	3.34	0.00	3.34	0.02
68	4.00	4.00	Round	1.23	6.61	19.4	3.30	0.00	3.30	0.02
69	4.00	4.00	Round	1.63	21.78	34.3	4.37	0.00	4.37	0.04
70	4.00	4.00	Round	1.69	22.01	32.1	4.44	0.00	4.44	0.04
71	4.00	4.00	Round	1.87	22.61	25.9	4.66	0.00	4.66	0.05
72	4.00	4.00	Round	2.00	22.86	22.8	4.79	0.00	4.79	0.06
73	4.00	4.00	Round	2.42	25.80	39.7	5.29	0.00	5.29	0.09
74	4.00	4.00	Round	2.50	26.14	38.4	5.38	0.00	5.38	0.09
75	4.00	4.00	Round	2.69	26.80	33.9	5.57	0.00	5.57	0.11
76	4.00	4.00	Round	2.80	26.90	31.3	5.67	0.00	5.67	0.12
77	4.00	4.00	Round	2.80	27.52	46.3	5.69	0.00	5.69	0.11
78	4.00	4.00	Round	2.95	27.63	45.2	5.82	0.00	5.82	0.13
79	4.00	4.00	Round	3.18	27.82	41.6	6.02	0.00	6.02	0.15
80	4.00	4.00	Round	3.28	27.90	39.1	6.10	0.00	6.10	0.16
81	4.00	4.00	Round	3.54	27.51	52.3	6.29	1.90	8.19	0.18
82	4.00	4.00	Round	3.77	27.28	51.1	6.45	3.54	10.00	0.21
83	4.00	4.00	Round	4.28	26.81	48.3	6.80	7.07	13.87	0.27
84	4.00	4.00	Round	4.44	26.62	46.4	6.91	8.17	15.08	0.29
85	4.00	4.00	Round	4.14	23.19	63.8	6.58	5.91	12.49	0.25
86	4.00	4.00	Round	4.14	21.84	59.3	6.52	5.80	12.32	0.25
87	4.00	4.00	Round	4.21	18.32	46.7	6.42	5.81	12.22	0.26
88	4.00	4.00	Round	4.28	17.01	44.2	6.40	5.93	12.33	0.27
89	4.00	4.00	Round	5.03	14.09	51.7	6.68	8.33	15.01	0.37
90	4.00	4.00	Round	5.48	12.63	50.6	6.83	9.35	16.18	0.44
91	4.00	4.00	Round	4.33	9.95	40.7	5.98	4.69	10.67	0.28
92	4.00	4.00	Round	3.74	9.09	34.8	5.55	2.85	8.40	0.21

Note - Pier scour calculated using CSU equation.

Existing Structure 25-year

*** PIER SCOUR REPORT ***

Pier No.	Pier Width (ft)	Pier Lngth (ft)	Pier Nose shape	Approach Flow Vel (ft/s)	Approach Flow Depth (ft)	Approach Flow Angle (deg)	Scour Depths Local (ft)	Scour Depths Genrl (ft)	Scour Depths Total (ft)	Riprap D50 (ft)
1	4.00	4.00	Round	5.11	9.27	35.9	6.36	6.59	12.95	0.38
2	4.00	4.00	Round	6.19	10.14	42.5	6.99	10.08	17.07	0.56
3	4.00	4.00	Round	7.72	12.89	49.9	7.94	17.11	25.05	0.87
4	4.00	4.00	Round	6.85	14.41	49.9	7.66	15.39	23.05	0.69
5	4.00	4.00	Round	5.36	17.22	44.6	7.06	10.89	17.95	0.42
6	4.00	4.00	Round	5.54	18.58	47.6	7.23	12.31	19.55	0.45
7	4.00	4.00	Round	5.53	22.27	59.6	7.41	13.73	21.13	0.45
8	4.00	4.00	Round	5.56	23.67	64.5	7.49	14.46	21.94	0.45
9	4.00	4.00	Round	6.10	27.06	47.4	7.93	19.24	27.17	0.55
10	4.00	4.00	Round	5.88	27.29	48.8	7.81	17.85	25.66	0.51
11	4.00	4.00	Round	5.03	27.82	51.1	7.33	12.38	19.71	0.37
12	4.00	4.00	Round	4.68	28.07	52.4	7.11	9.99	17.11	0.32
13	4.00	4.00	Round	4.37	28.46	39.1	6.92	7.88	14.80	0.28
14	4.00	4.00	Round	4.30	28.39	41.9	6.87	7.36	14.23	0.27
15	4.00	4.00	Round	3.98	28.23	44.7	6.64	5.07	11.71	0.23
16	4.00	4.00	Round	3.73	28.14	45.6	6.46	3.29	9.75	0.20
17	4.00	4.00	Round	3.78	27.52	31.0	6.47	3.60	10.07	0.21
18	4.00	4.00	Round	3.65	27.42	34.1	6.37	2.71	9.08	0.20
19	4.00	4.00	Round	3.42	26.79	39.2	6.18	1.18	7.36	0.17
20	4.00	4.00	Round	3.31	26.46	40.4	6.08	0.41	6.49	0.16
21	4.00	4.00	Round	2.69	23.52	22.4	5.47	0.00	5.47	0.11
22	4.00	4.00	Round	2.48	23.27	25.6	5.27	0.00	5.27	0.09
23	4.00	4.00	Round	2.20	22.68	32.4	5.00	0.00	5.00	0.07
24	4.00	4.00	Round	2.13	22.45	34.6	4.92	0.00	4.92	0.07
25	4.00	4.00	Round	1.67	7.28	19.5	3.80	0.00	3.80	0.04
26	4.00	4.00	Round	1.72	7.22	21.6	3.85	0.00	3.85	0.04
27	4.00	4.00	Round	1.73	7.06	25.1	3.85	0.00	3.85	0.04
28	4.00	4.00	Round	1.68	6.99	26.4	3.80	0.00	3.80	0.04
29	4.50	4.50	Round	4.13	10.07	35.2	6.34	8.12	14.46	0.25
30	4.50	4.50	Round	4.72	9.86	33.9	6.69	10.16	16.86	0.33
31	4.50	4.50	Round	5.52	9.44	28.6	7.11	12.60	19.71	0.45
32	4.50	4.50	Round	5.64	9.25	24.8	7.16	12.82	19.98	0.47
33	4.50	4.50	Round	3.38	11.70	37.8	5.93	5.68	11.61	0.17
34	4.50	4.50	Round	3.68	11.58	35.6	6.15	6.99	13.13	0.20
35	4.50	4.50	Round	4.28	11.31	31.5	6.53	9.38	15.92	0.27
36	4.50	4.50	Round	4.53	11.18	29.7	6.68	10.32	17.01	0.30
37	4.50	4.50	Round	2.79	11.79	40.2	5.47	3.07	8.54	0.11
38	4.50	4.50	Round	3.02	11.71	38.3	5.65	4.10	9.75	0.13
39	4.50	4.50	Round	3.48	11.54	35.1	5.99	6.08	12.07	0.18
40	4.50	4.50	Round	3.67	11.45	34.0	6.13	6.89	13.01	0.20
41	4.50	4.50	Round	2.93	11.88	35.4	5.59	3.72	9.31	0.13
42	4.50	4.50	Round	3.05	11.85	35.1	5.69	4.27	9.96	0.14
43	4.50	4.50	Round	3.32	11.78	33.7	5.89	5.47	11.37	0.16
44	4.50	4.50	Round	3.45	11.74	32.7	5.99	6.03	12.02	0.17
45	4.50	4.50	Round	4.00	11.18	34.4	6.33	8.14	14.47	0.23
46	4.50	4.50	Round	4.19	11.20	34.5	6.47	8.95	15.42	0.26
47	4.50	4.50	Round	4.42	11.24	33.3	6.62	9.93	16.55	0.29
48	4.50	4.50	Round	4.46	11.26	32.2	6.65	10.08	16.72	0.29
49	4.50	4.50	Round	4.25	10.29	35.9	6.44	8.69	15.13	0.27
50	4.50	4.50	Round	4.54	10.32	36.2	6.62	9.80	16.42	0.30
51	4.50	4.50	Round	4.87	10.40	35.3	6.83	11.10	17.93	0.35
52	4.50	4.50	Round	4.89	10.44	34.3	6.85	11.23	18.08	0.35
53	4.50	4.50	Round	3.50	9.40	39.5	5.84	5.45	11.29	0.18
54	4.50	4.50	Round	3.79	9.45	40.2	6.05	6.52	12.57	0.21
55	4.50	4.50	Round	4.20	9.57	39.4	6.34	8.07	14.41	0.26
56	4.50	4.50	Round	4.28	9.62	38.3	6.39	8.40	14.79	0.27
57	4.50	4.50	Round	2.85	9.12	37.5	5.33	3.03	8.37	0.12
58	4.50	4.50	Round	2.84	9.09	40.5	5.32	3.00	8.32	0.12
59	4.50	4.50	Round	2.95	9.03	43.9	5.40	3.36	8.76	0.13

60	4.50	4.50	Round	3.01	9.01	44.1	5.45	3.60	9.05	0.13
61	4.50	4.50	Round	3.66	9.74	31.8	5.99	6.19	12.18	0.20
62	4.50	4.50	Round	3.47	9.66	32.7	5.85	5.45	11.29	0.18
63	4.50	4.50	Round	3.28	9.50	33.9	5.69	4.67	10.37	0.16
64	4.50	4.50	Round	3.28	9.43	33.8	5.69	4.68	10.37	0.16
65	4.50	4.50	Round	4.56	10.36	36.3	6.64	9.92	16.55	0.31
66	4.50	4.50	Round	4.35	10.22	36.1	6.49	9.03	15.53	0.28
67	4.50	4.50	Round	3.99	9.97	35.0	6.23	7.52	13.75	0.23
68	4.50	4.50	Round	3.89	9.86	34.1	6.16	7.09	13.25	0.22
69	4.50	4.50	Round	4.23	11.06	39.4	6.48	9.04	15.53	0.26
70	4.50	4.50	Round	4.32	10.97	40.7	6.54	9.37	15.91	0.27
71	4.50	4.50	Round	4.38	10.72	41.2	6.56	9.46	16.01	0.28
72	4.50	4.50	Round	4.32	10.58	40.5	6.50	9.13	15.63	0.27
73	4.50	4.50	Round	5.03	11.98	34.4	7.06	12.99	20.06	0.37
74	4.50	4.50	Round	4.54	11.88	35.1	6.75	10.81	17.55	0.30
75	4.50	4.50	Round	3.99	11.80	36.6	6.38	8.43	14.81	0.23
76	4.50	4.50	Round	4.03	11.80	37.0	6.41	8.60	15.01	0.24
77	4.50	4.50	Round	5.73	15.04	40.4	7.70	18.87	26.57	0.48
78	4.50	4.50	Round	5.54	14.54	40.6	7.55	17.48	25.03	0.45
79	4.50	4.50	Round	5.17	13.57	39.2	7.26	14.87	22.14	0.39
80	4.50	4.50	Round	5.04	13.16	37.9	7.16	13.95	21.10	0.37
81	4.50	4.50	Round	4.65	15.33	42.4	7.06	13.50	20.56	0.32
82	4.50	4.50	Round	4.67	15.02	46.4	7.05	13.40	20.45	0.32
83	4.50	4.50	Round	4.78	14.18	50.9	7.06	13.42	20.48	0.33
84	4.50	4.50	Round	4.82	13.74	51.0	7.06	13.34	20.40	0.34
85	4.50	4.50	Round	5.73	11.71	34.8	7.44	15.67	23.11	0.48
86	4.50	4.50	Round	5.67	11.94	36.8	7.43	15.66	23.09	0.47
87	4.50	4.50	Round	5.30	12.21	43.1	7.24	14.34	21.58	0.41
88	4.50	4.50	Round	5.10	12.25	46.6	7.12	13.48	20.61	0.38
89	4.50	4.50	Round	4.81	11.13	22.1	6.86	11.45	18.31	0.34
90	4.50	4.50	Round	5.24	11.04	24.6	7.10	13.06	20.16	0.40
91	4.50	4.50	Round	5.88	10.94	36.1	7.46	15.48	22.94	0.51
92	4.50	4.50	Round	6.08	10.93	42.8	7.57	16.24	23.80	0.54

Note - Pier scour calculated using CSU equation.

Existing Structure 50-year

*** PIER SCOUR REPORT ***

Pier No.	Pier Width (ft)	Pier Lngth (ft)	Pier Nose shape	Approach Flow Vel (ft/s)	Approach Flow Depth (ft)	Approach Flow Angle (deg)	Scour Depths Local (ft)	Scour Depths Genrl (ft)	Scour Depths Total (ft)	Riprap D50 (ft)
1	4.50	4.50	Round	7.40	11.11	42.3	8.25	21.48	29.73	0.80
2	4.50	4.50	Round	7.28	11.09	35.9	8.19	21.00	29.19	0.78
3	4.50	4.50	Round	6.61	11.18	25.0	7.86	18.55	26.41	0.64
4	4.50	4.50	Round	6.10	11.27	22.4	7.61	16.67	24.28	0.55
5	4.50	4.50	Round	6.17	12.61	46.2	7.76	18.47	26.24	0.56
6	4.50	4.50	Round	6.41	12.53	42.3	7.88	19.42	27.31	0.60
7	4.50	4.50	Round	6.87	12.15	35.8	8.09	20.86	28.94	0.69
8	4.50	4.50	Round	6.93	11.86	34.0	8.09	20.73	28.82	0.70
9	4.50	4.50	Round	5.87	14.13	51.4	7.71	18.70	26.41	0.51
10	4.50	4.50	Round	5.82	14.54	51.4	7.71	18.85	26.56	0.50
11	4.50	4.50	Round	5.66	15.29	47.0	7.68	18.76	26.43	0.47
12	4.50	4.50	Round	5.61	15.57	43.0	7.67	18.78	26.45	0.46
13	4.50	4.50	Round	6.12	13.58	37.9	7.81	19.31	27.13	0.55
14	4.50	4.50	Round	6.27	13.95	39.3	7.92	20.42	28.35	0.58
15	4.50	4.50	Round	6.78	14.86	40.7	8.26	23.92	32.19	0.67
16	4.50	4.50	Round	7.06	15.33	40.5	8.44	25.90	34.35	0.73
17	4.50	4.50	Round	4.92	12.25	36.9	7.02	12.74	19.75	0.36
18	4.50	4.50	Round	4.86	12.22	36.6	6.97	12.42	19.39	0.35
19	4.50	4.50	Round	5.56	12.24	34.7	7.39	15.46	22.85	0.45
20	4.50	4.50	Round	6.23	12.31	33.9	7.77	18.41	26.18	0.57
21	4.50	4.50	Round	5.10	11.03	40.6	7.02	12.50	19.52	0.38
22	4.50	4.50	Round	5.18	11.16	41.2	7.08	12.92	20.00	0.39
23	4.50	4.50	Round	5.17	11.35	40.8	7.09	13.04	20.13	0.39
24	4.50	4.50	Round	5.10	11.42	39.6	7.05	12.81	19.86	0.38
25	4.50	4.50	Round	4.84	10.32	34.2	6.80	10.93	17.73	0.34
26	4.50	4.50	Round	4.92	10.41	35.1	6.86	11.30	18.16	0.35
27	4.50	4.50	Round	5.36	10.63	36.3	7.14	13.15	20.29	0.42
28	4.50	4.50	Round	5.65	10.74	36.5	7.31	14.36	21.67	0.47
29	4.50	4.50	Round	4.14	9.90	34.1	6.33	8.06	14.39	0.25
30	4.50	4.50	Round	4.12	9.95	34.2	6.32	7.99	14.31	0.25
31	4.50	4.50	Round	4.40	10.08	33.1	6.51	9.10	15.61	0.28
32	4.50	4.50	Round	4.69	10.15	32.3	6.70	10.24	16.93	0.32
33	4.50	4.50	Round	3.52	9.48	46.4	5.87	5.57	11.44	0.18
34	4.50	4.50	Round	3.45	9.49	46.3	5.81	5.29	11.11	0.17
35	4.50	4.50	Round	3.39	9.53	42.4	5.78	5.10	10.88	0.17
36	4.50	4.50	Round	3.47	9.55	39.0	5.83	5.39	11.22	0.18
37	4.50	4.50	Round	5.14	10.08	39.6	6.96	11.87	18.83	0.39
38	4.50	4.50	Round	5.04	10.02	40.9	6.90	11.45	18.35	0.37
39	4.50	4.50	Round	4.54	9.90	41.9	6.58	9.51	16.09	0.30
40	4.50	4.50	Round	4.19	9.84	41.2	6.36	8.20	14.56	0.26
41	4.50	4.50	Round	6.01	10.87	34.9	7.52	15.91	23.43	0.53
42	4.50	4.50	Round	5.99	10.84	36.0	7.51	15.79	23.30	0.53
43	4.50	4.50	Round	5.60	10.77	37.0	7.29	14.21	21.50	0.46
44	4.50	4.50	Round	5.25	10.73	36.7	7.08	12.83	19.92	0.40
45	4.50	4.50	Round	5.52	11.68	32.0	7.32	14.77	22.09	0.45
46	4.50	4.50	Round	5.48	11.67	33.2	7.30	14.61	21.91	0.44
47	4.50	4.50	Round	5.20	11.64	34.4	7.13	13.42	20.55	0.40
48	4.50	4.50	Round	4.95	11.63	34.3	6.99	12.40	19.38	0.36
49	4.50	4.50	Round	4.19	12.14	32.3	6.53	9.43	15.96	0.26
50	4.50	4.50	Round	4.02	12.19	33.1	6.43	8.74	15.17	0.24
51	4.50	4.50	Round	3.68	12.29	34.3	6.19	7.22	13.42	0.20
52	4.50	4.50	Round	3.52	12.33	34.5	6.08	6.53	12.61	0.18
53	4.50	4.50	Round	4.38	11.82	35.0	6.64	10.08	16.72	0.28
54	4.50	4.50	Round	4.14	11.92	36.0	6.48	9.10	15.58	0.25
55	4.50	4.50	Round	3.53	12.13	39.5	6.07	6.49	12.56	0.18
56	4.50	4.50	Round	3.21	12.22	41.9	5.83	5.06	10.89	0.15
57	4.50	4.50	Round	5.60	11.51	30.0	7.35	14.93	22.28	0.46
58	4.50	4.50	Round	5.28	11.66	31.9	7.18	13.77	20.95	0.41
59	4.50	4.50	Round	4.50	11.97	36.5	6.73	10.69	17.42	0.30

60	4.50	4.50	Round	4.09	12.11	39.1	6.47	8.98	15.45	0.25
61	4.50	4.50	Round	7.04	9.49	25.5	7.91	17.79	25.70	0.73
62	4.50	4.50	Round	6.93	9.72	29.6	7.88	17.74	25.62	0.70
63	4.50	4.50	Round	5.97	10.21	34.9	7.44	15.01	22.45	0.52
64	4.50	4.50	Round	5.24	10.45	35.8	7.05	12.55	19.60	0.40
65	4.00	4.00	Round	2.00	7.65	26.2	4.14	0.00	4.14	0.06
66	4.00	4.00	Round	2.06	7.72	24.9	4.20	0.00	4.20	0.06
67	4.00	4.00	Round	2.06	7.88	21.6	4.21	0.00	4.21	0.06
68	4.00	4.00	Round	1.99	7.95	19.6	4.15	0.00	4.15	0.06
69	4.00	4.00	Round	2.48	23.11	34.7	5.27	0.00	5.27	0.09
70	4.00	4.00	Round	2.56	23.33	32.4	5.35	0.00	5.35	0.10
71	4.00	4.00	Round	2.89	23.91	25.3	5.66	0.00	5.66	0.12
72	4.00	4.00	Round	3.17	24.16	22.0	5.89	0.00	5.89	0.15
73	4.00	4.00	Round	3.94	27.09	40.9	6.57	4.73	11.30	0.23
74	4.00	4.00	Round	4.08	27.42	39.8	6.68	5.73	12.41	0.24
75	4.00	4.00	Round	4.34	28.03	34.3	6.88	7.59	14.47	0.28
76	4.00	4.00	Round	4.48	28.12	30.7	6.98	8.56	15.54	0.29
77	4.00	4.00	Round	4.40	28.74	45.1	6.95	8.08	15.03	0.28
78	4.00	4.00	Round	4.72	28.83	44.2	7.16	10.40	17.56	0.33
79	4.00	4.00	Round	5.12	28.96	42.1	7.42	13.24	20.66	0.38
80	4.00	4.00	Round	5.15	29.01	39.1	7.44	13.47	20.91	0.39
81	4.00	4.00	Round	5.45	28.63	52.5	7.61	15.47	23.08	0.44
82	4.00	4.00	Round	5.90	28.36	51.3	7.87	18.45	26.32	0.51
83	4.00	4.00	Round	7.03	27.77	49.2	8.46	25.66	34.12	0.72
84	4.00	4.00	Round	7.31	27.51	48.1	8.59	27.29	35.88	0.78
85	4.00	4.00	Round	6.54	24.16	64.9	8.05	20.42	28.47	0.63
86	4.00	4.00	Round	6.49	22.71	59.5	7.95	19.26	27.22	0.62
87	4.00	4.00	Round	6.44	18.86	48.9	7.73	16.73	24.46	0.61
88	4.00	4.00	Round	5.97	17.45	45.8	7.41	13.74	21.14	0.52
89	4.00	4.00	Round	8.13	14.76	48.8	8.27	20.45	28.72	0.97
90	4.00	4.00	Round	9.30	13.18	49.7	8.63	22.67	31.30	1.27
91	4.00	4.00	Round	7.55	10.37	44.0	7.64	14.06	21.70	0.84
92	4.00	4.00	Round	6.08	9.47	36.9	6.87	9.30	16.18	0.54

Note - Pier scour calculated using CSU equation.

Existing Structure 100-year

*** PIER SCOUR REPORT ***

Pier No.	Pier Width (ft)	Pier Lngth (ft)	Pier Nose shape	Approach Flow Vel (ft/s)	Approach Flow Depth (ft)	Approach Flow Angle (deg)	Scour Depths Local (ft)	Scour Depths Genrl (ft)	Scour Depths Total (ft)	Riprap D50 (ft)
1	4.50	4.50	Round	8.75	11.34	42.3	8.89	26.96	35.86	1.12
2	4.50	4.50	Round	8.74	11.30	36.4	8.88	26.85	35.74	1.12
3	4.50	4.50	Round	8.05	11.36	26.0	8.58	24.35	32.93	0.95
4	4.50	4.50	Round	7.46	11.44	23.1	8.31	22.19	30.50	0.82
5	4.50	4.50	Round	7.22	13.08	45.7	8.34	23.60	31.94	0.76
6	4.50	4.50	Round	7.52	12.94	41.5	8.48	24.69	33.17	0.83
7	4.50	4.50	Round	8.11	12.42	35.0	8.71	26.37	35.08	0.96
8	4.50	4.50	Round	8.21	12.07	33.4	8.73	26.18	34.91	0.99
9	4.50	4.50	Round	6.85	14.62	51.9	8.28	23.95	32.23	0.69
10	4.50	4.50	Round	6.80	14.99	51.8	8.28	24.18	32.47	0.68
11	4.50	4.50	Round	6.60	15.64	47.5	8.23	23.98	32.20	0.64
12	4.50	4.50	Round	6.53	15.88	43.7	8.20	23.88	32.09	0.63
13	4.50	4.50	Round	7.21	14.10	38.0	8.42	24.97	33.39	0.76
14	4.50	4.50	Round	7.37	14.44	39.4	8.53	26.20	34.73	0.80
15	4.50	4.50	Round	8.00	15.27	40.8	8.91	30.48	39.39	0.94
16	4.50	4.50	Round	8.37	15.70	40.7	9.11	33.00	42.11	1.03
17	4.50	4.50	Round	5.84	12.81	36.7	7.60	17.25	24.84	0.50
18	4.50	4.50	Round	5.76	12.75	36.6	7.55	16.85	24.39	0.49
19	4.50	4.50	Round	6.66	12.70	34.6	8.03	20.66	28.69	0.65
20	4.50	4.50	Round	7.53	12.73	33.6	8.47	24.45	32.92	0.83
21	4.50	4.50	Round	5.72	11.60	40.9	7.43	15.52	22.95	0.48
22	4.50	4.50	Round	5.80	11.70	41.5	7.48	15.96	23.44	0.49
23	4.50	4.50	Round	5.89	11.83	40.9	7.54	16.45	24.00	0.51
24	4.50	4.50	Round	5.91	11.87	39.7	7.56	16.58	24.14	0.51
25	4.50	4.50	Round	5.84	10.89	34.5	7.43	15.25	22.68	0.50
26	4.50	4.50	Round	5.88	10.96	35.4	7.46	15.47	22.93	0.51
27	4.50	4.50	Round	6.35	11.13	36.8	7.72	17.48	25.20	0.59
28	4.50	4.50	Round	6.71	11.22	37.1	7.92	18.98	26.90	0.66
29	4.50	4.50	Round	5.15	10.48	34.3	7.01	12.25	19.26	0.39
30	4.50	4.50	Round	5.11	10.51	34.5	6.98	12.10	19.09	0.38
31	4.50	4.50	Round	5.48	10.60	33.6	7.21	13.61	20.81	0.44
32	4.50	4.50	Round	5.88	10.65	32.8	7.43	15.17	22.60	0.51
33	4.50	4.50	Round	3.97	10.06	48.2	6.23	7.50	13.74	0.23
34	4.50	4.50	Round	3.89	10.06	48.2	6.17	7.18	13.36	0.22
35	4.50	4.50	Round	3.95	10.07	43.6	6.21	7.41	13.63	0.23
36	4.50	4.50	Round	4.15	10.08	39.9	6.35	8.17	14.52	0.25
37	4.50	4.50	Round	5.91	10.64	41.0	7.44	15.24	22.68	0.51
38	4.50	4.50	Round	5.77	10.58	42.6	7.37	14.68	22.05	0.49
39	4.50	4.50	Round	5.19	10.45	43.7	7.03	12.38	19.41	0.40
40	4.50	4.50	Round	4.82	10.38	42.9	6.80	10.92	17.72	0.34
41	4.50	4.50	Round	7.09	11.41	35.6	8.13	20.73	28.86	0.74
42	4.50	4.50	Round	7.07	11.39	36.9	8.12	20.62	28.74	0.73
43	4.50	4.50	Round	6.61	11.32	38.0	7.88	18.75	26.63	0.64
44	4.50	4.50	Round	6.20	11.28	37.6	7.66	17.10	24.76	0.56
45	4.50	4.50	Round	6.65	12.19	31.7	7.98	19.99	27.96	0.65
46	4.50	4.50	Round	6.60	12.19	32.9	7.95	19.81	27.76	0.64
47	4.50	4.50	Round	6.26	12.19	34.2	7.77	18.38	26.15	0.57
48	4.50	4.50	Round	5.96	12.19	34.1	7.61	17.13	24.74	0.52
49	4.50	4.50	Round	4.99	12.63	31.5	7.08	13.29	20.38	0.36
50	4.50	4.50	Round	4.80	12.70	32.1	6.97	12.50	19.47	0.34
51	4.50	4.50	Round	4.39	12.83	32.8	6.72	10.71	17.43	0.28
52	4.50	4.50	Round	4.20	12.89	32.8	6.60	9.90	16.50	0.26
53	4.50	4.50	Round	4.98	12.28	36.3	7.05	13.00	20.06	0.36
54	4.50	4.50	Round	4.69	12.39	37.4	6.88	11.81	18.69	0.32
55	4.50	4.50	Round	3.91	12.63	41.4	6.38	8.41	14.79	0.22
56	4.50	4.50	Round	3.48	12.74	44.4	6.08	6.46	12.54	0.18
57	4.50	4.50	Round	6.63	11.93	30.4	7.95	19.61	27.56	0.65
58	4.50	4.50	Round	6.24	12.10	32.4	7.76	18.19	25.95	0.57
59	4.50	4.50	Round	5.26	12.44	37.6	7.23	14.34	21.57	0.41

60	4.50	4.50	Round	4.73	12.60	40.7	6.92	12.14	19.07	0.33
61	4.50	4.50	Round	8.44	9.80	26.2	8.58	22.93	31.51	1.04
62	4.50	4.50	Round	8.33	10.06	30.5	8.57	23.07	31.63	1.02
63	4.50	4.50	Round	7.22	10.63	35.8	8.11	20.09	28.20	0.76
64	4.50	4.50	Round	6.36	10.90	36.3	7.71	17.26	24.97	0.59
65	4.00	4.00	Round	2.30	8.43	26.1	4.45	0.00	4.45	0.08
66	4.00	4.00	Round	2.37	8.50	24.8	4.52	0.00	4.52	0.08
67	4.00	4.00	Round	2.39	8.66	21.6	4.54	0.00	4.54	0.08
68	4.00	4.00	Round	2.32	8.72	19.7	4.49	0.00	4.49	0.08
69	4.00	4.00	Round	2.83	23.88	34.6	5.61	0.00	5.61	0.12
70	4.00	4.00	Round	2.91	24.10	32.3	5.68	0.00	5.68	0.12
71	4.00	4.00	Round	3.26	24.67	24.8	5.98	0.29	6.27	0.16
72	4.00	4.00	Round	3.58	24.91	21.4	6.24	2.42	8.66	0.19
73	4.00	4.00	Round	4.50	27.85	41.2	6.98	8.68	15.66	0.30
74	4.00	4.00	Round	4.67	28.17	40.2	7.11	9.92	17.02	0.32
75	4.00	4.00	Round	4.98	28.76	34.5	7.33	12.21	19.54	0.36
76	4.00	4.00	Round	5.14	28.83	30.5	7.43	13.35	20.78	0.39
77	4.00	4.00	Round	5.00	29.46	44.7	7.37	12.54	19.91	0.37
78	4.00	4.00	Round	5.40	29.54	43.8	7.61	15.37	22.99	0.43
79	4.00	4.00	Round	5.88	29.64	42.2	7.90	18.82	26.72	0.51
80	4.00	4.00	Round	5.85	29.67	39.1	7.89	18.65	26.54	0.50
81	4.00	4.00	Round	6.12	29.30	52.6	8.03	20.40	28.43	0.55
82	4.00	4.00	Round	6.66	29.01	51.4	8.31	23.96	32.28	0.65
83	4.00	4.00	Round	8.09	28.36	49.5	9.01	33.02	42.03	0.96
84	4.00	4.00	Round	8.42	28.07	48.6	9.15	34.88	44.03	1.04
85	4.00	4.00	Round	7.43	24.75	65.4	8.53	26.01	34.54	0.81
86	4.00	4.00	Round	7.36	23.25	59.3	8.42	24.46	32.88	0.79
87	4.00	4.00	Round	7.18	19.21	50.9	8.12	20.46	28.58	0.76
88	4.00	4.00	Round	6.34	17.76	48.0	7.62	15.58	23.19	0.59
89	4.00	4.00	Round	9.28	15.21	47.8	8.79	25.25	34.04	1.26
90	4.00	4.00	Round	10.72	13.58	49.6	9.21	27.98	37.19	1.69
91	4.00	4.00	Round	8.90	10.68	45.2	8.23	18.16	26.39	1.16
92	4.00	4.00	Round	7.10	9.76	37.9	7.38	12.24	19.62	0.74

Note - Pier scour calculated using CSU equation.

Existing Structure 500-year

*** PIER SCOUR REPORT ***

Pier No.	Pier Width (ft)	Pier Lngth (ft)	Pier Nose shape	Approach Flow Vel (ft/s)	Approach Flow Depth (ft)	Approach Flow Angle (deg)	Scour Depths Local (ft)	Scour Depths Genrl (ft)	Scour Depths Total (ft)	Riprap D50 (ft)
1	4.00	4.00	Round	9.62	10.76	38.8	8.52	20.27	28.79	1.36
2	4.00	4.00	Round	11.98	11.69	45.8	9.46	28.49	37.96	2.10
3	4.00	4.00	Round	13.34	14.77	48.2	10.23	39.08	49.31	2.61
4	4.00	4.00	Round	11.30	16.54	44.6	9.67	34.95	44.63	1.87
5	4.00	4.00	Round	6.65	18.68	52.6	7.83	17.60	25.43	0.65
6	4.00	4.00	Round	8.33	20.25	54.5	8.72	26.89	35.61	1.02
7	4.00	4.00	Round	9.46	24.79	56.7	9.46	37.72	47.18	1.31
8	4.00	4.00	Round	9.39	26.46	63.5	9.52	39.27	48.79	1.29
9	4.00	4.00	Round	10.53	29.63	49.0	10.15	50.22	60.37	1.62
10	4.00	4.00	Round	10.22	30.02	49.8	10.04	48.69	58.73	1.53
11	4.00	4.00	Round	8.27	30.86	52.4	9.20	36.35	45.55	1.00
12	4.00	4.00	Round	7.54	31.22	54.0	8.86	31.52	40.37	0.83
13	4.00	4.00	Round	7.19	31.54	39.6	8.69	29.22	37.91	0.76
14	4.00	4.00	Round	7.27	31.55	42.9	8.73	29.78	38.51	0.77
15	4.00	4.00	Round	6.66	31.51	43.8	8.41	25.33	33.73	0.65
16	4.00	4.00	Round	6.01	31.46	44.4	8.04	20.55	28.60	0.53
17	4.00	4.00	Round	6.47	30.82	29.5	8.28	23.62	31.90	0.61
18	4.00	4.00	Round	6.28	30.76	34.4	8.17	22.22	30.39	0.58
19	4.00	4.00	Round	5.94	30.21	40.2	7.96	19.49	27.44	0.52
20	4.00	4.00	Round	5.73	29.91	40.8	7.83	17.90	25.73	0.48
21	4.00	4.00	Round	4.26	26.98	19.7	6.79	6.93	13.72	0.27
22	4.00	4.00	Round	3.86	26.75	23.4	6.51	4.22	10.72	0.22
23	4.00	4.00	Round	3.59	26.21	31.8	6.29	2.40	8.69	0.19
24	4.00	4.00	Round	3.56	25.99	34.3	6.26	2.20	8.46	0.19
25	4.00	4.00	Round	3.09	10.85	19.9	5.23	0.96	6.19	0.14
26	4.00	4.00	Round	3.14	10.79	21.7	5.26	1.11	6.37	0.14
27	4.00	4.00	Round	3.07	10.62	24.8	5.20	0.90	6.10	0.14
28	4.00	4.00	Round	2.97	10.56	26.1	5.13	0.60	5.73	0.13
29	4.50	4.50	Round	8.60	12.29	36.9	8.92	28.12	37.04	1.08
30	4.50	4.50	Round	9.77	11.94	35.9	9.39	32.05	41.44	1.40
31	4.50	4.50	Round	11.21	11.17	30.1	9.87	35.58	45.45	1.84
32	4.50	4.50	Round	11.27	10.82	25.6	9.85	34.85	44.70	1.86
33	4.50	4.50	Round	6.07	14.08	44.0	7.83	19.63	27.46	0.54
34	4.50	4.50	Round	6.69	13.87	40.5	8.14	22.29	30.43	0.66
35	4.50	4.50	Round	7.88	13.42	34.7	8.69	26.99	35.68	0.91
36	4.50	4.50	Round	8.37	13.20	32.4	8.90	28.76	37.66	1.03
37	4.50	4.50	Round	4.98	14.31	45.8	7.20	14.53	21.73	0.36
38	4.50	4.50	Round	5.57	14.16	43.3	7.54	17.27	24.82	0.45
39	4.50	4.50	Round	6.56	13.83	39.1	8.07	21.65	29.72	0.63
40	4.50	4.50	Round	6.90	13.67	37.5	8.23	23.01	31.24	0.70
41	4.50	4.50	Round	7.12	14.54	31.5	8.41	25.17	33.58	0.74
42	4.50	4.50	Round	7.38	14.45	32.0	8.54	26.27	34.80	0.80
43	4.50	4.50	Round	7.87	14.26	31.6	8.76	28.26	37.02	0.91
44	4.50	4.50	Round	8.05	14.16	31.0	8.84	28.94	37.78	0.95
45	4.50	4.50	Round	7.82	13.84	34.4	8.70	27.39	36.09	0.90
46	4.50	4.50	Round	8.29	13.83	34.9	8.92	29.51	38.43	1.01
47	4.50	4.50	Round	8.89	13.81	33.9	9.19	32.13	41.32	1.16
48	4.50	4.50	Round	9.00	13.79	32.7	9.24	32.57	41.80	1.19
49	4.50	4.50	Round	7.22	12.93	39.1	8.33	23.42	31.75	0.77
50	4.50	4.50	Round	7.74	12.96	39.9	8.59	25.68	34.26	0.88
51	4.50	4.50	Round	8.36	13.02	39.3	8.88	28.41	37.29	1.02
52	4.50	4.50	Round	8.41	13.04	38.0	8.91	28.67	37.58	1.04
53	4.50	4.50	Round	6.09	12.02	41.6	7.67	17.47	25.13	0.54
54	4.50	4.50	Round	6.36	12.09	43.3	7.82	18.70	26.52	0.59
55	4.50	4.50	Round	6.90	12.24	43.3	8.11	21.11	29.22	0.70
56	4.50	4.50	Round	7.06	12.30	41.9	8.20	21.86	30.06	0.73
57	4.50	4.50	Round	6.63	11.68	37.4	7.92	19.27	27.20	0.64
58	4.50	4.50	Round	6.20	11.69	39.5	7.70	17.57	25.27	0.56
59	4.50	4.50	Round	5.81	11.73	42.2	7.49	16.00	23.49	0.49

60	4.50	4.50	Round	5.86	11.75	42.0	7.52	16.24	23.76	0.50
61	4.50	4.50	Round	8.74	12.17	35.3	8.97	28.45	37.42	1.12
62	4.50	4.50	Round	8.32	12.17	35.5	8.78	26.76	35.54	1.01
63	4.50	4.50	Round	7.88	12.16	35.6	8.58	25.02	33.60	0.91
64	4.50	4.50	Round	7.91	12.17	35.3	8.59	25.12	33.71	0.92
65	4.50	4.50	Round	8.51	12.67	39.8	8.92	28.45	37.37	1.06
66	4.50	4.50	Round	8.18	12.64	39.7	8.77	27.04	35.80	0.98
67	4.50	4.50	Round	7.87	12.59	38.4	8.62	25.66	34.27	0.91
68	4.50	4.50	Round	7.92	12.58	37.5	8.64	25.84	34.48	0.92
69	4.50	4.50	Round	7.89	13.24	39.7	8.68	26.77	35.45	0.91
70	4.50	4.50	Round	7.35	13.28	41.4	8.43	24.47	32.89	0.79
71	4.50	4.50	Round	6.89	13.30	42.9	8.20	22.47	30.67	0.70
72	4.50	4.50	Round	6.91	13.28	42.6	8.21	22.52	30.72	0.70
73	4.50	4.50	Round	10.39	14.03	33.7	9.85	39.20	49.05	1.58
74	4.50	4.50	Round	9.06	14.08	34.8	9.29	33.40	42.70	1.20
75	4.50	4.50	Round	7.65	14.32	36.8	8.66	27.37	36.03	0.86
76	4.50	4.50	Round	7.76	14.46	36.7	8.73	28.10	36.82	0.88
77	4.50	4.50	Round	11.11	16.85	41.0	10.39	49.11	59.50	1.81
78	4.50	4.50	Round	10.61	16.52	40.9	10.16	45.84	56.00	1.65
79	4.50	4.50	Round	9.80	15.90	39.4	9.77	40.48	50.25	1.41
80	4.50	4.50	Round	9.63	15.66	38.3	9.68	39.14	48.82	1.36
81	4.50	4.50	Round	8.45	16.86	45.0	9.24	35.34	44.58	1.05
82	4.50	4.50	Round	8.55	16.75	48.2	9.28	35.69	44.97	1.07
83	4.50	4.50	Round	8.69	16.35	52.3	9.31	35.74	45.06	1.11
84	4.50	4.50	Round	8.66	16.10	52.7	9.28	35.12	44.40	1.10
85	4.50	4.50	Round	11.21	12.81	32.2	10.05	39.74	49.80	1.84
86	4.50	4.50	Round	10.99	13.34	33.4	10.02	40.14	50.16	1.77
87	4.50	4.50	Round	10.04	14.20	39.9	9.72	38.05	47.77	1.48
88	4.50	4.50	Round	9.56	14.50	44.5	9.55	36.47	46.02	1.34
89	4.50	4.50	Round	10.57	11.99	25.4	9.72	35.25	44.96	1.64
90	4.50	4.50	Round	11.33	11.95	28.8	10.01	38.02	48.02	1.88
91	4.50	4.50	Round	11.93	12.05	37.9	10.24	40.55	50.79	2.09
92	4.50	4.50	Round	11.58	12.19	42.5	10.13	39.59	49.72	1.97

Note - Pier scour calculated using CSU equation.

VITA

Gabriel A. Bruehl

Candidate for the Degree of

Master of Science

Thesis: HYDRAULIC AND SCOUR MODELING OF EXISTING AND ORIGINAL STRUCTURES AT INTERSTATE-35 AND CIMARRON RIVER

Major Field: Civil Engineering

Biographical:

Personal Data: Born in Norman, Oklahoma, on December 19, 1973, the son of Dennis and Mary Bruehl.

Education: Graduated from Oklahoma State University, Stillwater, Oklahoma in May 1998. Completed the requirements for the Master of Science degree with a major in Civil Engineering at Oklahoma State University in July, 2000.

Experience: GIS Analyst for The Benham Group from May 1998 to April 2000. Research Assistant at Oklahoma State University from May 1998 to August 1998 and September 1999 to December 2000. Teachers Assistant at Oklahoma State University from January 1999 to April 2000. Associate Engineer, K.C. Engineering from April 2000 to present.

Professional Organizations: National Society of Professional Engineers, Oklahoma Society of Professional Engineers, American Society of Civil Engineers. Texas Water Conservation Association.